

ATMOSPHERIC DEPOSITION IN SOUTHEASTERN NORTH CAROLINA AND ITS  
IMPACT ON THE CAPE FEAR RIVER ESTUARY

Michael S. Long

A Thesis Submitted to the  
University of North Carolina at Wilmington in Partial Fulfillment  
Of the Requirements for the Degree of  
Master of Science

Center for Marine Science

University of North Carolina at Wilmington

2003

Approved by

Advisory Committee

\_\_\_\_\_  
Joan D. Willey  
Co-Chair

\_\_\_\_\_  
Robert Kieber  
Co-Chair

\_\_\_\_\_  
Douglas Gamble

Accepted by

\_\_\_\_\_  
Robert Roer  
Dean, Graduate School

## TABLE OF CONTENTS

ABSTRACT .....	iv
ACKNOWLEDGMENTS.....	vi
DEDICATION .....	vii
LIST OF TABLES .....	viii
LIST OF FIGURES.....	x
INTRODUCTION.....	1
METHODS.....	13
Reagents and Standards.....	13
Study Sites.....	14
UNCW.....	14
Cape Fear River Estuary (CFRE).....	14
Sample Collection and Storage .....	15
Rainwater .....	15
Particle Dry Deposition.....	15
Gas-phase Ammonia .....	16
CFRE Water Column and Atmosphere.....	17
Analytical Methods .....	19
NH <sub>x</sub> and Free Amino Acid Determination.....	19
Inorganic Anion Determination .....	21
Total Nitrogen Determination .....	23
Organic Nitrogen Determination.....	24
Detection Limits and Standard Error .....	25

Air Mass Back-trajectory Classification .....	26
Regional Rainfall Estimation and Validation.....	27
Data Analysis .....	28
Sample Storage Experiments .....	28
<b>RESULTS AND DISCUSSION .....</b>	<b>33</b>
Rainwater Chemistry.....	33
Correlation Patterns.....	38
Spatial Variability .....	40
Temporal Variability.....	48
Air Mass Back-trajectories.....	58
Particle Dry Deposition.....	64
Gas-phase Ammonia .....	70
Deposition to the Cape Fear River Estuary (CFRE) .....	72
Hurricane Isabel .....	81
<b>SUMMARY AND CONCLUSIONS .....</b>	<b>91</b>
<b>REREFENCES.....</b>	<b>95</b>

## ABSTRACT

Concentrations of  $\text{NH}_x$ ,  $\text{NO}_3^-$ , free amino acids, total and organic nitrogen, and inorganic anions were determined for 78 rain events between September 1, 2002 and August 31, 2003, on the campus of the University of North Carolina at Wilmington in southeastern North Carolina.

The majority of N in Wilmington rain (78%) is inorganic, occurring as  $\text{NO}_3^-$  and  $\text{NH}_x$  in approximately equal proportions. Free amino acids make up a small portion of ON (11%). Correlation analysis and back trajectory analysis indicate that regional sources, rather than local emissions, determine the concentrations of inorganic N in UNCW rainwater and particle dry deposition.  $\text{NO}_3^-$  concentration in rainwater at UNCW has decreased from 1990 to the present while wet deposition increased due to increased rainfall and possibly increased emissions from growing population and expanding industry in North Carolina.

Wet and dry deposition of  $\text{NH}_x$  are respectively 53% and 26% higher than a decade ago reflecting an increase in regional and possibly local emissions. Similar temporal patterns in are seen at UNCW and the NADP monitored sites with the greatest increase in Clinton, NC, where  $\text{NH}_x$  concentrations and depositions have increased 58% and 107% respectively. Concentrations of  $\text{H}^+$  and major N analytes, with the exception of ON, vary significantly as a function of air mass origin with major increases in analytes correlating with locations of known anthropogenic sources. Seasonal and diurnal influences have a significant impact on the concentrations of  $\text{H}^+$  and N analytes in UNCW rainwater with significant concentration maximums in the spring and significantly lower concentrations from 6:00AM to 10:00PM.

Direct atmospheric deposition is not a major source of bioavailable nitrogen to the Cape Fear River Estuary. The average total daily  $\text{NH}_x$  and  $\text{NO}_3^-$  dry depositions were small in comparison to their total amounts in the CFRE. Wet depositions of  $\text{NH}_x$  reached 20% for a single event with

an average per event deposition equivalent to 1.3% of  $\text{NH}_x$  in the CFRE. Dry deposition accounts for 17% of inorganic N deposition to the CFRE; though it is possibly underestimated in this study.

## ACKNOWLEDGMENTS

Special thanks to my advisors – Drs. Joan Willey, Robert Kieber, and Doug Gamble. Myself being new to the laboratory environment and pursuant of such a potentially broad project, they gave me the freedom to do things the way I determined was best, the endless patience to let me figure out on my own whether or not my decisions were correct, the resources for continued attempts, and ultimately the self-respect that only those factors can entrain.

Thanks to MACRL lab for the continued effort and depth of resolve that is absolutely necessary when your work (and often daily life) is governed by the weather. “Schedule” has a new meaning to me. As well, I thank them for the “smooth-ship” that lets work get done without unbearable speed bumps.

Thanks to Dr. Robert Whitehead for the time and energy put into total nitrogen analysis. Thanks to Dr. Joanne Halls for providing the way and means to visualize my endless streams of numbers. To Dr. Larry Cahoon for data, info, scoops, support, and chats (and equipment that you never knew I had borrowed. It is all back now). To Richard Lancaster for his tools, time, space, and patience. To Allan Randall and the UNCW Computer Science Department for letting me onto TORVALDS, giving me space, technical assistance, and the resources to out-do myself. To David Glenn, Drs. Dargan Friersen and James Blum, and the UNCW Department of Mathematics and Statistics for all you help, coordination, knowledge, and resources. Thanks to Dr. Ward because he is the closest thing to Santa Claus a graduate student can get. J.J. Gourley and the QPESUMS group at the NOAA-NSSL was especially helpful with getting me set up and moving with a tool that will prove to be exceptionally useful in studies of this sort.

## DEDICATION

This thesis is dedicated to Dr. Tom Hopkins at NCSU for opening big doors. Also, to my parents, and Emily, Gray and Stephen for being there to make sure I made it through them OK. To Piero, Nixon, Antonio, the CEAB, ICTP for strength. To Fiona, Uli, Hugh, Marco, Tafo, Mastro di Casa, Crispo, Abu, Marcus, and Jonas for being on the other side of the doors when I went through. And God for the endless opportunities to see how incredible the universe really is through people, places, and events, good and bad, in the past present and future.

## LIST OF TABLES

Table	Page
1.	Volume-weighted average concentration and standard deviations of pH, and N-species in rainwater collected at Wilmington, NC between September 1, 2002 and August 31, 2003. The %NH <sub>x</sub> and %ON are relative to TN concentration, and n is the number of samples included in their respective calculations. .... 33
2.	Volume-weighted average concentrations of SO <sub>4</sub> <sup>2-</sup> , NSS, H <sub>2</sub> O <sub>2</sub> , and DOC in rainwater collected at Wilmington, NC between September 1, 2002 and August 31, 2003 ..... 34
3.	Volume-weighted average concentrations of ON, TN, and AA from the present study and for various geographic locations. %ON value is in comparison to TN. The asterisk (*) values represent coastal sampling sites. .... 35
4.	Correlation matrix for rainwater components. Results are Pearson correlation coefficients for natural log-transformed concentration data for events during the sampling period. Bold values indicate significance at 95% C.I. .... 37
5.	Rainwater VWA concentrations of NH <sub>x</sub> , NO <sub>3</sub> <sup>-</sup> , SO <sub>4</sub> <sup>2-</sup> (NSS), and H <sup>+</sup> , as well as rainfall amounts from UNCW, and the NADP sampling sites at Clinton, Lewiston, and Jordan Creek. The 1990 values from UNCW are averages of rainwater collected from 1988 to 1990 taken from Willey and Kiefer (1993) ..... 41
6.	Comparisons of VWA concentrations for rainfall collected at UNCW for the periods of 1988 through 1990 and September 1, 2002 through August 31, 2003 and the present change between the two periods..... 49
7.	Total potential and actual wet deposition of NH <sub>x</sub> (tons per year) at UNCW and Clinton, NC ..... 50
8.	Change in VWA concentration (Δ) of H <sup>+</sup> , NH <sub>x</sub> , NO <sub>3</sub> <sup>-</sup> , NSS, and SO <sub>4</sub> <sup>2-</sup> based on values given in Table 1 for UNCW, Clinton, Jordan Creek, and Lewiston NADP sampling sites. The values for Finley Farm and Kennedy Space Center (KSC) are from the NADP datasets representing the same time periods as those presented in table 1. .... 52
9.	Total rain, rainfall per event, and VWA concentrations, by trajectory category, of H <sup>+</sup> and N analytes in rainwater at UNCW for the current sampling period. Red and blue values are maximum and minimum values respectively. Statistically significant values (p<0.05) based on a Student's T-test are marked with an asterisk..... 60
10.	Average overall and seasonal particle dry deposition in μmoles m <sup>-2</sup> d <sup>-1</sup> measured at UNCW between August 21, 2002 and August 21, 2003. .... 62

11.	Particle dry deposition of $\text{NH}_x$ and $\text{NO}_3^-$ in $\mu\text{moles m}^{-2} \text{d}^{-1}$ for UNCW and for various geographic locations.....	65
12.	Particle dry deposition ( $\text{mmoles m}^{-2} \text{y}^{-1}$ ) and %Change of $\text{NH}_x$ , $\text{NO}_3^-$ , $\text{SO}_4^{2-}$ , NSSm and $\text{Cl}^-$ at UNCW for the periods from 1988 through 1990 and between August 2002 and August 2003. ....	66
13.	A comparison of $\text{NH}_3(\text{g})$ measurements (ppbv) made at UNCW and different geographical locations in N. America.....	68
14.	Wet, dry, and total (wet + dry) deposition of $\text{NH}_x$ , $\text{NO}_3^-$ , AA, and TN to the CFRE. The %Dry values are calculated relative to total depositions.....	72
15.	Potential change in concentration of $\text{NH}_x$ , $\text{NO}_3^-$ and TN for the entire CFRE due to wet, dry, and total direct atmospheric depositions ( $\mu\text{M d}^{-1}$ ). Percentages are calculated relative to 2002 average surface concentrations of each analyte based on data from the Lower Cape Fear River Program (LCFRP). ....	77

## LIST OF FIGURES

Figure .....	Page
1. Concentrations of $\text{NO}_3^-$ and $\text{NH}_x$ in the CFRE from M61 to M18 for the period from 1995 to 2002 based on data from the Lower Cape Fear River Program (LCFRP). The lines represent simple regressions of the plotted data.....	3
2. Annual volume-weighted average rainwater concentrations of $\text{NH}_x$ , $\text{NO}_3^-$ and $\text{SO}_4^{2-}$ measured at Clinton, NC from 1988 to 2002 (NADP-NC35). The lines represent simple regressions of the plotted data. ....	6
3. Annual volume-weighted average rainwater concentrations of $\text{NH}_x$ , $\text{NO}_3^-$ and $\text{SO}_4^{2-}$ measured at Lewiston, NC from 1988 to 2002 (NADP-NC03). The lines represent simple regressions of the plotted data. ....	7
4. Annual volume-weighted average rainwater concentrations of $\text{NH}_x$ , $\text{NO}_3^-$ and $\text{SO}_4^{2-}$ measured at Jordan Creek, NC from 1988 to 2002 (NADP-NC36). The lines represent simple regressions of the plotted data. ....	8
5. North Carolina map indicating the location of NADP collection sites. Shaded regions are counties that experienced extensive growth in livestock farming during the 1990's. ....	9
6. Diagram of the CFRE indicating locations of water column sampling sites used in this study. ....	18
7. Replicate profiles of fluorescence signals (in arbitrary fluorescence units) versus time for 1, 2, and 4 $\mu\text{M}$ glycine standards. ....	21
8. Results from a before and after test of sample $\text{NH}_x$ stability for samples frozen at $-20^\circ\text{C}$ . Results are grouped by number of days the samples were stored frozen.....	29
9. Results from repetitive, same-bottle $\text{NH}_x$ of 7 samples. ....	30
10. Plot of rate of $\text{NH}_x$ loss versus initial sample concentration for results from analyses of samples stored in separate bottles. Line is a simple regression of plotted data. ....	31
11. Map of North and South Carolina $\text{NH}_3$ emissions by county based on 1999 EPA-NEI data. The general locations of the NADP and UNCE collection sites are indicated by arrows. White coloring represents data only in North and South Carolina.....	43
12. Map of North and South Carolina $\text{NO}_x$ emissions by county based on 1999 EPA-NEI data. The general locations of the NADP and UNCE collection sites are indicated by arrows. White coloring represents data only in North and South Carolina.....	44

13.	Map of North and South Carolina SO <sub>x</sub> emissions by county based on 1999 EPA-NEI data. The general locations of the NADP and UNCE collection sites are indicated by arrows. White coloring represents data only in North and South Carolina. ....	45
14.	Seasonal averages from VWA concentrations in rainwater at UNCW for the current study (163 cm rainfall) and from 1988-1990 in Willey and Kiefer (1993) (120 cm rainfall) ....	53
15.	Seasonal VWA concentrations of H <sup>+</sup> , NH <sub>x</sub> , NO <sub>3</sub> <sup>-</sup> , AA, ON and TN at UNCW. ....	54
16.	Diurnal VWA concentrations of H <sup>+</sup> , NH <sub>x</sub> , NO <sub>3</sub> <sup>-</sup> , AA, ON and TN at UNCW. ....	56
17.	Plots of air mass back-trajectories calculated from the HYSPLIT model grouped by trajectory classification. ....	59
18.	NH <sub>3</sub> (g) (ppbv) measured by condensate collection at UNCW throughout the day of July 29, 2003. ....	70
19.	CFRE water column measurements of NH <sub>x</sub> from M18, M35, M42, M54, and M61 from 0 to 5 meters depth (based on measurements of the entire water column) taken on April 22, 2003. C <sub>sfc</sub> is the surface water concentration of NH <sub>x</sub> (μM) calculated from NH <sub>3</sub> (g) measurements taken over the CFRE on the same day. ....	75
20.	Results from sequential samples taken at UNCW during hurricane Isabel (September 18, 2003): a) NH <sub>x</sub> concentration and Sequential rainfall amounts, b) AA concentration and sequential rainfall amounts, c) H <sup>+</sup> concentrations, d) NH <sub>x</sub> wet deposition amounts per sequential sample, and e) AA wet deposition amounts per sequential sample. ....	81
21.	Concentrations and depositions of Cl <sup>-</sup> , NO <sub>3</sub> <sup>-</sup> , and NSS in sequential samples taken at UNCW during hurricane Isabel (September 18, 2003). Bars in the Cl <sup>-</sup> concentration plot represent rainfall amounts for individual sequential samples. ....	82
22.	Plots of back trajectories (calculated using the HYSPLIT model) and interpolated rainfall intensity field for hurricane Isabel sequential samples. Rainfall intensity (mm/h) is calculated from values given at each trajectory point. ....	84
23.	Plots of back trajectories (calculated using the HYSPLIT model) and interpolated wind intensity field for hurricane Isabel sequential samples. Wind intensity (arbitrary wind units) is calculated from the spatial displacement between model generated trajectory points. ....	85

## INTRODUCTION

The Cape Fear River basin is the largest river basin in North Carolina draining approximately 23,700 km<sup>2</sup> from the Piedmont through the Coastal Plain. It contains over 25% of the state's population, many of its largest industries, and one of its two major ports (Wilmington). Because of a rapidly growing population, the Cape Fear estuary is under increasing pressure from residential, agricultural, and industrial development. Detrimental impacts of this increased anthropogenic activity, mainly through point source pollution from municipal and industrial discharges, hog lagoon spills, and river dredging; and from non-point sources including urban and agricultural runoff and atmospheric deposition, have been documented for the Cape Fear system. These impacts include episodes of hypoxia (reduced oxygen levels), increased turbidity, and eutrophication in certain portions of the estuary (Mallin et al., 1996, 1998; Cahoon et al., 1999). The potential for these inputs to continue is high, given the expanding development projected for the lower Cape Fear region within the next ten years.

One of the most alarming aspects of increasing development within the Cape Fear watershed is the increasing input of nutrients in the estuary. Nutrient enrichment (eutrophication) in estuarine waters can engender a number of water quality problems. One of the most direct environmental impacts of eutrophication is the overgrowth of algae and other phytoplankton species whose eventual death and decomposition lead to increased consumption of oxygen in the water column and surface sediments. This oxygen depletion leads to subsequent hypoxic (low oxygen) or anoxic (no oxygen) conditions, which have been observed at times in many of the state's major estuaries including the Cape Fear River. A second problem associated with eutrophication is the potential for changes in biotic community composition and structure that are dependent upon the concentrations and types of nutrient species available. A drastic example

of the type of changes that may result from eutrophication in some locales is harmful algal blooms, which pose threats to higher trophic levels including important fisheries and ultimately, humans (e.g., Paerl, 1988; Burkholder et al., 1995).

Nitrogen is a nutrient of particular concern for the Cape Fear River Estuary (CFRE) since most of the regions coastal and estuarine ecosystems seem to be sensitive to N-loading. Average concentrations of  $\text{NH}_x$  (considered for the duration of this document as  $\text{NH}_4^+ + \text{NH}_3$  in aqueous form) in the Cape Fear are increasing rapidly and have almost doubled in the last six years while  $\text{NO}_3^-$  concentrations show signs of a very slight decline (Figure 1). Also, total nitrogen loading to the CFRE has increased considerably over the past 10-15 years due to the proliferation of intensive agricultural operations, as well as increasing municipal and industrial development. The importance of the individual pathways by which N is put into the CFRE is not known. The three rivers (Cape Fear around Navassa, Black and Northeast Cape Fear) that feed into the CFRE are all lower in  $\text{NH}_x$  concentrations than the estuarine waters (Mallin et al., 2000), so there must be an  $\text{NH}_x$  source in addition to river input. Ammonium is a key species for understanding the cycling of nitrogen in estuarine waters because it is the dominant nitrogen species that fluxes from bottom sediments. As well, there are significant levels of  $\text{NO}_3^-$  input into the CFRE from the atmosphere and surface runoff. Ammonium appears to be the dominant form of inorganic nitrogen in the CFRE during hurricane flooding, probably because the lowered oxygen concentrations in the estuary during these events favor  $\text{NH}_x$  over  $\text{NO}_3^-$  and  $\text{NO}_2^-$  (Mallin et al., 1999c, 2000).

Ammonium and nitrate are of critical importance for understanding estuarine biogeochemistry. Ammonia, free amino acids, and other reduced forms of nitrogen are believed to be preferred by phytoplankton (Gilbert et al., 1982; Paasche and Kristiansen, 1982; Pennock,

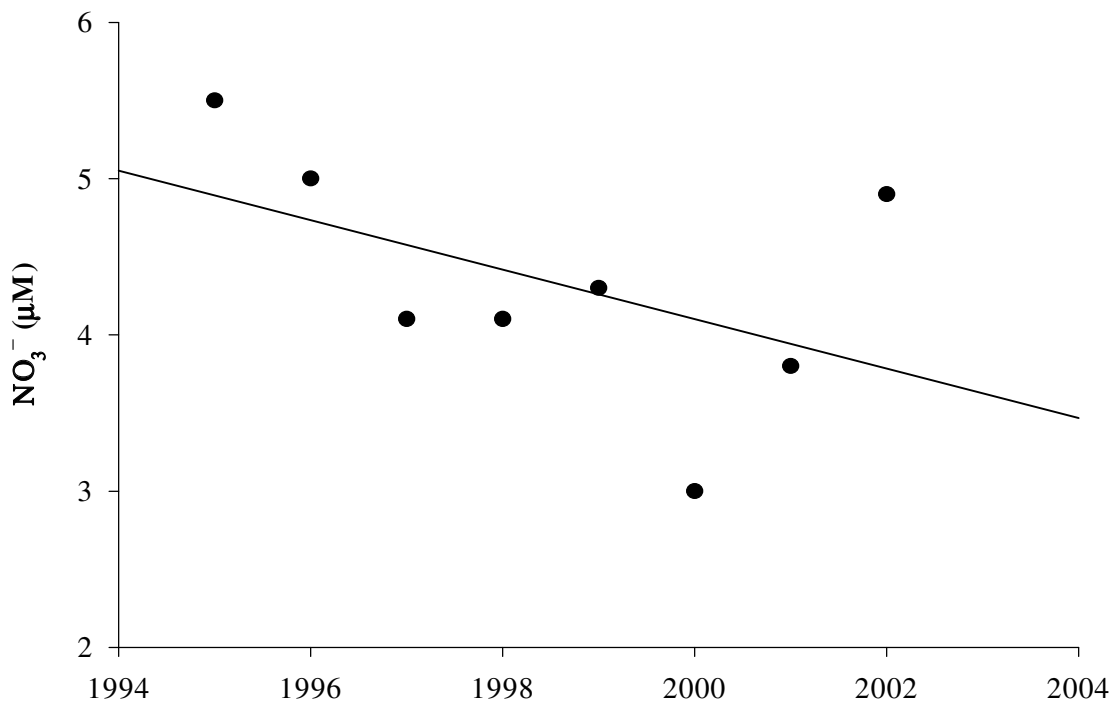
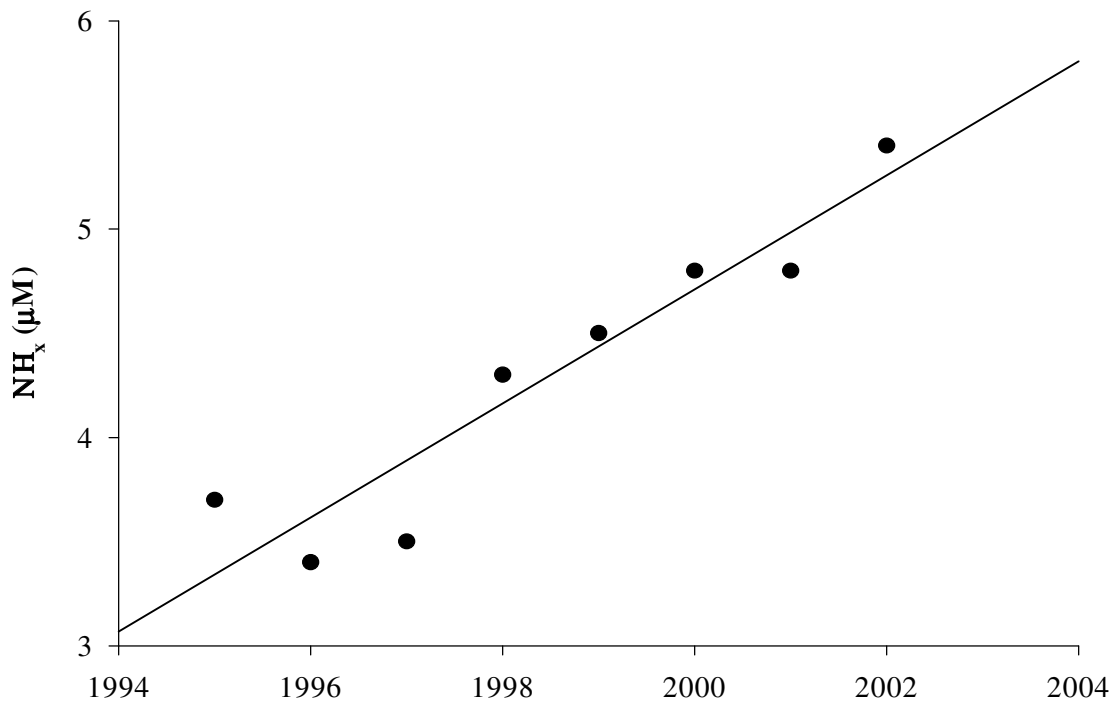


Figure 1. Concentrations of  $\text{NO}_3^-$  and  $\text{NH}_x$  in the CFRE from M61 to M18 for the period from 1995 to 2002 based on data from the Lower Cape Fear River Program (LCFRP). The lines represent simple regressions of plotted data.

1987) while nitrate is the dominant form of dissolved inorganic nitrogen in the CFRE. In addition, ammonium plays an important role in maintaining bacterial productivity by processes such as nitrification (Wofsy et al., 1981; Wofsy, 1983; Lipshultz et al., 1985; Pennock, 1987). Such bacterial processes may be particularly important in the Cape Fear estuary, which contains very high levels of dissolved organic carbon, a substrate for bacterial growth, yet relatively low phytoplankton productivity typically due to light limitation imposed by turbidity (Mallin et al., 1999a).

It is necessary to approach the issue from a systems standpoint. As such, various possible sources and pathways of N input must be considered: these include atmospheric deposition of ammonia released from waste lagoons in concentrated animal operations (Walker et al., 2000), industrial and municipal point and non-point sources (e.g., outfalls, wastewater treatment plants, septic systems, runoff), release from resuspended sediments, and fluxes from bottom sediments. The purpose of this project will focus on the atmospheric component as a source of nitrogen in the CFRE.

The deposition of atmospheric nitrogen may be responsible for a significant portion of nitrogen input into the CFRE due to its relative close proximity to high  $\text{NH}_3$  emissions from animal operations in southeastern North Carolina. As a result of the fourfold increase in swine population during the 1990's, it is estimated that emissions from swine operations represent approximately 48% of all North Carolina  $\text{NH}_3$  emissions, and approximately 21% of total atmospheric nitrogen (Mallin et. al., 2000; Walker et al., 2000). According to the EPA, nearly half of all nitrate emissions in the US are from automobiles. Figures 2, 3 and 4 present trends average annual rainfall concentrations of  $\text{SO}_4^{2-}$ ,  $\text{NO}_3^-$ , and  $\text{NH}_x$  for the period between 1988 and 2002 at Clinton, Lewiston, and Jordan Creek in eastern North Carolina monitored by the

National Atmospheric Deposition Program (NADP). These trends directly reflect trends in regional emissions (EPA, 2002). The impact of increasing agricultural development on atmospheric nitrogen is evidenced by ammonia deposition measured at all three NADP sites – most remarkably in Clinton. There is a steady increasing trend in  $\text{NH}_x$  deposition since 1989 when explosive agricultural growth occurred in this region of the state. Figure 5 shows the counties where this growth is most concentrated and the location of the NADP monitored sites. Less pronounced increases in ammonia deposition were observed at Lewiston and Jordan Creek, North Carolina primarily because these regions did not undergo similar increases in agricultural development. Atmospheric deposition of nitrate showed a slight decreasing trend at all three sites indicating increasing agricultural processes are primarily influencing ammonia deposition. As the population in Wilmington and surrounding areas continues to grow, the impact of increased traffic emissions in the immediate region could serve to reverse the decreasing trend in atmospheric  $\text{NO}_3^-$  deposition seen in the southeast over the past decade.

These trends in atmospheric deposition of ammonia and nitrate at Clinton closely track trends in water column ammonia and nitrate measured in the CFRE by the LCFRP suggesting atmospheric processes may be influencing water column concentrations.

The atmospheric behavior of these nitrogen compounds requires that they all be considered in an investigation of atmospheric deposition. Atmospheric nitrate is formed by the oxidation of  $\text{NO}$  and  $\text{NO}_2$ , emitted from fossil fuel combustion, to form nitric acid ( $\text{HNO}_3$ ). Sulfate is formed by the oxidized emissions of  $\text{SO}_2$  from power plants to form sulfuric acid ( $\text{H}_2\text{SO}_4$ ). In vapor forms,  $\text{HNO}_3$  and  $\text{H}_2\text{SO}_4$  have short lifetimes in the atmosphere (Metzger et al., 2002). Ammonia is emitted from numerous sources though mainly from agriculture. Atmospheric ammonia is lost

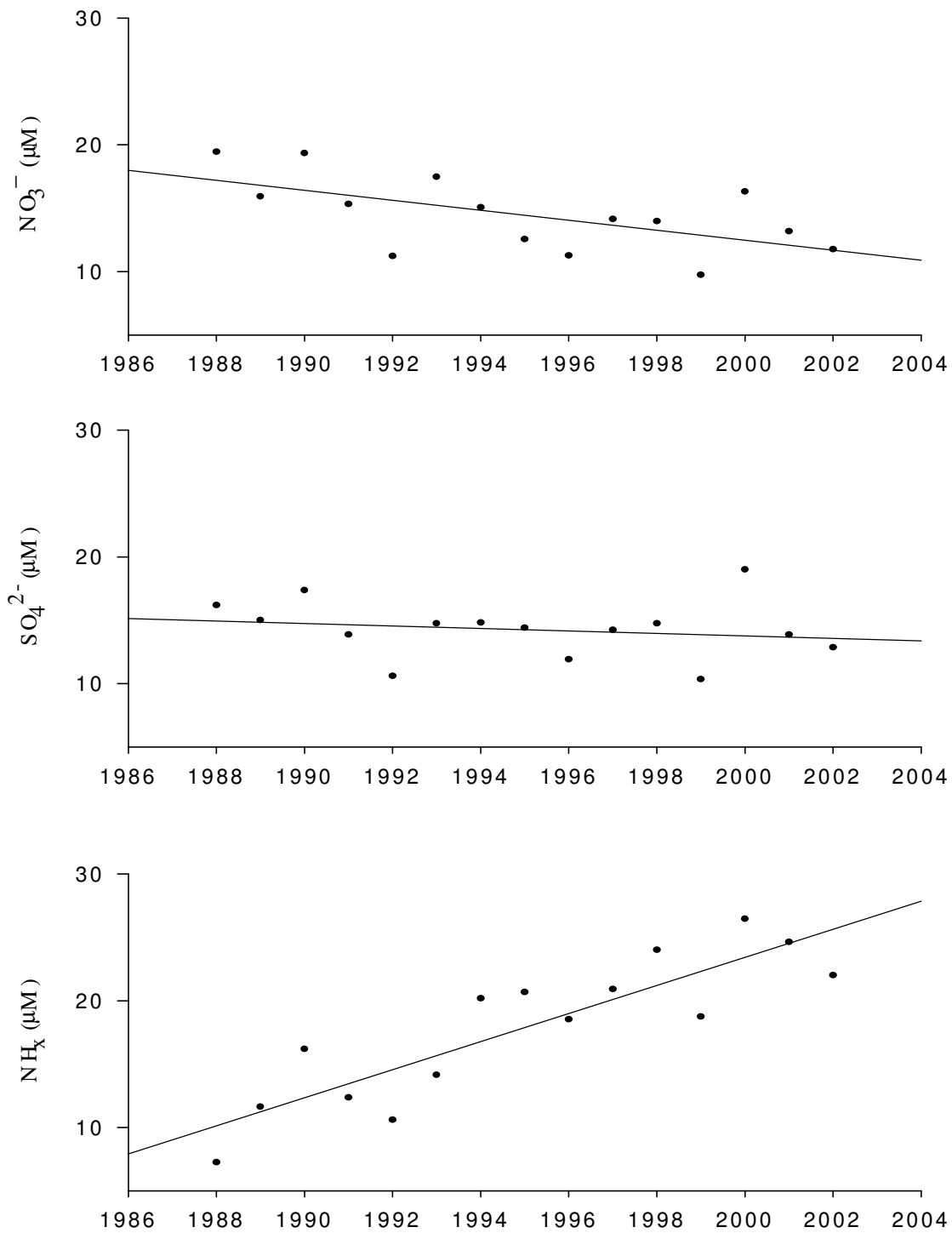


Figure 2. Annual volume-weighted average rainwater concentrations of  $\text{NH}_x$ ,  $\text{NO}_3^-$ , and  $\text{SO}_4^{2-}$  measured at Clinton, NC from 1988 to 2002 (NADP-NC35) based on data collected by the NADP. The lines represent simple regressions of the plotted data.

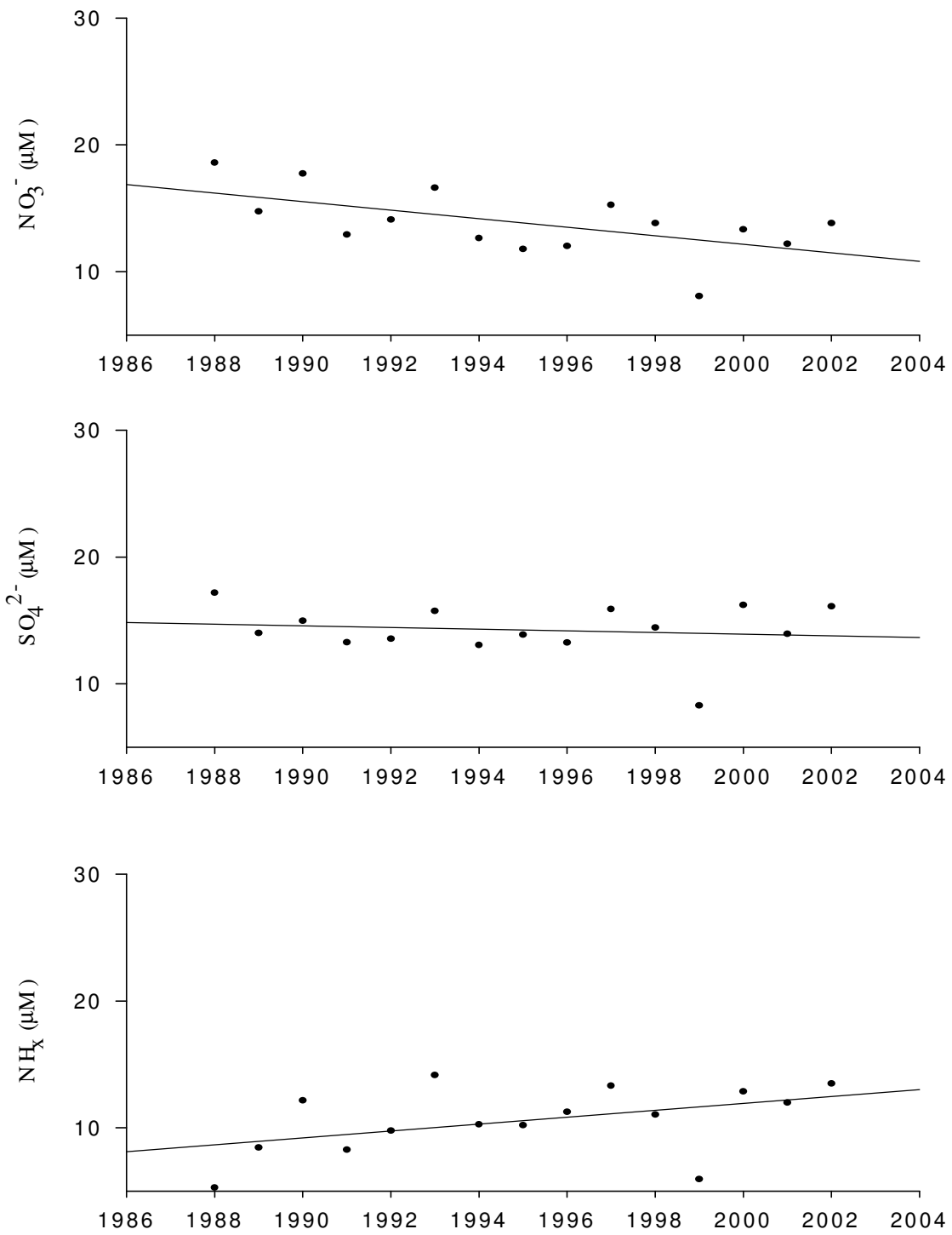


Figure 3. Annual volume-weighted average rainwater concentrations of  $\text{NH}_x$ ,  $\text{NO}_3^-$ , and  $\text{SO}_4^{2-}$  measured at Lewiston, NC from 1988 to 2002 (NADP-NC03) based on data collected by the NADP. The lines represent simple regressions of the plotted data.

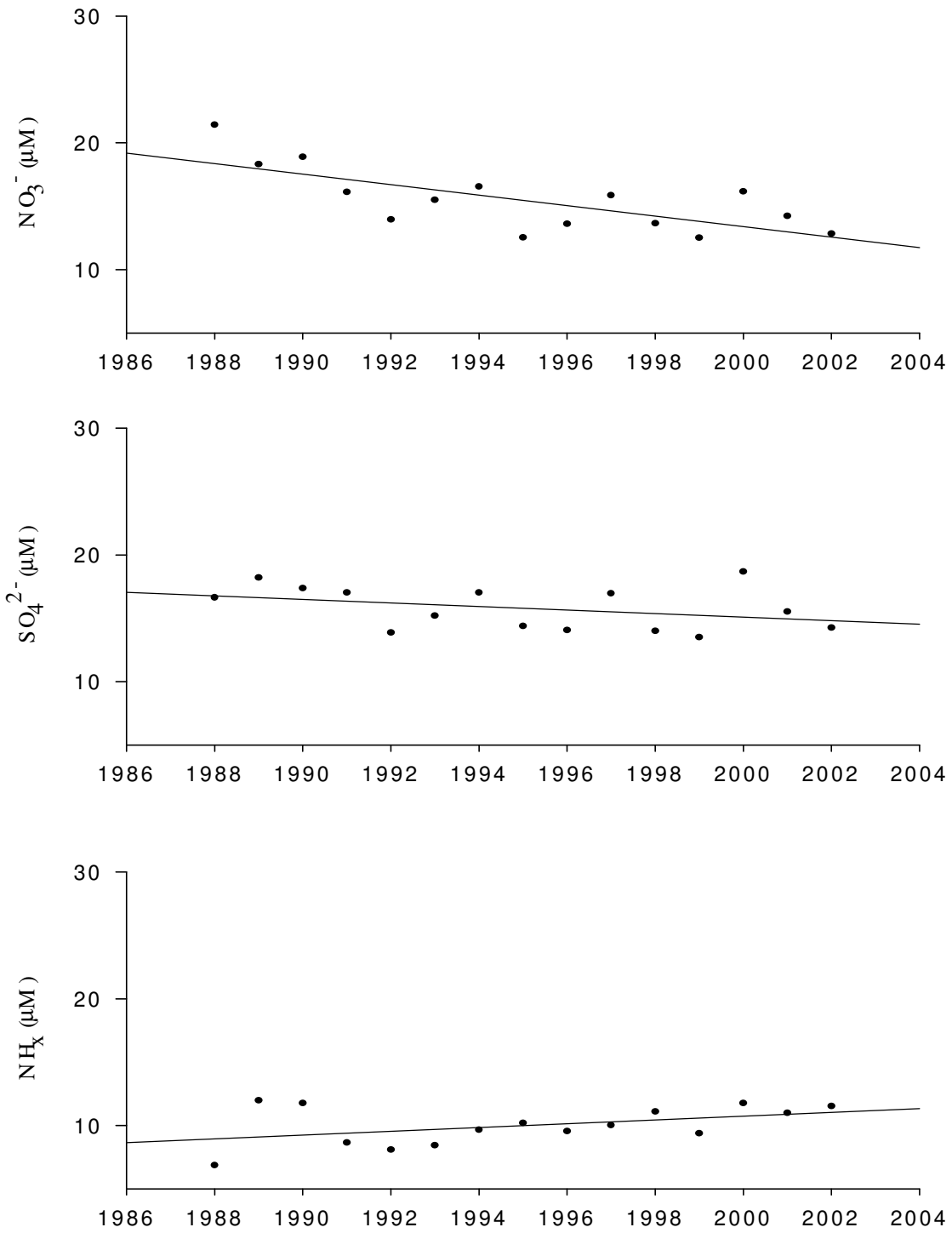


Figure 4. Annual volume-weighted average rainwater concentrations of  $\text{NH}_x$ ,  $\text{NO}_3^-$ , and  $\text{SO}_4^{2-}$  measured at Jordan Creek, NC from 1988 to 2002 (NADP-NC36) based on data collected by the NADP. The lines represent simple regressions of the plotted data.

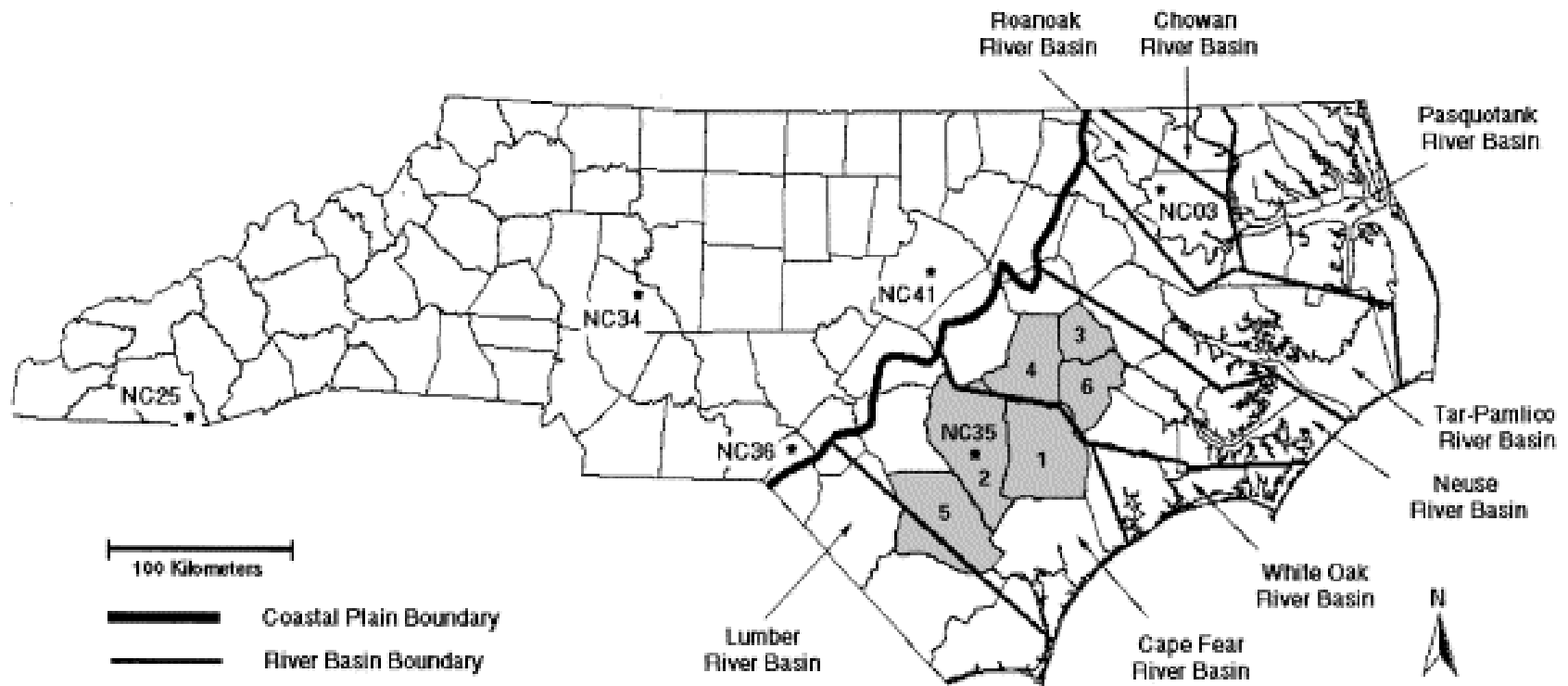


Figure 5. North Carolina map indicating the location of NADP collection sites. Shaded regions are counties that experienced extensive growth in livestock farming during the 1990's.

via deposition and conversion to ammonium very close to its source with an atmospheric residence time of 1 to 5 days (Warneck, 1988). Model calculations estimate that up to 46% of ammonia is deposited within 50 km of its source (Asman and van Jaarsveld, 1992). Dragosits et al. (2002) determined from modeled results that high  $\text{NH}_3(\text{g})$  emissions were not distinguishable from background concentrations beyond 2.5 km of the source.

The rapid conversion of ammonia to ammonium by reaction with, and neutralization of, acids in the atmosphere - primarily  $\text{HNO}_3$ , and  $\text{H}_2\text{SO}_4$  - forms aerosol particles with relatively low deposition velocities. This enhances transport lifetime to between 1 and 15 days for each of the compounds (Lawrence, 2000; Aneja, 2000). As a result, high regional emissions of  $\text{NH}_3$ ,  $\text{NO}_x$  ( $\text{NO} + \text{NO}_2 + \text{NO}_3^-$ ) and  $\text{SO}_x$  ( $\text{SO}_2 + \text{SO}_4^{2-}$ ) have the potential to impact a relatively large geographic area. In North Carolina, 82% of all  $\text{NH}_3$  emissions are the result of the livestock industry mainly concentrated in the eastern portion of the state (Aneja et al., 2001). Emissions from this region have been shown to impact precipitation concentrations up to 80 km away (Walker et al, 2000); while Wilmington is approximately 50 km from this region. As well, the transport of  $\text{NO}_x$  and  $\text{SO}_x$  emissions in the eastern US over long distances is well documented (Lawrence et al., 2000).

Nitrogen loading from the atmosphere includes wet deposition by precipitation and fog, and gaseous and particle dry deposition. They are highly susceptible to specific meteorological conditions including temperature, wind speed, relative humidity, storm type and source, vertical mixing, and the depth of the atmospheric boundary layer (Aneja et.al., 2001).

Wet deposition is the process by which the chemical constituents in the atmosphere are removed by precipitation. The incorporation of aerosols and gases into precipitation consists of both in-cloud and below-cloud scavenging mechanisms (Walker, 2000). In-cloud processes are

generally believed to be the predominant mechanism for removal by precipitation though below-cloud scavenging by adsorption of aerosols onto falling raindrops can be significant (Asman, 1995). The solubility of gases and particulates, for the most part, determines the efficiency of wet removal processes (Pryor and Barthelmie, 2000).

Dry deposition is the transfer of particles and gases to surfaces via air motions and gravitational settling. The flux, to a surface, of dry deposited material can generally be calculated from

$$F_i = v_d \cdot C_i$$

where  $C_i$  is the atmospheric concentration of species  $i$  and  $v_d$  is the deposition rate (deposition velocity). Deposition velocity can be computed from the inverse sum of aerodynamic, viscous sub-layer, and surface resistances that incorporate gravitational settling for larger particle sizes (Pryor and Barthelmie, 2000; Wesely and Hicks, 2000). It is a function of surface type and roughness, wind speed, atmospheric stability, chemical species, and particle size thus making dry deposition very hard to determine for large areas.

There is generally a widespread size distribution of atmospheric particles depending on a number of factors including concentration and type of chemical species, relative humidity, and temperature. In the case of deposition to a water surface, it is hypothesized that the efficiency is dramatically increased for moderate and highly hygroscopic chemicals (Pryor et al., 1998; Slinn and Slinn, 1980). Near the water surface, a much higher relative humidity will enhance the condensation of water vapor onto these hygroscopic particles increasing their size and the effect of gravitational settling (versus diffusive transport (Brownian motion)). Under normal conditions, though, N-aerosols exist in a bimodal size distribution consisting of accumulation mode (0.1 to 1  $\mu\text{m}$  diameter) and coarse mode (>1  $\mu\text{m}$  diameter) though the exact partitioning

process is not well known (Pryor and Sorensen, 2002; Raes et al., 2000; Zhuang and Chan, 1997).

Gas-phase deposition calculations generally follow those of particle dry deposition (Wesely and Hicks, 2000). Though, in the case of deposition to water surfaces, the solubility (generally based on Henry's law calculations) of the species in question dominates the process (Sorensen et al., 2003). Many methods of direct dry deposition measurement to a surrogate surface, though, do not sample gasses (Shahin et al., 1999; Dasch, 1985). As well, the small-scale variability of  $\text{HNO}_3$ ,  $\text{NH}_3$ , and  $\text{H}_2\text{SO}_4$  undermines the validity of regional calculations based on local measurements.

This study attempts to determine the impact of atmospheric nitrogen deposition on the nutrient load of the CFRE. As well, temporal (long-term, seasonal, and diurnal) and spatial trends in wet and dry deposition of nitrogen species ( $\text{NH}_x$ ,  $\text{NO}_3^-$ ,  $\text{ON}$ ), sulfate, rainfall acidity, and gaseous ammonia at a sampling site on the campus of the University of North Carolina at Wilmington are addressed.

## METHODS

### Reagents and Standards

The working reagents (WR) used for  $\text{NH}_x$  and free amino acid analysis were reagent grade materials obtained from Sigma Chemical Company (St. Louis, MO, USA) unless otherwise indicated. All standards were prepared from reagent grade materials. All deionized water was made using an ultra-pure Milli Q water system (18.2 M $\Omega$  resistance) (Millipore, Bedford, MA, USA).

A 240  $\mu\text{M}$   $\text{NH}_4\text{Cl}$  standard is made by diluting 120  $\mu\text{L}$  of 0.5 M  $\text{NH}_4\text{Cl}$  solution to 250 mL in deionized water. For  $\text{NH}_x$  working reagent, a borate buffer is made by dissolving 80g of sodium borate ( $\text{Na}_2\text{B}_4\text{O}_7 \cdot 10\text{H}_2\text{O}$ ) in 2 L of deionized water. 2 g of sodium sulfite ( $\text{NaSO}_2$ ) was added to 250 mL of deionized water and allowed to dissolve. Four grams of OPA (o-Phthaldialdehyde,  $\text{C}_8\text{H}_6\text{O}_2$ ) are dissolved in 100 mL of HPLC grade acetonitrile obtained from Fisher Scientific (Fair Lawn, NJ). OPA is light sensitive and was prepared and stored in the dark. To complete the working reagent, 100 mL of the OPA solution, and 10 mL of sodium sulfite solution are added to 2 L of borate buffer and mixed for five minutes. The complete reagent is stored in a large HDPE bottle covered with aluminum foil to eliminate light degradation. It can be used after 24 h and is stable for up to three months when stored at room temperature (Holmes, 1999).

A 100  $\mu\text{M}$  glycein standard is made by diluting 1 mL of a 10 mM glycein stock solution to 100 mL with deionized water. The working reagent used in AA analysis is prepared with a 0.4 M borate buffer made by dissolving 24.7 g of sodium borate in 2 L of deionized water. The pH of the buffer is adjusted to  $9.5 \pm 0.02$  with 1N NaOH. 20 mg of OPA are dissolved in 20 mL of HPLC grade acetonitrile. This solution is prepared and stored in the dark. For the final reagent, 1 mL of electrophoresis grade 2-mercaptoethanol (Fisher Scientific) and 20 mL of the OPA solution are added to 400 mL of pH adjusted borate buffer and stirred for five minutes. The reagent can be used after 1 h and is good for 1 to 2 weeks when stored at  $5^\circ\text{C}$  in a 500 mL light-sealed HDPE bottle.

## Study Sites

### UNCW

The primary sample collection site is located in a large open area, approximately one-hectare,

within a turkey oak, long leaf pine, and wiregrass community, typical of inland coastal areas in southeastern North Carolina. This site ( $34^{\circ}13.9\text{N}$ ,  $77^{\circ}52.7\text{W}$ ) is on the UNCW campus, approximately 8.5 km from the Atlantic Ocean. Rain samples were collected on an event basis in Teflon bottles using an Aerochem-Metrics Automatic Wet-Dry Precipitation Collector. Collectors of this type isolate the collection apparatus until the onset and after the completion of a precipitation event.

#### Cape Fear River Estuary (CFRE)

The Cape Fear River Estuary (CFRE) is located between Brunswick and New Hanover Counties in SE North Carolina. The narrow estuary (generally 1 to 3 km wide) runs north to south for approximately 50 km from Wilmington at the northernmost portion to Southport and Cape Fear at the meeting point with the Atlantic Ocean.

#### Sample Collection and Storage

##### Rainwater

Rain samples were collected on an event basis in 2L trace metal clean Teflon bottles using an Aerochem-Metrics Automatic Wet-Dry Precipitation Collector. Collectors of this type isolate the collection apparatus until the onset and after the completion of a precipitation event. Rain samples were generally collected within 6 hours of the end of an event. In the case of overnight rain events, samples were collected before 8:00 AM the following morning and noted in the data log. Upon collection, rainwater was immediately analyzed for pH and hydrogen peroxide. Samples for inorganic anions, and N analysis were transferred to clean 125 mL HDPE bottles on-

site and stored frozen until analysis. Nearly all samples were analyzed for inorganic nitrogen and amino acids ( $\text{NO}_3^-$ ,  $\text{NH}_x$ , AA) within one week of collection.

#### Particle Dry Deposition

Dry deposition samples were collected using polyethylene collector surfaces located in the dry collection side of the ACM rain collector. This configuration isolates the dry collectors during precipitation events. Collection surfaces were soaked in ethanol, thoroughly scrubbed with a Citranox solution, rinsed with deionized water, and allowed to dry in a reverse-flow particle free hood before being deployed. Collection surfaces were tightly covered at all times during transfer to and from the collection site. Collection surfaces were left exposed for one to two week periods before analysis for particle content. Samples determined by visual inspection to be contaminated by birds or insects were discarded. Dry-deposited material was extracted by soaking the bottom of the buckets in 200 mL of deionized water for 24 hours. The subsequent water was then filtered through 0.2  $\mu\text{m}$  filters and stored frozen in HDPE bottles until analysis.

#### Gas-Phase Ammonia

Gas-phase ammonia measurements were made both at the UNCW collection site and on the Cape Fear River based on the condensate method described by Heffern et al. (1997). The method is valid for highly soluble gases while discriminating against particulates; therefore it is applicable for the measurement of ammonia gas (Farmer and Dawson, 1982). Water vapor is transported across a diffusive boundary layer onto a cooled surface and condensed out of the air. Highly soluble gases (assumed to be completely incorporated into the condensate) are transported across the boundary layer at a rate proportional to the ratio of the diffusion

coefficients of water vapor to the gas in question. Therefore, the concentration of the gas in the aqueous phase of the collected condensate is directly proportional to the ambient gas concentration and water vapor content of the air.

Condensate collections measuring  $\text{NH}_3$  gas were conducted on a weekly or biweekly basis for the duration at the UNCW rain collection site for the sample period. Since the collection method is based on water vapor diffusion gradient, there is a minimum temperature and humidity requirement below which samples cannot be collected. Though this minimum is not known, there are many instances during the fall and winter where the collector did not generate samples. As a result, there are few reported values for these portions of the sampling period for this study. The condensate collection apparatus used was the same as described in Heffern et al. (1997). Collections took place between 10:00AM and 3:00PM for duration of one hour. The collector was placed on the main platform of the rainwater collection site (about 1m high). Pre-sized ice cylinders made of DI water were inserted in 3 large, clean glass tubes and oriented above a funnel situated above three 60 mL Nalgene HDPE bottles. Mean values - based on measurements taken at the beginning and end of the sampling hour - of temperature, wind, and relative humidity were determined using a Kestrel 3000 hand-held weather station (Kestrelmeters, Minneapolis, MN, USA). Temperature readings are given to within  $1.0^\circ\text{C}$  and relative humidity to  $\pm 3\%$ . Upon completion, the tubes and funnels were removed from the collector and the bottles tightly capped. The samples were immediately returned to the lab and analyzed for  $\text{NH}_x$  within 30 minutes of completion of the experiment. Clean plastic gloves were worn for every portion of this experiment to aid in prevention of sample contamination.

CFRE Water Column and Atmosphere

In situ water column and atmospheric sampling was conducted on the RV Cape Fear. The RV Cape Fear is a 70 ft. diesel powered vessel maintained and operated by the Research Vessel Fleet at the UNCW Center for Marine Science. Cape Fear River surface, bottom and water column samples were taken using a Seabird SBE 32 H2O Bottle Carousel and SBE 33 Real Time Deck Unit (Sea-Bird Electronics, Bellvue, WA, USA) deployed at predetermined sampling sites. The sites are shown in Figure 6. Samples were filtered through Whatman 0.2  $\mu\text{m}$  filters (Whatman, Maidstone, Kent, UK) and analyzed for ammonium and free amino acids upon collection. For  $\text{NH}_3$  gas measurements conducted on the RV Cape Fear, a condensate collector was secured to the bow of the boat at an approximate height of 2 m above the water. The position of the boat was maintained to prevent contamination of condensate samples by the boat's exhaust fumes.  $\text{NH}_x$  analysis in condensate samples was performed on the boat immediately upon collection. All other procedures were followed as at the UNCW rain collection site.

## Analytical Methods

### $\text{NH}_x$ and Free Amino Acid Determination

$\text{NH}_x$  in all samples was determined using a modified version of a fluorometric method described by Holmes et al. (1999). The method is based on the reaction of o-phthaldialdehyde (OPA) with ammonia forming a fluorescent chromophore. OPA in the presence of sulfite blocks the fluorescent signal of free amino acids (Kerouel and Aminot, 1997). For free amino acid concentrations a modified version of the fluorometric technique described in Parsons et al. (1994) was used. OPA, in the presence of 2-mercaptoethanol, reacts with primary amines to form a fluorescent chromophore with free amino acids instead of ammonia.  $\text{NH}_x$  and AA were determined using the method of standard additions to eliminate analytical error due to matrix

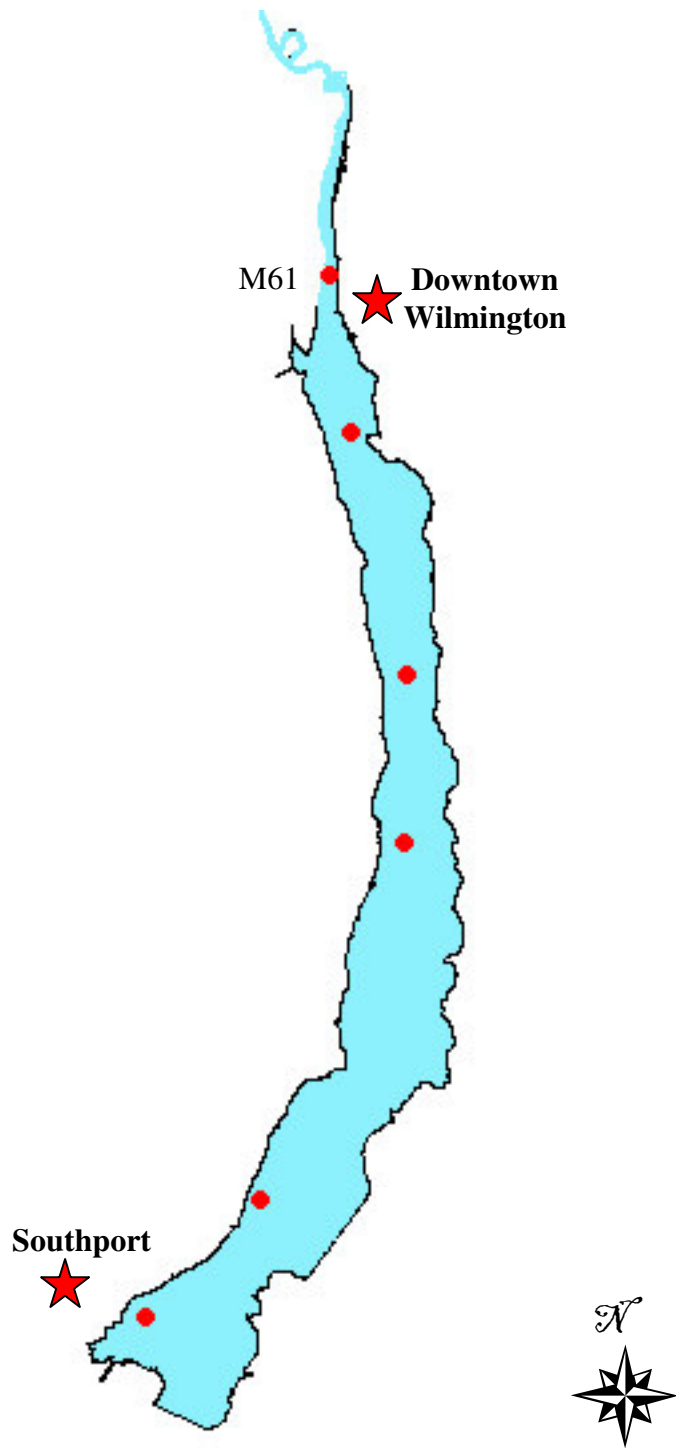


Figure 6. Diagram of the CFRE indicating locations of water column sampling sites used in this study.

effects. The addition of small volumes of an analyte at known concentrations will not significantly alter the overall matrix of a sample. Thus, the signal perturbation from the sample matrix is also generated for the calibration signal. In this case,

$$\frac{\Delta F}{F_{Sample}} = \frac{C_{SA}}{C_{Sample}}$$

where  $F_{sample}$  is the signal of a pure sample aliquot, and  $\Delta F$  is the difference between the signals of standard addition sample ( $F_{SA}$ ) and of the sample aliquot ( $F_{sample}$ ).  $C_{SA}$  is the standard addition concentration and  $C_{sample}$  is the sample concentration. Background fluorescence signal (BF) is subtracted from all actual recorded fluorescence signals (e.g.  $F_{SA} = F_{SA-actual} - BF$ ;  $F_{sample} = F_{sample-actual} - BF$ ). This corrects for fluorescence from the analytical reagent and particles in the sample. From the above relation, the sample concentration can be determined by

$$C_{sample} = \frac{(F_{SA} - F_{sample})}{F_{sample}} \cdot \frac{(C_{Std} \cdot V_{SA})}{(V_{Sample} + V_{SA})}$$

where  $C_{Std}$  is the concentration of the analytical standard,  $V_{SA}$  is the volume of the standard addition, and  $V_{sample}$  is the volume of the sample.

Fluorescence for  $NH_x$  and AA is measured on a Turner Designs Model 450 Fluorometer (Turner Designs, Sunnyvale CA, USA) with 360 nm excitation and 440 nm emission filters. For  $NH_x$  analysis, 1.5 mL sample aliquots are pipetted into six 8 mL Nalgene HDPE sample vials. 50, 100, and 200  $\mu$ L of 240  $\mu$ M  $NH_4Cl$  standard were added to three of the vials making 7.74, 15.0 and 28.2  $\mu$ M  $NH_4Cl$  standard solutions. 5 mL of WR was then added to all of the vials, which were allowed to incubate for 3 to 8 hours in the dark before fluorescence was measured. An additional 1.5 mL sample aliquot was pipetted into a seventh vial and set aside for determination of the background fluorescence.

For AA analysis, 2 mL sample aliquots are pipetted into six 8 mL Nalgene HDPE sample vials. Three additional vials are filled with 2 mL of deionized water to measure background fluorescence (BF). 100  $\mu$ L of the glycine standard is pipetted into three of the vials containing sample aliquots. Sample, standard addition, and BF vials are then filled with 2 mL of room temperature working reagent. The fluorescence is immediately recorded for the BF vials and after a short incubation period for the sample and standard addition vials. The duration of the incubation is the minimum time needed for a sample to reach peak fluorescence. To determine this, two standards each of 1, 2, and 4  $\mu$ M glycine were analyzed following the outlined procedures above. Figure 7 presents the results of these tests. The minimum time required for a sample to reach peak fluorescence was approximately 4 minutes.

#### Inorganic Anion Determination

Inorganic anions ( $\text{Cl}^-$ ,  $\text{NO}_2^-$ ,  $\text{NO}_3^-$ ,  $\text{SO}_4^{2-}$ ) were measured using ion-suppressed chromatography. Samples were analyzed using a Dionex CD25 Conductivity Detector/GP50 Gradient Pump system in conjunction with an AS14A/AG14A Analysis/Guard column and an ASRS – Ultra 4mm anion self-regenerating suppressor flow path. Samples and standards (200  $\mu$ L) are injected directly into the guard/analysis column. The conductivity of samples and standards is then measured above that of the carbonate/bicarbonate eluant solution (0.8M  $\text{Na}_2\text{CO}_3$  / 0.1M  $\text{NaHCO}_3$ ) at a flow rate of 1.00 mL/min and a suppressor current of 43 mV.

Standards of 1/20, 1/50, and 1/100 dilutions were prepared from a concentrated stock solution of 0.569 mM NaCl, 1.61 mM  $\text{KNO}_3$ , 1.05 mM  $\text{K}_2\text{SO}_4$ , and 0.193 mM  $\text{NaNO}_2$ . Sample concentrations were calculated from a linear regression standard curve of concentration as a function of peak area. All calculations are performed automatically on Dionex Peaknet v 6.4

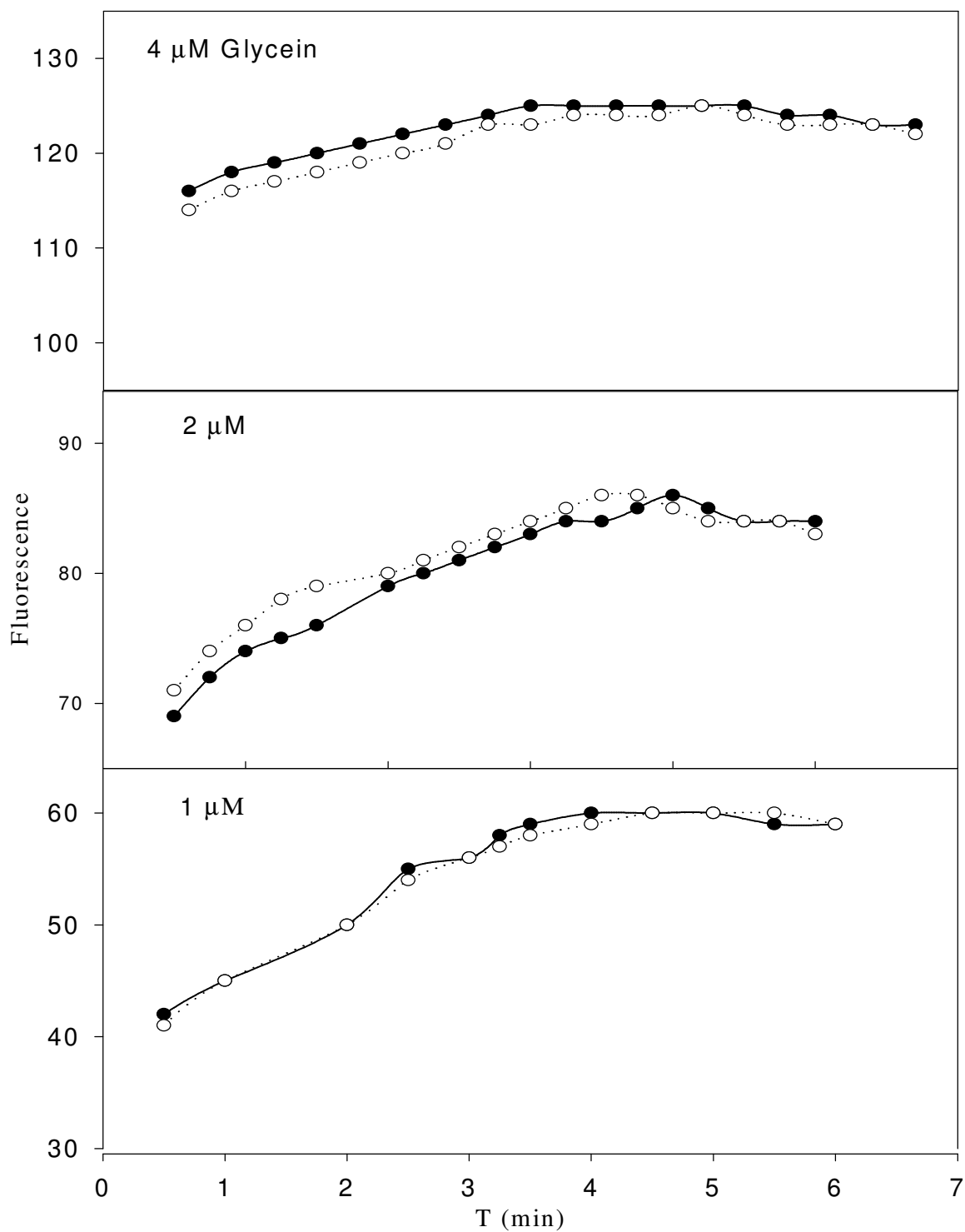


Figure 7. Replicate profiles of fluorescence signals (in arbitrary fluorescence units) versus time for 1, 2, and 4  $\mu\text{M}$  glycein standards.

software run on a Dell OPTIPLEX GX260 PC.

#### Total Nitrogen Determination

Total nitrogen was analyzed by the method of Alvarez-Salgado et al. (1998). HTCO measurements were performed using a commercial Shimadzu TOC-5050A coupled to an Antek 9000N nitrogen-specific chemiluminescence detector (Antek Instruments, TX, USA). Nitrate was used as the standard due to its good recovery (Merriam et al. 1996). A Hansel Laboratory Deep Seawater Reference (Lot # 06-00, Bermuda Biological Station for Research Inc.) was measured to confirm the accuracy of the analysis. The reference ran at  $21.3 \pm 0.24 \mu\text{M N}$  ( $n = 10$ ) with accepted values ranging from 20.5 to 21.5  $\mu\text{M N}$  (W.Chen, personal communication).

Samples are injected (50 $\mu\text{L}$  injection volume) from pre-treated and capped glass cuvettes into the Shimadzu TOC-5050A furnace, filled with a preconditioned Shimadzu catalyst ( $\text{Al}_2\text{O}_3$  impregnated with 0.5% platinum), at 680°C. The combustion products ( $\text{CO}_2$ ,  $\text{NO}\bullet$ ,  $\text{H}_2\text{O}$ , etc.) are carried by high purity oxygen (99.999%; Linde Gas UK, Manchester, UK) through a 25%  $\text{H}_3\text{PO}_4$  solution (IC reaction vessel) to prevent dissolution of  $\text{CO}_2$  into water vapor. The stream then passes through a Peltier cooler at  $\sim 1^\circ\text{C}$  (electronic dehumidifier) for removal of water vapor, and finally through a Shimadzu particle filter (20mm  $\text{\O}$ , sub-micron membrane), which enters the measuring cell of the Shimadzu IRGA (which is necessary to control the automatic injection system of the Shimadzu TOC-5050A).

The combustion gases are routed to the Antek 9000N detector by pulling with a Vacuubrand MZ 2D diaphragm vacuum pump (ABM, Germany) at the exit of the Antek permeation-tube drier to the lower the pressure within the  $\text{NO}_x/\text{O}_3$  reaction chamber. This minimizes background luminescence and increases sensitivity (Walsh, 1989). A high precision controller (Orme

Scientific, Manchester, UK) is used to keep a constant vacuum of -25" Hg (-635mm Hg). This is critical in maintaining the constant flow through the reaction cell necessary to perform precise measurements. To keep the vacuum from drawing water through the Shimadzu TOC-5050A, a T-piece has been installed after the Shimadzu IRGA. The flow through the Antek 9000N is set to ~75% of the total flow ( $=150\text{mL}\cdot\text{min}^{-1}$ ) by means of an extra-fine Nupro (swage-lock) metering valve (Bristol Valve and Fitting, Bristol UK). The remaining ~25% ( $=37.5150\text{mL}\cdot\text{min}^{-1}$ ) is vented to the atmosphere. This configuration avoids all backpressure problems derived from running both systems in-line.

The dried  $\text{NO}\bullet$  is then mixed with  $\text{O}_3$ , leading to production of the excited chemiluminescent  $\text{NO}_2$  species, which emits quantifiable light energy upon decay to its ground state. Oxygen flow through the ozone generator is set to  $\sim 25\text{mL}\cdot\text{min}^{-1}$  and at 0.5 bar pressure. Such low oxygen inflow increases residence time of oxygen in the ozone generator. This enriches the outflow, and enhances the baseline stability. For the TDN levels usually found in seawater ( $5\text{-}50\mu\text{M N L}^{-1}$ ), the Antek 9000N photomultiplier (PMT) voltage must be set to 800mV, in the range of  $\times 10$ .

#### Organic Nitrogen Determination

Organic nitrogen (ON) is determined by difference:

$$\text{ON} = \text{TN} - \text{IN}$$

(Cornell, 2003; Peierls and Pearl, 1997; Gorzelska, 1997). Inorganic nitrogen (IN) is the sum  $\text{NO}_3^-$  and  $\text{NH}_x$ . While  $\text{NO}_2^-$  is sometimes detected, normal atmospheric oxidation and the acidic pH of rainwater rapidly converts it to  $\text{NO}_3^-$ ; therefore it is not considered in IN.

Due to its volatility, it is important that  $\text{NH}_x$ , for the purposes of IN calculation, be measured at the same time of TN analysis. Many samples showed significant losses of  $\text{NH}_x$  between initial

analysis and TN analysis due to exposure and handling (see figures 9 and 10 in Sample Storage Experiments section). These values were corrected by reanalysis of  $\text{NH}_x$  in approximately 80% of samples after TN analysis was performed.

The calculation of ON, which is often low relative to TN and IN, compounds the uncertainty in the initial measurements resulting in the generation of small but negative concentrations of ON in 13 of samples. Of these samples, the average negative value was about 9% of TN per sample (ranging from BDL to  $-4.9 \mu\text{M N}$ ). All of the samples within their standard error were set equal to zero for calculation purposes. Two samples whose values significantly greater than the standard error were removed from the dataset. Values significantly below zero (outside the range of standard error) were removed from the dataset. Remaining negative values were said to be zero or BDL.

#### Detection Limits and Standard Error

Detection limits (DL) for  $\text{NH}_x$ , AA, and TN analysis were estimated from the standard deviation of replicates of a blank (MilliQ) taken after a complete incubation period. DL was determined from

$$DL = 3 \cdot S_o$$

where  $S_o$  is the standard deviation of the blank replicates. For  $\text{NH}_x$ , AA, and TN the DL was  $0.17 \mu\text{M}$  (n=10),  $0.13 \mu\text{M}$  (n=14), and  $0.51 \mu\text{M}$  (n=21), respectively.

The standard error for  $\text{NH}_x$ , TN, and AA analyses was calculated as the average of the variance of all samples measured – each sample was measured in triplicate. The standard error for  $\text{NH}_x$  and AA was determined to be 8% RSD and 3% RSD respectively. For TN, the standard error

was found to be 2% RSD. For ON, standard error was based on Hansell (1993) that incorporated the errors of TN ( $S_{TN}$ ) and IN ( $S_{IN}$ ) where

$$s_{ON} = \sqrt{(s_{TN}^2 + s_{IN}^2)}.$$

The resulting standard error for ON is 8% RSD.

#### Air Mass Back-trajectory Classification

Precipitation events were categorized using air-mass back-trajectories generated using version 4 of the Hybrid Single Particle Lagrangian Integrated Trajectory Model (HYSPLIT) developed at the National Oceanic Atmospheric Administration – Air Resources Laboratory (NOAA/ARL) (Draxler and Rolph, 2003). Trajectories were generated using a stand-alone PC version of the model; and calculated using pre-processed gridded horizontal and vertical wind fields generated at 6-hour intervals from the National Center for Environmental Prediction’s Global Data Assimilation System (GDAS) using the Medium Range Forecast model (MRF) to produce the forecast wind fields (Kanamitsu, 1989).

Single back-trajectories were run for each measured precipitation event collected at UNCW starting at the recorded onset of precipitation. Trajectories were generated for a 72 h hind-cast since this is a mid-range value for the residence time of  $NH_x$  in the atmosphere (Aneja, 2000). Trajectories were run starting at the 500m level to represent the air-mass near the well mixed boundary layer likely to contribute more heavily to in-cloud processes contributing to wet deposition (Walker, 2000). They were then visually categorized based on origin (compass direction) and path (terrestrial, oceanic, or mixed): 1) N-Terrestrial, 2) W/SW-Terrestrial, 3) N/NW-Mixed, 4) SW-Coastal, 5) E-Oceanic. Terrestrial air masses are those whose pathway for the 72h period was predominantly over a landmass, and like-wise over the ocean for oceanic

types. Mixed trajectories were determined to have the same potential for oceanic as terrestrial influence based on a visual analysis of their pathway. Trajectories unclassifiable by either origin or pathway were not included in the dataset.

### Regional Rainfall Estimation and Validation

The estimation of rainfall to the CFRE for the sampling period was calculated using two methods of total rainfall depth: 1) depth determined from measurements made at the UNCW rain collection site, and 2) depth determined from summation of daily rainfall to the CFRE computed from the QPESUMS (Quantitative Precipitation Estimation and Segregation Using Multiple Sensors) algorithm. The QPESUMS 24-hour rainfall estimates for the region are generated from WSR-88D (Weather Surveillance Radar 88 Doppler) located at Wilmington International Airport (ILM) and run by the National Weather Service (Maddox, et al., 2002). Digitized datasets are retrieved via FTP from the National Severe Storms Laboratory (NSSL) in Norman, OK, USA.

A comparison of QPESUMS predicted rainfall versus rainfall measured at UNCW shows that the QPESUMS overestimates the rainfall at UNCW by 9%. Given the spatial variability of rainfall, this result validates the use of rainfall measured at UNCW to estimate the total wet deposition to the CFRE.

### Data Analysis

All rainwater concentration averages and standard deviations are volume weighted (Topol, 1985). Rainwater pH values were computed from volume weighted hydrogen ion concentrations. All other averages are simple averages with standard deviations based on  $n-1$ . Comparisons between averages employed Student's  $t$  at the 95% probability level. Pearson Correlation Tests

were also used where correlation coefficients were considered significant at the 95% probability level.

Non Sea-Salt Sulfate (NSS) concentrations were calculated from

$$NSS = TotalSO_4^{2-} - [Cl^-] \cdot 0.052$$

based on the constancy-of-composition principle for seawater. Assuming all chloride present in rainwater samples is from seawater, the sea-salt ratio of  $Cl^- / SO_4^{2-}$  can be used to determine the fraction of total rainwater  $SO_4^{2-}$  is not of sea-salt origin (Willey and Kiefer, 1993).

### Sample Storage Experiments

Experiments were performed to determine if storage by freezing was sufficient for preservation of sample relative to  $NH_x$  and AA concentration. For AA, 6 rain samples and one dry deposition sample were analyzed for AA immediately upon collection and after subsequent freezing at  $-20^\circ C$  for 14 days. Initial sample concentrations ranged from 0.2 to  $9.4 \mu M$  AA. Two samples ( $1.1 \mu M$  and  $0.7 \mu M$  AA) showed significant increases in AA concentration ( $0.3, 0.4 \mu M$  AA increases;  $p < 0.05$ ). The remaining samples had no measurable change: the results were below BDL and they failed Student's T-tests ( $p > 0.05$ ). Given these results, freezing can be considered sufficient for sample preservation since nearly all samples were analyzed within one week of collection.

Similarly, initial, unfrozen  $NH_x$  concentrations were measured from 25 rain samples – ranging from  $0.95$  to  $40.5 \mu M$   $NH_x$ . Samples were reanalyzed after being stored frozen at  $-20^\circ C$  for periods ranging from 1 day to over one year. The results, given in Figure 8, demonstrate that rain samples are stable for up to 2 weeks - losing less than 5%  $NH_x$  during the storage period

(ranging from  $-2.5 \mu\text{M}$  to  $2.5 \mu\text{M}$   $\text{NH}_x$ ; 8 increasing samples, 7 decreasing samples, 2 with no change ( $p>0.05$ )). A more dramatic loss is seen in samples stored up to 100 days.  $\text{NH}_x$  increased in 6 of 7 samples stored longer than 100 days ( $p>0.05$ ; ranging from BDL to  $4.5 \mu\text{M}$  increases).

Figure 9 presents results from multiple  $\text{NH}_x$  analyses of individual samples. Seven frozen samples were analyzed 3 or more times, aliquots being taken from the same sample bottle for each analysis, over periods ranging from 1 day to 1.5 years. Given both the positive and negative  $\text{NH}_x$  changes for all sample groups, it seems likely that sample contamination due to handling is a significant factor in these results. To address this issue 7 rain events were divided into two identical samples and stored in clean 125mL HDPE bottles. Initial, unfrozen  $\text{NH}_x$  concentrations were measured from samples in one bottle (bottle-*a*) while the other was frozen at  $-20^\circ\text{C}$  (bottle-*b*). Initial measurements from bottle-*a* samples ranged from  $0.64$  to  $57.6 \mu\text{M}$   $\text{NH}_x$ . Subsequent measurements were taken from the frozen samples (bottle-*b*) after periods ranging from 221 to 297 days. The results (Figure 10) show a linear relationship between  $\text{NH}_x$  loss rate and initial sample concentration. There was an average loss of less than  $0.01\%$  per day in samples where losses occurred. Samples with higher initial concentrations experienced the greatest loss rate while  $\text{NH}_x$  in the sample with the lowest initial concentration showed no change (ranging from  $-0.06$  to  $0 \mu\text{M}$   $\text{NH}_x \cdot \text{d}^{-1}$ ). This suggests that  $\text{NH}_x$  loss is a function of initial  $\text{NH}_x$  concentration. As well, these results support both the hypothesis that sample contamination was indeed a factor in previous stability tests of frozen samples, and that the method of preservation of  $\text{NH}_x$  in rainwater samples employed in this study is effective in the short term.

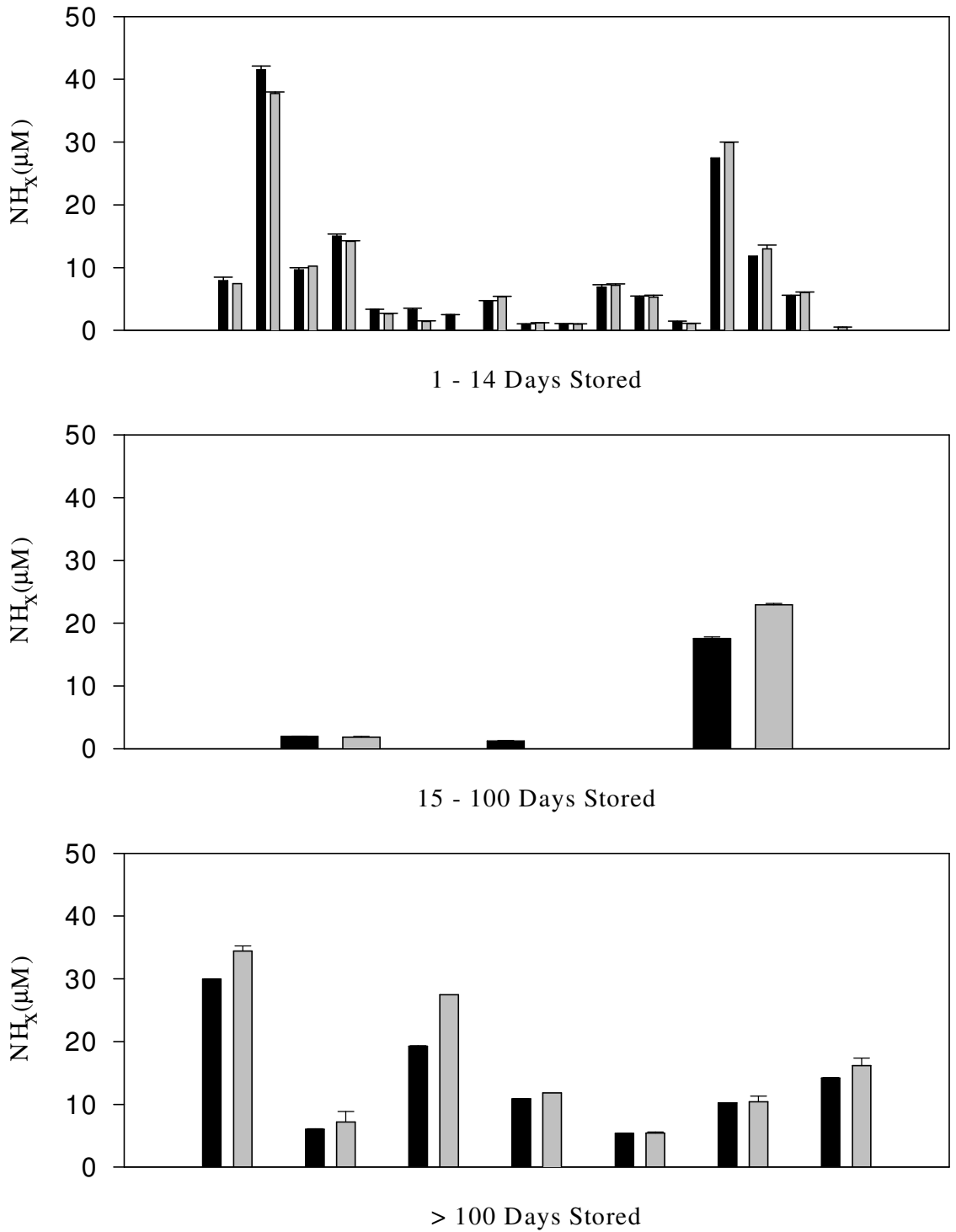


Figure 8. Results from a before (black) and after (gray) test of sample  $\text{NH}_x$  stability for samples frozen at  $-20^\circ\text{C}$ . Results are grouped by number of days the samples were stored frozen.

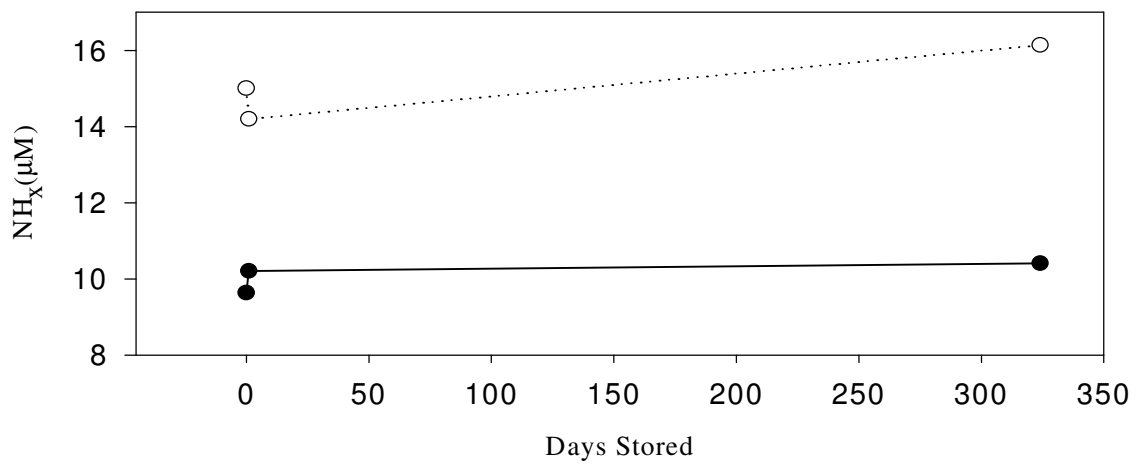
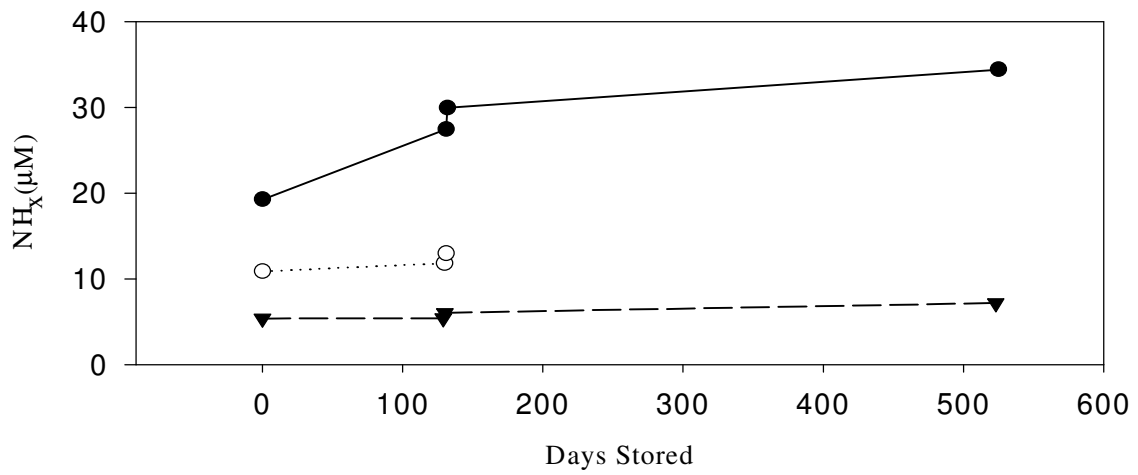
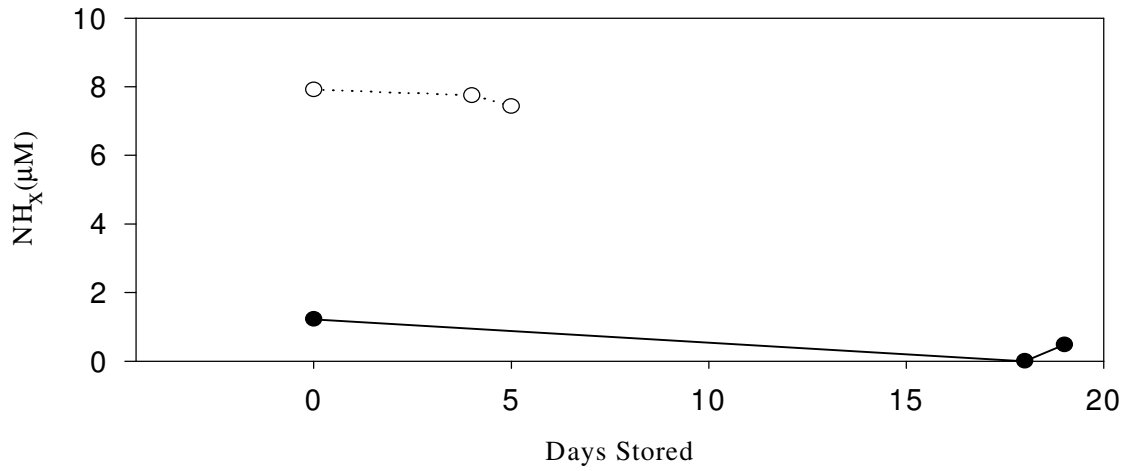


Figure 9. Results from repetitive, same-bottle  $\text{NH}_x$  analysis of 7 samples.

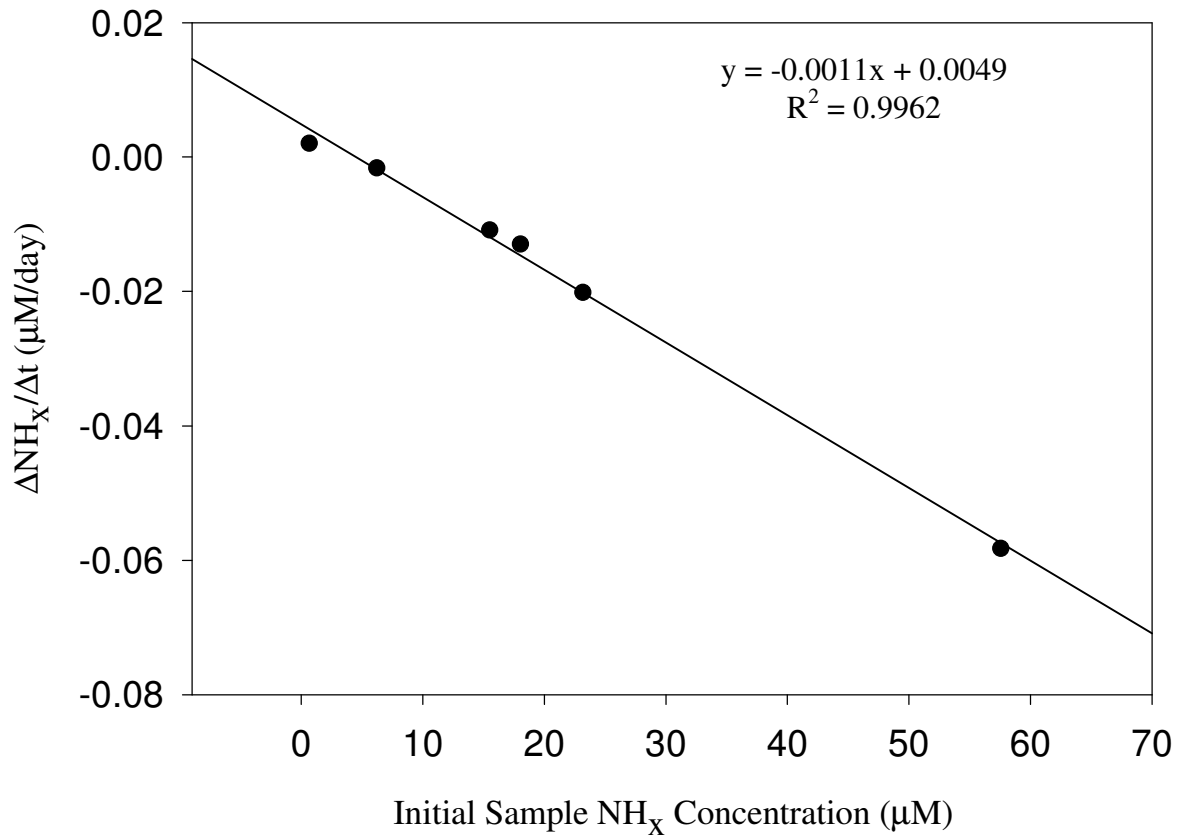


Figure 10. Plot of rate of  $\text{NH}_x$  loss versus initial sample concentration for results from analyses of samples stored in separate bottles. Line is a simple regression of plotted data.

## Results and Discussion

### Rainwater Chemistry

Rain samples were collected from February 2002 through August 2003 on an event basis. Samples from September 1, 2002 to August 31, 2003 (78 rain events) were used in this study representing a calendar year. The sample year netted 163.4 cm of rain (21.0 mm per event) compared to 147 cm per year average at the Wilmington International Airport (ILM) based on data from the last 10 years collected by the National Weather Service.

Tables 1 and 2 show volume-weighted averages of rainwater analytes for the sample period. Inorganic nitrogen was the dominant form of N representing nearly 86% of total nitrogen based on volume-weighted averages. For the sample period,  $\text{NO}_3^-$ ,  $\text{NH}_x$ , and NSS concentrations were similar (11.1  $\mu\text{M}$ , 10.1  $\mu\text{M}$ , and 11.1  $\mu\text{M}$  respectively).  $\text{NH}_x$  and  $\text{NO}_3^-$  made up approximately the same amount of inorganic-N. This is dissimilar to other nearby where  $\text{NO}_3^-:\text{NH}_x$  ratios are about 2 to 1 (Peierls, 1997; Russel, 1998; Lawrence, 2000) and 1.4 to 1 at the UNCW site in an earlier study (Willey and Kiefer, 1993). Rainwater ammonium concentrations ranged from below detection to 77.2  $\mu\text{M}$  (median: 4.42  $\mu\text{M}$ ).  $\text{NO}_3^-$  ranged from 0.3 to 55.8  $\mu\text{M}$  (median: 11.2  $\mu\text{M}$ )

Values for TN, ON and AA for various general and specific locations are presented in Table 3. Organic nitrogen (ON) average of 5.5  $\mu\text{M}$  was very similar to other locations and somewhat lower than more Anthropogenically impacted environments. Rainwater ON ranged from below detection to 83.3  $\mu\text{M}$  (median: 2.54). Both ON and TN concentrations are comparable to values for a 1994 – 1996 study (3.6  $\mu\text{M}$  and 17.4  $\mu\text{M}$  respectively) at a similar site in Morehead City on the North Carolina coast (Peierls and Pearl, 1997). TN is similar to other coastal locations and at the low end of other reported values. Free amino acids make up 17% rainwater ON. Their concentrations ranged from 0.03  $\mu\text{M}$  to 4.56  $\mu\text{M}$  (median: 0.64); and the average of 0.93  $\mu\text{M}$

Table 1. Volume-weighted average concentration and standard deviations of pH, and N-species in rainwater collected at Wilmington, NC between September 1, 2002 and August 31, 2003. The % NH<sub>x</sub> and %ON are relative to TN concentration, and n is the number of samples included in their respective calculations.

<b>n</b>		<b>Rain (mm)</b>	<b>pH</b>	<b>NH<sub>x</sub> (μM)</b>	<b>NO<sub>3</sub><sup>-</sup> (μM)</b>	<b>AA (μM)</b>	<b>ON (μM)</b>	<b>TN (μM)</b>	<b>%NH<sub>x</sub></b>	<b>%ON</b>
129	All Data	2602.9	4.62	9.8±1.3	11.5±1.1	0.86±0.1	4.6±1.3	22.0±0.4	45%	21%
78	AvgYear	1633.9	4.72	10.1±1.6	11.1±1.0	0.93±0.10	5.5±1.1	24.8±0.5	41%	22%
13	Winter	234.2	4.85	6.8±1.7	15.5±3.7	0.84±0.22	2.4±0.6	24.2±1.2	28%	10%
21	Spring	566.7	4.69	18.6±4.5	12.4±2.0	1.37±0.25	7.5±2.3	32.7±0.9	57%	23%
31	Summer	617.7	4.65	6.0±0.7	8.9±1.2	0.70±0.09	5.5±0.4	20.2±0.2	30%	27%
13	Fall	215.4	4.87	3.0±0.6	7.7±1.1	0.55±0.10	3.3±1.6	14.6±0.4	21%	23%

Table 2. Volume-weighted average concentrations of  $\text{SO}_4^{2-}$ , NSS,  $\text{H}_2\text{O}_2$ , and DOC in rainwater collected at Wilmington NC between September 1, 2002 and August 31, 2003.

<b>n</b>		<b><math>\text{SO}_4^{2-}</math> (<math>\mu\text{M}</math>)</b>	<b>NSS (<math>\mu\text{M}</math>)</b>	<b><math>\text{H}_2\text{O}_2</math> (<math>\mu\text{M}</math>)</b>	<b>DOC (<math>\mu\text{M}</math>)</b>
78	<b>AvgYear</b>	13.2±1.1	11.1±1.0	13.6±1.1	70.7±10.4
13	<b>Winter</b>	15.2±2.9	12.4±2.8	5.9±1.4	59.8±17.1
21	<b>Spring</b>	15.5±2.1	12.9±1.9	15.9±1.4	84.9±28.8
31	<b>Summer</b>	10.3±1.3	9.0±1.4	15.8±2.0	70.7±11.6
13	<b>Fall</b>	13.0±0.8	10.5±1.6	9.1±2.3	45.5±11.4

Table 3. Volume-weighted average concentrations of ON, TN, and AA from the present study and for various geographic locations. The %ON Value is in comparison to TN. The asterisk (\*) values represent coastal sampling sites.

<b>Location</b>	<b>ON (<math>\mu\text{M}</math>)</b>	<b>TN (<math>\mu\text{M}</math>)</b>	<b>%ON</b>	<b>AA (<math>\mu\text{M}</math>)</b>	<b>n</b>	
UNCW–Present Study	5.5*	24.8*	22*	0.93*	78	
Marine	7	11	67		3	Cornell, 2003
Coastal	19*	57*	33*		24	“
Continental	21	58	36		12	“
N. America	17	49	35	0.002 – 6.4	39	“
NH, DE, VA	0.6, 4.2, 3.1	23.8, 53.8, 48.5	2.6, 7.8, 6.5		12, 50, 83	Keene, 2002
Morehead City, NC	3.6*	17.4*	20.7*		43	Peierls and Pearl, 1997
Chesapeake Bay	6.2*				60	Russel, 1998
Norwich, UK	33				12	Cornell, 1997

falls within the reported range of .002 – 6.4  $\mu\text{M}$  by Cornell (2003); while Mopper and Zika (1987) found AA concentrations in marine rain ten times that of terrestrial rain (6.5  $\mu\text{M}$  AA for marine versus 0.61  $\mu\text{M}$  AA for coastal) is possibly the result of degradation of more complex ON forms by constituents of the marine troposphere. These results indicate other ON species not measured in our analysis scheme constitutes the majority of ON in Wilmington rainwater. Keene et al (2002) present that ON in rainwater consists of numerous N-species usually in the form of organic nitrates, soluble reduced-N forms (urea, amino acids, and amines), and primary bio-material. Cornell (1998), in Norwich, UK, found urea to be ~11% of rainwater DON; which suggests that ON incorporates many different N species. All analytes are log-normally distributed. In conjunction with standard precipitation studies the data set was natural log-normally transformed (Yevjevich, 1971). This permits the use of standardized statistical analyses with our dataset. The TN value is not a composite of (IN+ON) values reported in Table 1. The discrepancy is a result of an ON value adjustment based on corrections of negative data points (see methods).

### Correlation Patterns

Interactions between specific rainwater components based on general properties of the system generate discernible patterns that reflect these processes and aid in the interpretation of data. Table 4 is a correlation matrix of the chemical components (concentration units) and amounts of rainfall (mm per event) used in this study. Due to its calculation as a composite value, TN auto-correlates with many components and is therefore left out. The results support a number of conclusions.

Table 4. Correlation matrix for rainwater components. Results are Pearson correlation coefficients for natural log-transformed concentration data for events during the sampling period. Bold values indicate significance at 99% C.I.

	NH <sub>x</sub>	NO <sub>3</sub> <sup>-</sup>	SO <sub>4</sub> <sup>2-</sup>	NSS	Cl <sup>-</sup>	AA	ON	H <sup>+</sup>
Amount	-0.1229	<b>-0.3902</b>	<b>-0.3447</b>	<b>-0.3127</b>	-0.0960	-0.2006	-0.1689	-0.2254
NH <sub>x</sub>		<b>0.6819</b>	<b>0.7288</b>	<b>0.6407</b>	0.2555	<b>0.8215</b>	-0.0236	<b>0.3845</b>
NO <sub>3</sub> <sup>-</sup>			<b>0.8551</b>	<b>0.7368</b>	<b>0.3350</b>	<b>0.7142</b>	0.0941	<b>0.5318</b>
SO <sub>4</sub> <sup>2-</sup>				<b>0.9214</b>	0.2408	<b>0.7421</b>	0.0265	<b>0.4728</b>
NSS					-0.1553	<b>0.6279</b>	0.0377	<b>0.4431</b>
Cl <sup>-</sup>						<b>0.3147</b>	-0.0251	0.1015
AA							0.1965	<b>0.5523</b>
ON								0.0975
NH <sub>x</sub> +H <sup>+</sup>		<b>0.719</b>	<b>0.716</b>	<b>0.662</b>	-0.069	<b>0.739</b>	<b>0.263</b>	

1. Increased rainfall dilutes concentrations of several chemical species – especially those associated with aerosols.  $\text{NH}_x$ , AA, and ON concentrations are controlled by more dominant sources of variability.
2. Concentrations of inorganic acids and bases in Wilmington rainwater occur as both aerosols and gas vapors. In their simplest atmospheric form, acids and bases ( $\text{HNO}_3$ ,  $\text{H}_2\text{SO}_4$ ,  $\text{NH}_3$ , organic acids) will correlate strongly with  $\text{H}^+$ .  $\text{NO}_3^-$ , and  $\text{SO}_4^{2-}$  correlate strongly with both  $\text{H}^+$  and  $\text{NH}_x$ . Since the sources of these compounds are all different, it can be inferred that any similarities are due to atmospheric interactions, such as the formation of aerosols, rather than co-varying emissions.
3. AA and  $\text{NH}_x$  correlate with pollutant indicators suggesting an anthropogenic source. ON did not correlate with anything implying that it behaves differently than other N species.
4. Correlations for  $(\text{NH}_x + \text{H}^+)$  to  $\text{SO}_4^{2-}$  and  $(\text{NH}_x + \text{H}^+)$  to  $\text{NO}_3^-$  could mean that other cations present in the atmosphere (mainly  $\text{Ca(II)}$ ) may form aerosols with  $\text{SO}_4^{2-}$  and  $\text{NO}_3^-$  near the coast as noted by Minoura and Iwasaka (1996).
5. The amphoteric properties of amino acids compound their atmospheric behavior. Free amino acids are known to become more soluble in water with increasing  $\text{H}^+$  (Pradhan and Vera, 1998; Carta, 1998). Thus it could be possible that free amino acids are more efficiently scavenged by more acidic rainfall. This is evidenced in the strong correlation between AA and  $\text{H}^+$ .

Conclusion 2 cannot hold up in comparison to AA and ON. It is possible that, in contrast to inorganic nitrogen, AA and ON concentrations are functions of numerous processes: these could include factors controlling both emissions and atmospheric interactions.

## Spatial Variability

A comparison of measured analytes for the current sampling period and an earlier study conducted from 1988-1990 at UNCW is given in Table 5. Measurements of the same analytes from nearby sites monitored by the National Atmospheric Deposition Program (NADP) are also presented in Table 5. The values used for the NADP sites at Clinton, Lewiston, and Jordan Creek are from 1990 and from July 2002 through June 2003: representing available sampling periods closest to those analyzed for the UNCW site. At the time of writing, NADP data for the entirety of the sample period of this study were not yet available. Figures 11, 12, and 13 show the location of the NADP sites and UNCW in reference to U.S. Environmental Protection Agency – National Emissions Inventory (EPA-NEI) 1999 emissions data for  $\text{NH}_3$ ,  $\text{NO}_x$ , and  $\text{SO}_x$ . The NADP site at Clinton, NC is located within the region of high  $\text{NH}_3$  emissions. While the Jordan Creek, and Lewiston NADP sites, as well as the UNCW site, are outside of this region, they are within the fallout range of these  $\text{NH}_3$  emissions (Walker, 2000). UNCW alone is located within a region of high  $\text{SO}_x$  emissions; though the uniform distribution of both  $\text{NO}_x$  and  $\text{SO}_x$  emission sources, in contrast to  $\text{NH}_x$ , leaves the potential for high levels of deposition at all sites.

An examination of the right portion of Table 5 reveals the regional variability of rainwater composition and atmospheric wet deposition. Currently, VWA concentrations of  $\text{NO}_3^-$  and NSS at UNCW were similar to those from the NADP collection sites. Higher concentrations of these analytes given the urban setting of the UNCW site might be expected; though widespread  $\text{NO}_x$  emissions support similar deposition patterns. Our result is possibly due, in part, to increased dilution from greater rainfall for the current period at UNCW than the NADP sites (26% above average total rainfall). An elevated  $\text{SO}_4^{2-}$  concentration indicates higher natural sulfate inputs due to the proximity of the UNCW

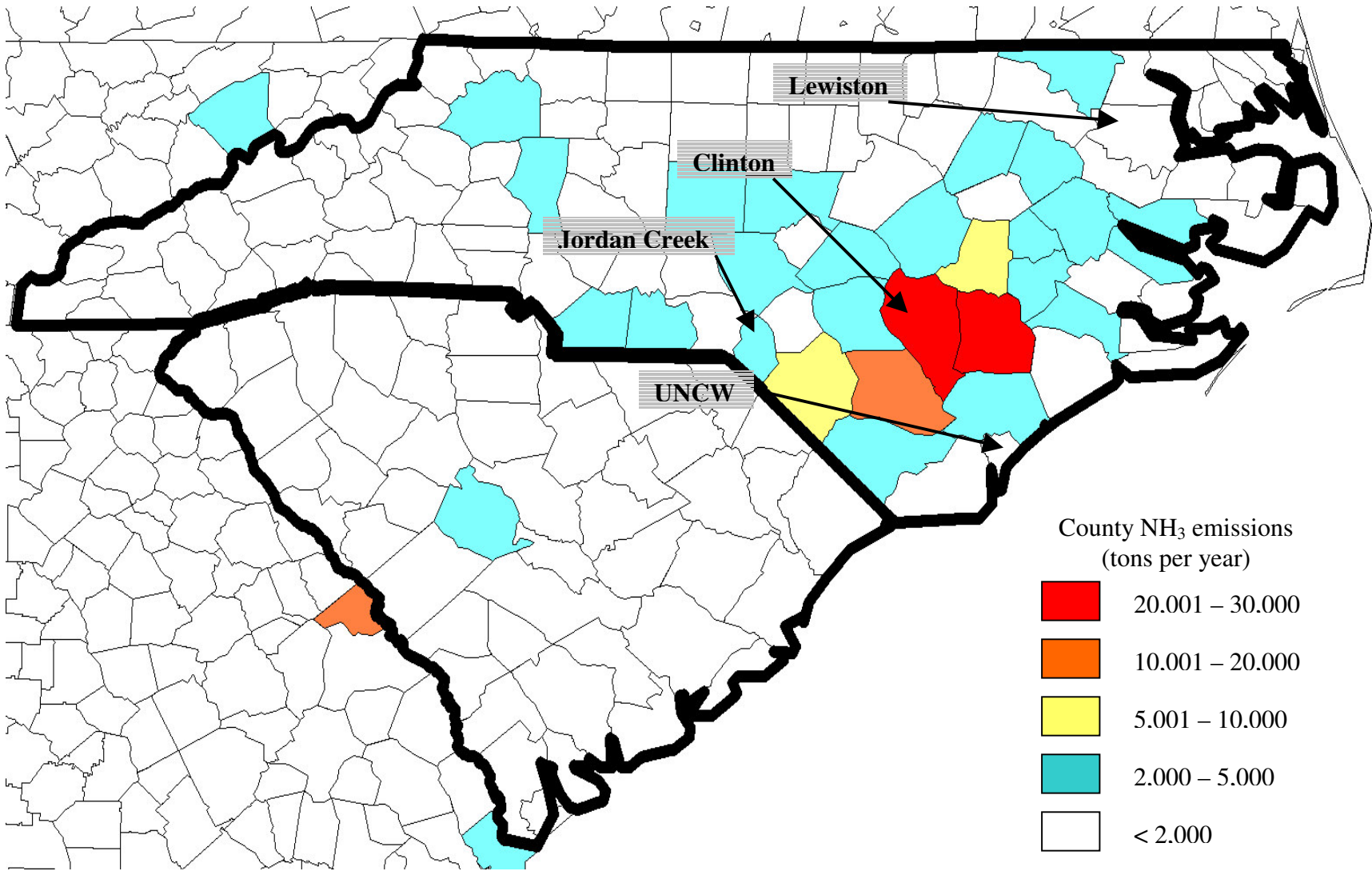
Table 5. Rainwater VWA concentrations of  $\text{NH}_x$ ,  $\text{NO}_3^-$ ,  $\text{SO}_4^{2-}$  (NSS), and  $\text{H}^+$ , and rainfall amounts from UNCW, and the NADP sampling sites at Clinton, Lewiston, and Jordan Creek. The 1990 values from UNCW are averages of rainwater collected from 1988 to 1990 taken from Willey and Kiefer (1993).

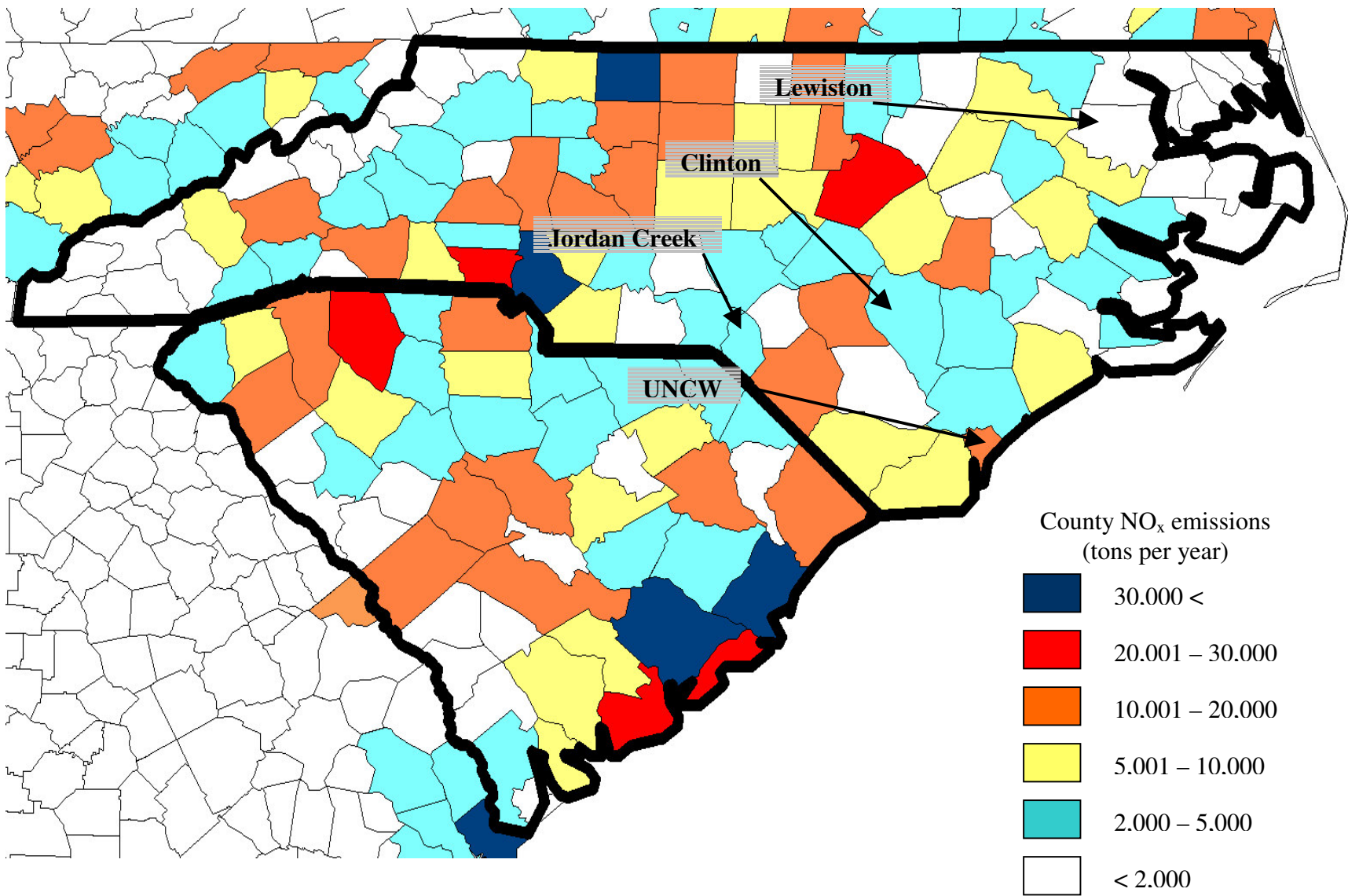
Jan. 1, 1990 – Dec. 31, 1990			Sept. 1, 2002 – Aug. 31, 2003	
<b><u>NH<sub>4</sub><sup>+</sup></u></b>	<b>μM</b>	<b>Deposition (mmol m<sup>-2</sup> yr<sup>-1</sup>)</b>	<b>μM</b>	<b>Deposition (mmol m<sup>-2</sup> yr<sup>-1</sup>)</b>
UNCW	9.00	10.8	10.1	16.5
Clinton	16.1	15.1	25.4	31.3
Lewiston	12.2	13.4	12.1	17.1
Jordan Creek	11.6	12.7	12.6	18.5
<b><u>NO<sub>3</sub><sup>-</sup></u></b>	<b>μM</b>	<b>Deposition (mmol m<sup>-2</sup> yr<sup>-1</sup>)</b>	<b>μM</b>	<b>Deposition (mmol m<sup>-2</sup> yr<sup>-1</sup>)</b>
UNCW	12.8	15.4	11.1	18.1
Clinton	17.4	16.2	12.2	15.1
Lewiston	15.0	16.5	13.5	19.1
Jordan Creek	17.4	18.7	14.2	20.9
<b><u>SO<sub>4</sub><sup>2+</sup> (NSS)</u></b>	<b>μM</b>	<b>Deposition (mmol m<sup>-2</sup> yr<sup>-1</sup>)</b>	<b>μM</b>	<b>Deposition (mmol m<sup>-2</sup> yr<sup>-1</sup>)</b>
UNCW	14.5(12.8)	17.4(15.3)	13.2(11.1)	21.6(18.1)
Clinton	19.4(18.4)	18.0(17.1)	11.9(11.3)	14.7(13.9)
Lewiston	17.6(17.0)	19.3(18.7)	11.9(11.3)	16.8(16.0)
Jordan Creek	18.8(18.0)	20.4(19.4)	13.5(13.1)	19.9(19.3)
<b><u>H<sup>+</sup></u></b>	<b>μM</b>	<b>Deposition (mmol m<sup>-2</sup> yr<sup>-1</sup>)</b>	<b>μM</b>	<b>Deposition (mmol m<sup>-2</sup> yr<sup>-1</sup>)</b>
UNCW	30.9	3.7	19.3	3.2
Clinton	32.4	3.0	9.55	1.2
Lewiston	31.6	3.5	20.0	2.8
Jordan Creek	34.7	3.8	24.0	3.5
<b><u>Rain</u></b>	<b>cm</b>		<b>cm</b>	
UNCW	120.0		163.4	
Clinton	93.1		123.4	
Lewiston	109.8		141.2	
Jordan Creek	108.0		147.1	

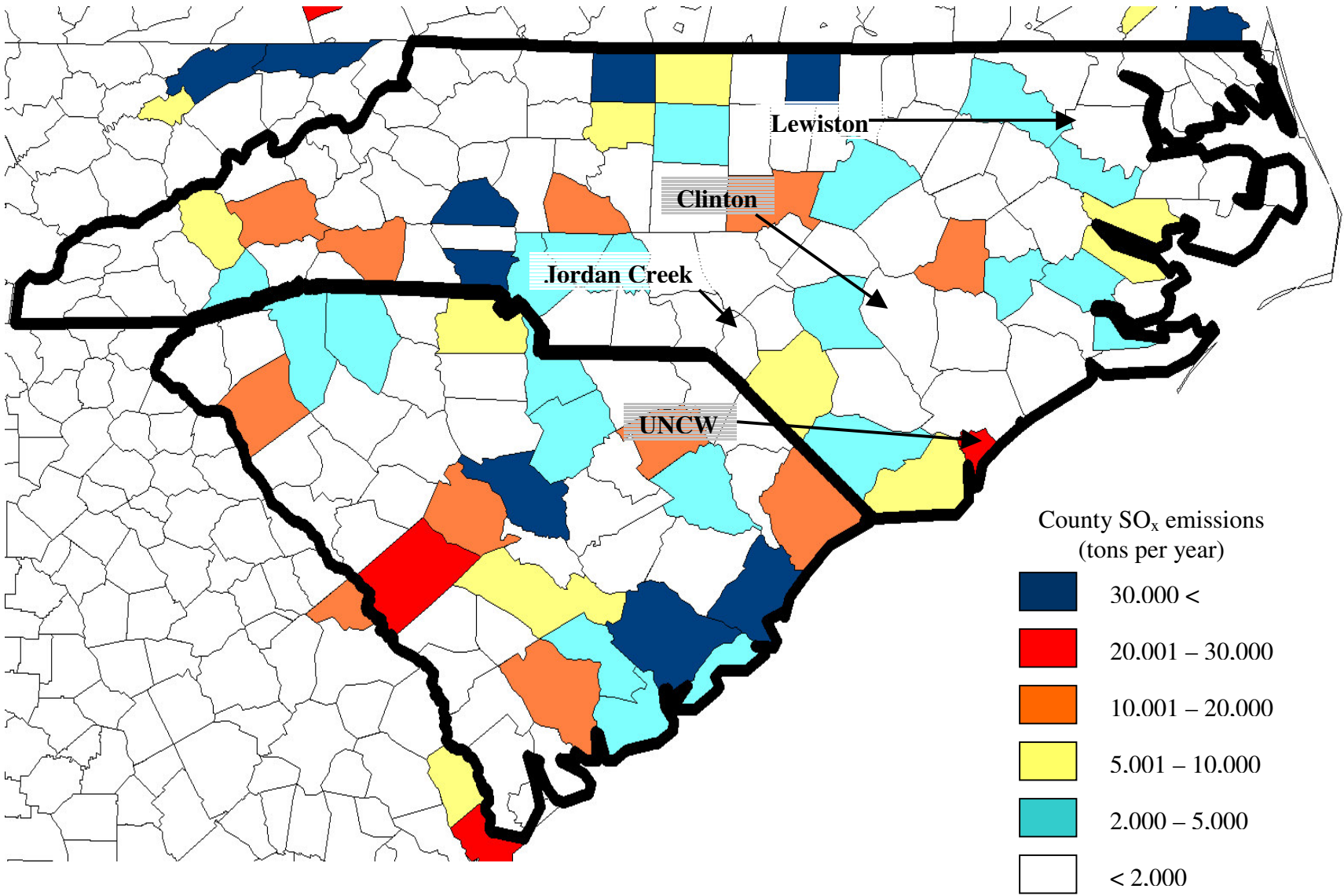
Figure 11. Map of North and South Carolina NH<sub>3</sub> emissions by county based on 1999 EPA-NEI data. The general locations of the NADP and UNCW collection sites are indicated by arrows. White coloring represents data only in North and South Carolina.

Figure 12. Map of North and South Carolina NO<sub>x</sub> emissions by county based on 1999 EPA-NEI data. The general locations of the NADP and UNCW collection sites are indicated by arrows. White coloring represents data only in North and South Carolina.

Figure 13. Map of North and South Carolina SO<sub>x</sub> emissions by county based on 1999 EPA-NEI data. The general locations of the NADP and UNCE collection sites are indicated by arrows. White coloring represents data only in North and South Carolina.







collection site to the ocean, which is known to be a significant source of sulfate to the atmosphere. Similarly, the entrainment of the  $\text{NH}_x$  -low marine atmosphere in the vicinity of UNCW during many rain events (see Air-mass Back Trajectories section), in addition to increased rainfall, could explain why the UNCW  $\text{NH}_x$  concentration is slightly lower than other sites in the region. The combined effect of these factors could lessen the influence of localized high  $\text{NH}_x$  emissions from nearby livestock farming operations (<50 km). The elevated  $\text{SO}_4^{2-}$  and NSS concentrations at Jordan Creek could possibly be due to its central location relative to  $\text{SO}_x$  emissions (see Fig 3).

Rainfall pH is comparable between UNCW and the region with the exception of Clinton. High  $\text{NH}_3$  emissions in the vicinity of Clinton (and consequential acid neutralization in rainwater) likely contributed to its higher pH. The influence of emissions associated with urban areas cannot be discounted here; though the extent of the urban influence on the UNCW dataset is not implicit in this study. Proximity to the ocean could affect pH in UNCW rainfall; but a Pearson Correlation test did not demonstrate a significant correlation between  $\text{Cl}^-$  (a primary component of sea-water) and  $\text{H}^+$  concentration ( $p \gg 0.05$ ).

$\text{NO}_3^-$ , and NSS wet deposition values were not significantly different at UNCW compared to the NADP sites. Though UNCW experienced more potential for wet deposition from increased rainfall, the regional uniformity of wet deposition implies that the atmospheric concentrations of these analytes are similar. UNCW displayed a higher  $\text{SO}_4^{2-}$  deposition likely due to both its proximity to the ocean (as a source) and greater rainfall. Clinton displays a remarkably high  $\text{NH}_x$  deposition due to the high input of livestock-derived  $\text{NH}_x$  in the local atmosphere.

#### Temporal Variability

Comparing the left and right portions of Table 5 exhibits the change in rainfall composition and wet deposition for the region from 1990 through 2002/2003.  $\text{NO}_3^-$ ,  $\text{SO}_4^{2-}$ , NSS, and  $\text{H}^+$  concentrations decreased for all sites. This could be due to either dilution (all sites experienced more rainfall) or a decrease in atmospheric  $\text{NO}_3^-$  and  $\text{SO}_4^{2-}$  concentrations.

The decrease in NSS deposition at the NADP sites, though, in conjunction with increased rain implies a decrease of NSS in the atmosphere for the region. This is also supported by the decrease in rainfall acidity for the region implying significant changes in overall atmospheric composition. A portion of the decline in  $\text{H}^+$  concentration for NADP sites could be a result of increased alkalinity due to higher  $\text{NH}_x$  concentrations – particularly at Clinton.

$\text{NH}_4^+$  concentrations increased at all sites except Lewiston where there was no change. This most likely reflects the growth in livestock farming in the region, and the potential for transport of airborne ammonium to remote locations. Livestock waste lagoons are known to release large amounts of ammonia and ammonium into the atmosphere (Aneja, 2001). The concentration at Lewiston - which is located the furthest from the livestock farming region - showed no change though it is not out of the immediate influence of downwind transport of agricultural emissions (Walker, 2000). At UNCW, the average  $\text{NH}_4^+$  concentration showed an increase (from 9.00  $\mu\text{M}$  to 10.1  $\mu\text{M}$ ). Wilmington is located approximately 50 km to the south - southeast of the livestock region and is well within the theoretical fallout range of agricultural emission from nearby livestock farming (Asman, 2001; Aneja, 2001; Walker, 2000) This validates an increased  $\text{NH}_x$  concentration; though dilution from increased rainfall for the period helps hide this.

If atmospheric concentrations of an analyte have not changed, then, assuming efficient aerosol scavenging and adequate rainfall intensity, an increase in rainfall per event will result in an equally proportional decrease in analyte concentration as described by

$$\frac{Rain1}{Rain2} = \frac{Concentration2}{Concentration1}$$

A comparison of average rainfall per event and VWA concentrations for the two periods at UNCW is given in Table 6. A 22% increase in rainfall coincides with a 12% increase in  $NH_4^+$  concentration. This indicates an overall increase in atmospheric concentration of  $NH_4^+$  during the 1990's. Decreases in  $NO_3^-$ ,  $SO_4^{2-}$  and NSS rainwater concentration indicate a decline in regional anthropogenic emissions for these components.

To address the influence of local versus regional emissions on  $NH_x$  deposition at UNCW,  $NH_3$  emissions data from the EPA National Emissions Inventory (NEI) were compared to total wet-deposited  $NH_x$  at UNCW and Clinton from values in Table 1. Total wet depositions of  $NH_x$  (tons per year) per county area for 1990 and 1999 were calculated for New Hanover (334 km<sup>2</sup>) and Sampson (2454 km<sup>2</sup>) counties in North Carolina. As well, total potential wet deposited  $NH_x$  estimations (tons per year) per county area for 1990 and 1999 were calculated from

$$D_{potential} = E_d \cdot N_r$$

$D_{potential}$  is the total possible wet deposition of  $NH_x$  (tons per year) if, during a given rain event, all of the  $NH_3$  emissions for that day were deposited in that county.  $E_d$  is the daily  $NH_3$  emissions based on EPA-NEI data, and  $N_r$  is the number of rain-days per year at the reference collection sites.  $N_r$  for Sampson county (Clinton) is estimated at 100 d · y<sup>-1</sup> (based on daily NADP precipitation data for 1990 and 1999). The results are presented in Table 7.

From Table 7, it is clear that a large portion of  $NH_x$  wet-deposited in New Hanover County in recent years has to originate from outside of the county. As well, the increase in emissions in New Hanover County does not account for the larger increase in deposition at

Table 6. Comparison of VWA concentrations for rainfall collected at UNCW for the periods of 1988 through 1990 and September 1, 2002 through August 31, 2003 and the percent change between the two periods.

	<b>1988-1990</b>	<b>2002-2003</b>	<b>% Change</b>
<b>Rain</b>	17.2 <sup>mm</sup> /event	21.0 <sup>mm</sup> /event	22%
<b>NH<sub>4</sub><sup>+</sup></b>	9.00 $\mu\text{M}$	10.1 $\mu\text{M}$	12%
<b>NO<sub>3</sub><sup>-</sup></b>	12.8 $\mu\text{M}$	11.1 $\mu\text{M}$	-13%
<b>SO<sub>4</sub><sup>2-</sup> (NSS)</b>	14.5(12.8) $\mu\text{M}$	13.2(11.1) $\mu\text{M}$	-9%(-13%)
<b>H<sup>+</sup></b>	30.9 $\mu\text{M}$	19.3 $\mu\text{M}$	-38%

Table 7. Total potential and actual wet depositions of NH<sub>x</sub> (tons per year) at UNCW and Clinton, NC.

		<b>1990</b>	<b>1999</b>	<b>ΔD</b>
<b>New Hanover County</b> <b>(UNCW)</b>	D <sub>Potential</sub>	43	66	23
	D <sub>Actual</sub>	68	104	36
<b>Sampson County</b> <b>(Clinton)</b>	D <sub>Potential</sub>	1992	4696	2704
	D <sub>Actual</sub>	695	1353	658

UNCW further supporting the hypothesis that much of the  $\text{NH}_x$  deposition is seen at UNCW is due to regional rather than local sources. On the other hand, less than one quarter of 1999  $\text{NH}_3$  emissions in Sampson County were deposited at Clinton suggesting that they are transported out of the county. Since rain events rarely last longer than a few hours, and much of an area's emissions would be transported out of that area in less than one day,  $D_{\text{potential}}$  is likely overestimated for both New Hanover and Sampson Counties, which further supports the aforementioned hypotheses.

Increases in  $\text{NH}_4^+$  deposition were seen at all sites though most dramatically at Clinton (x 2.1), and minimally at Lewiston (x 1.3). All sites but Clinton saw increases in  $\text{NO}_3^-$  deposition, while  $\text{SO}_4^{2-}$  and NSS increased at UNCW alone. A population increase and resultant emissions from increased automobile traffic, as well as an increase in industrial activity and energy production in the region is probably reflected in the increased wet deposition of  $\text{NO}_3^-$  and NSS at UNCW. Table 8 compares the measured change in  $\text{H}^+$  concentration from 1990 – 2002/3 to the change in  $\text{H}^+$  predicted from changes in major rainwater components affecting acidity for four NADP sites and UNCW. The predicted  $\Delta\text{H}^+$  value is based on a simple ion balance condition where  $\Delta\text{H}^+_{\text{actual}} \cong \Delta\text{H}^+_{\text{Predicted}} = \Delta\text{NO}_3^- + 2\Delta\text{NSS} - \Delta\text{NH}_4^+$ . This condition will not be met if there are either additional components in rainwater affecting acidity not measured here. Overall sites considered in this calculation meet the condition.  $\Delta\text{H}^+$  predicted regressed to  $\Delta\text{H}^+$  measured for all sites gives an  $R^2$  of 0.863. UNCW, though, underestimates the measured  $\Delta\text{H}^+$  by 47%. Ion balance calculations for Clinton and Lewiston overshoot the measured  $\text{H}^+$  concentration by 26% and 21% respectively. The greater change than predicted at UNCW could be a result of some component of rainwater in our more industrialized region not measured in this study. Rainfall data was further subdivided to determine seasonal and diurnal trends and compared to older data.

Table 8. Change in VWA concentration ( $\Delta$ ) of  $H^+$ ,  $NH_x$ ,  $NO_3^-$ , and  $SO_4^{2-}$  based on values given in Table 1 for UNCW, and Clinton, Jordan Creek, and Lewiston NADP sampling sites. The values for Finley Farm and the Kennedy Space Center (KSC) are taken from the NADP datasets representing the same time periods as those in Table 1.

	<b>UNCW</b>	<b>Clinton</b>	<b>Lewiston</b>	<b>Jordan Creek</b>	<b>Finley Farm</b>	<b>KSC</b>
$\Delta H^+$	-11.6	-22.9	-11.6	-10.7	-11.9	-15.0
$\Delta NH_x$	1.1	9.3	-0.1	1.0	-1.6	-1.1
$\Delta NO_3^-$	- 1.7	-5.2	-1.5	-3.2	-3.1	-4.2
$\Delta NSS$	- 1.7	-7.1	-6.3	-4.9	-5.6	-5.4
$\Delta SO_4^{2-}$	- 1.3	-7.5	-5.7	-5.3	5.9	-5.9
% $\Delta$ Rain	36%	33%	29%	36%	32%	35%
$\Delta H^+_{\text{predicted}}$	-6.2	-28.7	-14.0	-14.0	-12.7	-16.2
$(\Delta H^+ - \Delta H^+_{\text{predicted}})$	-5.4	5.9	2.4	3.3	0.7	1.2
%Difference	47%	-26%	-21%	-31%	-6%	-8%

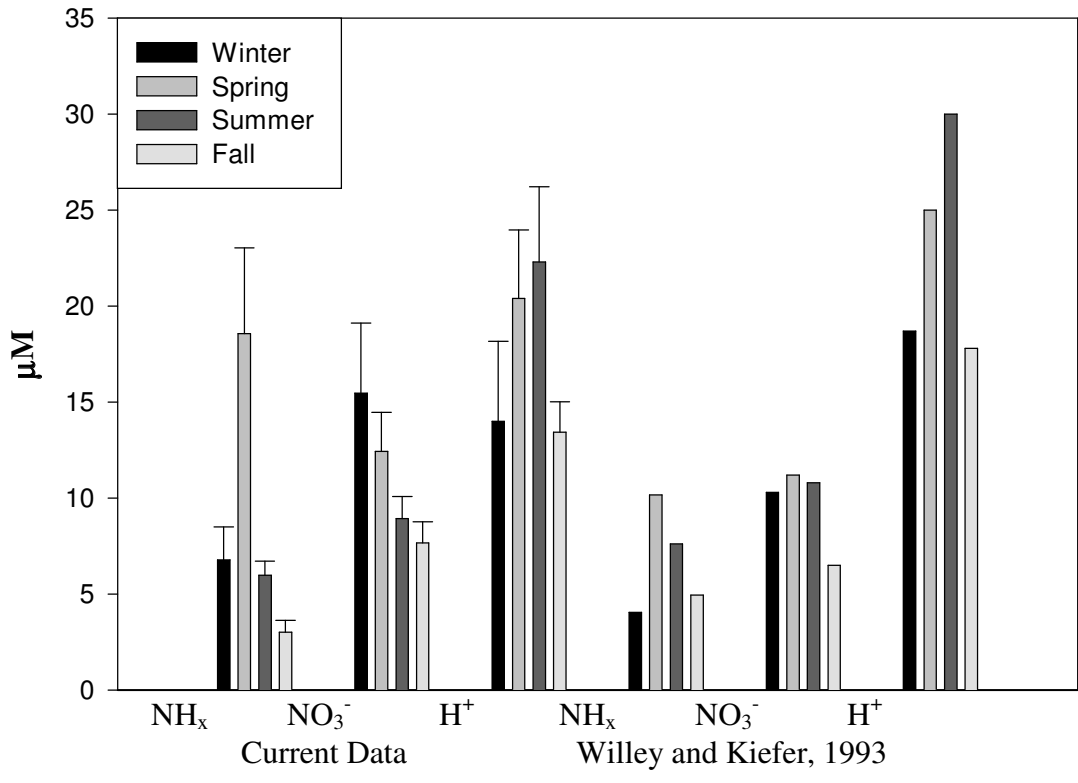


Figure 14. Seasonal averages from VWA concentrations in rainwater at UNCW for the current study (163 cm rainfall) and from 1988-1990 in Willey and Kiefer (1993) (120 cm rainfall).

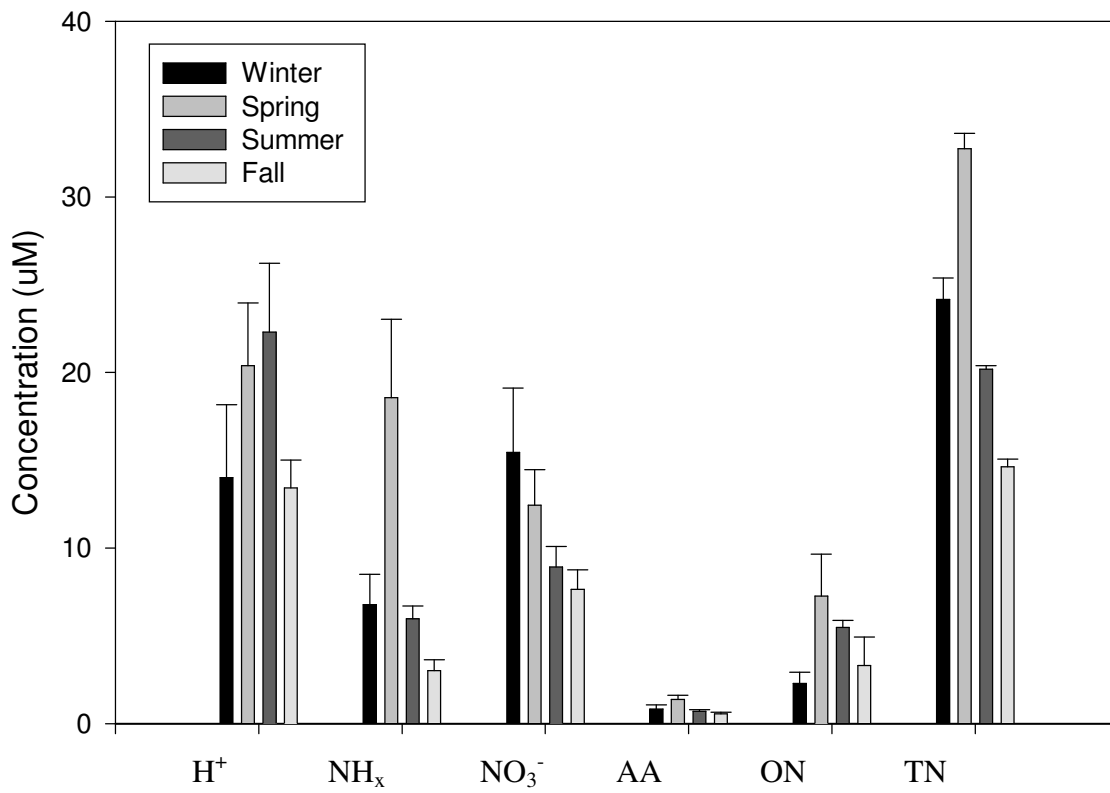


Figure 15. Seasonal VWA concentrations of H<sup>+</sup>, NH<sub>x</sub>, NO<sub>3</sub><sup>-</sup>, AA, ON and TN at UNCW.

Seasons were defined as winter: January 1 – March 31, and summer: July 1-September 30. The data are presented in Figures 14 and 15. Seasonal averages of N analytes reach a maximum ( $p < 0.05$ ) in the spring with the exception of  $\text{NO}_3^-$ . The springtime maximums of  $\text{NH}_4^+$ , AA, and TN are believed to be a result of increased agricultural activity: this includes emissions from fertilizer application and volatilization from livestock waste lagoons (Aneja, 2001; Walker, 2000). For  $\text{NH}_x$ , the marked increase in springtime concentration for both the 1988-1990 and current data could be due to a large decrease in  $\text{NH}_3$  solubility associated with a seasonal increase in temperature. According to Stumm and Morgan (1996), a temperature increase from  $10^\circ\text{C}$  to  $25^\circ\text{C}$  reduces the gassolubility constant (Henry's Law constant) by more than a factor of 2. This fits well with the near tripling of  $\text{NH}_x$  in rain from winter to spring. The large difference, though, in the  $\text{NH}_x$  springtime maximums between 1988-1990 and the present seen in Figure 14 could be directly linked to a jump in emissions associated with the liming of livestock lagoons and crop soils, and the application of fertilizers. In the spring, livestock waste is applied as fertilizer to crop fields; additionally, soil and waste liquid pH is controlled by the addition of basic compounds (Barker, 1996a; Barker, 1996b). These common practices increase  $\text{NH}_3$  volatility from soils, waste slurries and fertilizers. In conjunction with the increase in livestock farming in the region, this would explain the extreme increase in the springtime rainwater  $\text{NH}_x$  concentrations between the two periods at UNCW.

Time-of-day analysis included four categories: 1. 12:00AM – 6:00AM, 2. 6:00AM – 12:00PM, 3. 12:00PM – 6:00PM, 4. 6:00PM – 12:00AM. The time classifications were the same as those in earlier studies of rainwater composition at this site. Figure 16 presents the results of the diurnal analysis for the major N species in rainwater measured during this study. A minimum for all analytes occurs from 6:00 AM – 12:00 PM ( $p < 0.05$ ). A similar study done at this site

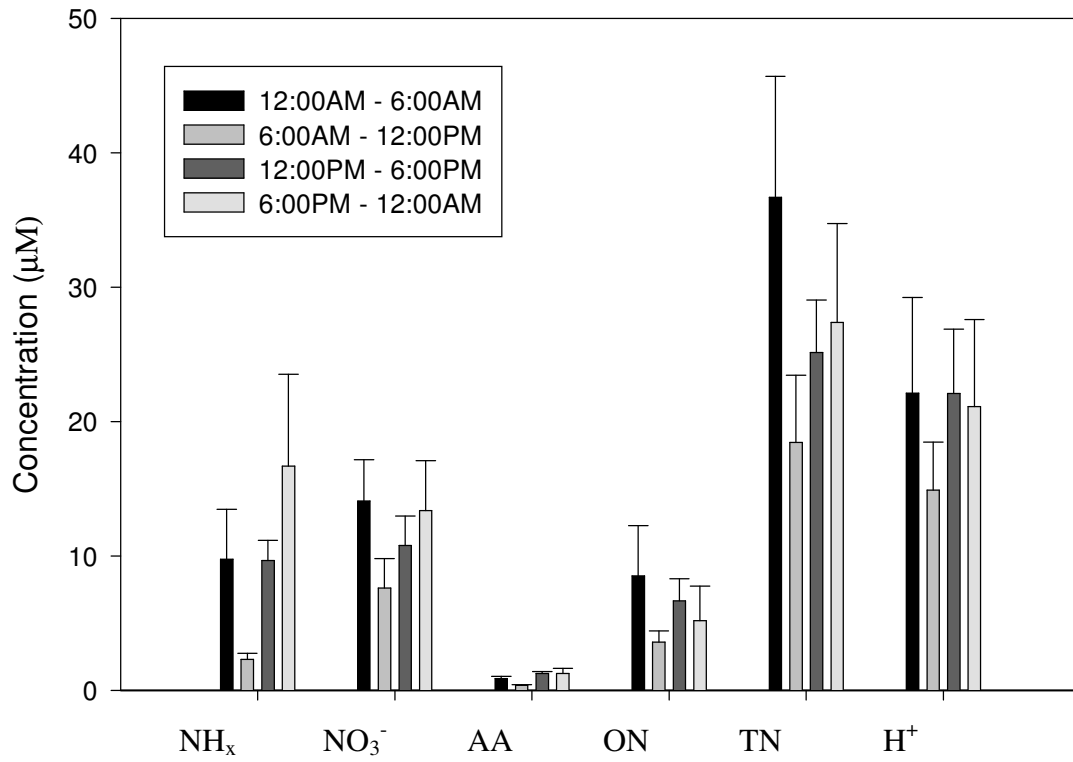


Figure 16. Diurnal VWA Concentrations of H<sup>+</sup>, NH<sub>x</sub>, NO<sub>3</sub><sup>-</sup>, AA, ON and TN at UNCW.

determined that the early morning minimum of rainwater components of gas-phase origin is a result of wet-removal by dew condensation (Avery, 2001).

#### Air mass Back-trajectories

In order to assess any variability in rainwater concentrations that can be linked to general meteorological conditions, air mass back trajectories were calculated for each precipitation event. These trajectories are shown in Figure 17. Table 9 shows volume-weighted average concentrations for analytes versus trajectory category based on the five categories outlined in the methods section. An analysis of concentrations as a function of air-mass origin shows a maximum from trajectory 2 for all N analytes ( $p < 0.05$ ) except ON. Acid ( $H^+$ ) deposition also has a maximum from trajectory 2 ( $p < 0.05$ ). In contrast to trajectory 2, the event air masses of marine origin in trajectory 5 had the lowest concentration of  $NH_x$  ( $p < 0.05$ ) and were near the minimum concentration of the remaining analytes with the lone exception, again, being ON.

These results illustrate that a majority of rainfall acidity and N content originates from regions containing urban centers and industry – mainly to the south and west. This includes both trajectories 2 and 4. While trajectory 2 is characterized as terrestrial and number 4 as coastal, both of the pathways cross major urban centers in the southeast.

Nitrate in rainfall shows a distinct directional based on broad sources: trajectory 5 contributes less due to the lack of  $NO_x$  emissions in oceanic air masses, while the terrestrially affected trajectories (2, 3 and 4) are much higher in  $NO_3^-$ . This pattern is consistent with the location of the collection site at UNCW. It is surrounded by widespread  $NO_x$  sources except in the direction of the Atlantic Ocean (Figure 12). The maximum in trajectory 2 is consistent with the location all of the major urban centers in the southeast. A minimum from trajectory 1 is possibly due to the

Figure 17. Plots of air mass back-trajectories calculated from the HYSPLIT model grouped by trajectory classification.

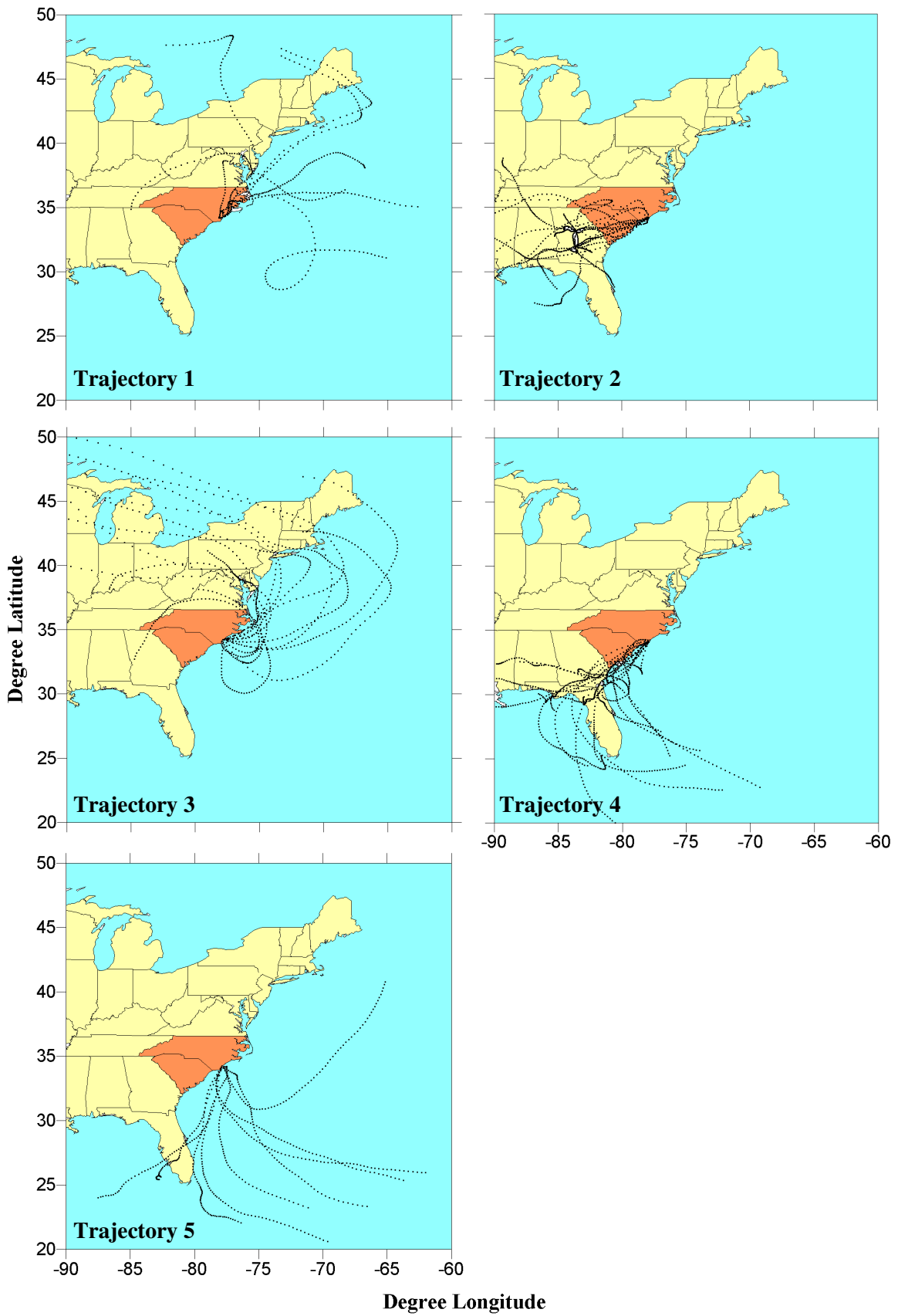


Table 9. Total rain, rainfall per event, and VWA concentrations, by trajectory category, of H+ and N analytes in rainwater at UNCW for the current sampling period. Red and blue values are maximum and minimum values respectively. Statistically significant values (p<0.05) based on a Student's T-test are marked with an asterisk.

Trajectory (n)	Total Rain (cm)	Rain per Event (cm)	NH <sub>4</sub> <sup>+</sup> (μM)	NO <sub>3</sub> <sup>-</sup> (μM)	AA (μM)	TN (μM)	ON (μM)	H <sup>+</sup> (μM)
1 (8)	<b>232.4</b>	<b>29.1</b>	5.5	<b>4.7*</b>	<b>0.49</b>	<b>16.1</b>	<b>4.3</b>	<b>9.9</b>
2 (15)	257.3	17.2	<b>22.8*</b>	<b>16.2*</b>	<b>1.7*</b>	<b>39.3*</b>	5.3	<b>35.6*</b>
3 (15)	304.8	20.3	16.0	13.2	1.5	29.5	4.7	15.4
4 (15)	294.1	19.6	7.0	12.6	0.84	24.6	<b>6.6</b>	27.6
5 (23)	<b>391.0</b>	<b>17.0</b>	<b>4.0*</b>	8.2	0.50	18.4	6.1	13.6

combined effects of higher a rainfall average, better dry deposition due to turbulent mixing, and relatively lower emissions to the north of Wilmington.

$\text{NH}_x$  had a maximum from trajectory 2 and a minimum from trajectory 5 ( $p < 0.05$ ). Rainfall amounts associated with these trajectories were low which might explain the higher concentrations. Trajectories 1, 2, and 4 could potentially be affected by emissions from livestock farms. While trajectories 2 and 3 contributed higher amounts of  $\text{NH}_x$  in accordance with these emissions, trajectory 1 had a very low concentration. AA followed a similar pattern. Amino acids are not known to be components of urban emissions, though some compounds in the urban and coastal atmosphere are known to be involved in the breakdown of organic aerosols (Bari, 2003; Blando, 2000; Mopper and Zika, 1987). This mechanism could increase the AA signal as more complex ON forms are reduced to free amino acids in the region. The similar trend in AA concentration from trajectory 3 suggests a similar source though this has yet to be revealed. Air masses of purely oceanic origin contribute the least to  $\text{NH}_x$  and AA in rainfall (Trajectory 5).

Organic nitrogen (ON) demonstrates more uniformity between trajectories. This would suggest that ON has a different source function than the other N species studied.

### Particle Dry Deposition

Table 10 presents the overall and seasonal particle dry deposition totals. Dry deposition rates of  $\text{NH}_4^+$ ,  $\text{NO}_3^-$  and AA represent 11%, 22% and 24% of their respective total depositions (wet + dry).  $\text{SO}_4^{2-}$  and NSS dry deposition rates are 15% and 16% of their respective total depositions. An  $\text{NH}_4^+$  maximum occurs in the summer ( $p < .05$ ), which fits a seasonal pattern resembling that of modeled results (Robarge, 2002). The dissimilarity between dry and wet deposition  $\text{NH}_x$  seasonality patterns (particularly the summer versus springtime maximum) could be caused by

Table 10. Average overall and seasonal particle dry deposition in  $\mu\text{moles} \cdot \text{m}^2 \cdot \text{d}^{-1}$  measured at UNCW between August 21, 2002 and August 21, 2003.

	<b>n</b>	<b>NH<sub>4</sub><sup>+</sup></b>	<b>NO<sub>3</sub><sup>-</sup></b>	<b>AA</b>	<b>SO<sub>4</sub><sup>2-</sup></b>	<b>NSS</b>
<b>Overall</b>	32	5.6 ± 7	14 ± 11	1.3 ± 0.6(n=11)	12 ± 10	9.9 ± 9.6
<b>Winter</b>	4	2.9 ± 2.3	11 ± 11	2.3 ± n/a (n=1)	7.5 ± 9.4	6.8 ± 9.5
<b>Spring</b>	7	3.9 ± 3.6	15 ± 17	0.9 ± 0.6(n=4)	12 ± 11	10 ± 11
<b>Summer</b>	17	7.6 ± 8.7	14 ± 8	1.4 ± 0.4(n=6)	12 ± 10	10 ± 9.6
<b>Fall</b>	4	2.2 ± 1.2	n/a	n/a	n/a	n/a

local NH<sub>3</sub> emissions affecting dry deposition while regional transport governs rainfall amounts. ANOVA results show no significant extremes for other analytes. Zhang et al. (2003) demonstrated that, in Northern California, amino acid aerosols (PM<sub>2.5</sub>) maintain consistent concentrations throughout the year consistent with the lack of seasonality observed in this study. The uniformity of dry-deposited NO<sub>3</sub><sup>-</sup> and SO<sub>4</sub><sup>2-</sup> between seasons seems to reflect a continuous emission from local anthropogenic sources. In contrast to dry deposition, a seasonal pattern in rainfall was observed, though the reason for this dissimilarity are not clear, it is possibly a result of different mechanisms contributing to rainfall concentrations than those of dry deposition amounts (Asman, 1995; Aneja, 1998; Chate, 2003; Zhang, 2001; Pryor, 2002).

One possible source of error exists in the difference between the collection efficiency of gravitationally settled particles in polyethylene buckets and the common form of NH<sub>4</sub><sup>+</sup>, and NO<sub>3</sub><sup>-</sup> aerosols. A deposition study by Willey and Kiefer (1993) at the same UNCW site using polyethylene buckets showed a similar lack of seasonality for NO<sub>3</sub><sup>-</sup>, and SO<sub>4</sub><sup>2-</sup>. Buckets tend to collect only aerosol particles that deposit by gravitational settling (1 – 10 μm size range) (Willey and Kiefer, 1993). A substantial portion of NO<sub>3</sub><sup>-</sup> and a majority of NH<sub>4</sub><sup>+</sup> aerosols, though, exist as accumulation mode particles (0.1 – 2 μm size range) that are controlled by Brownian motion and not deposited by gravitational settling (Zhuang, 1997; Pryor and Barthelmie, 2000; Yeatman, 2001). Therefore, the measurement of dry deposition by our method is possibly and underestimation and not representative of actual dry deposition at UNCW.

In order to test the validity of our dry deposition results, a rough NH<sub>4</sub><sup>+</sup> dry deposition amount can be estimated based on the flux calculation,

$$F_d = V_d \cdot C_A$$

where  $F_d$  is the flux of  $\text{NH}_4^+$  ( $\mu\text{M}\cdot\text{m}^{-2}\cdot\text{s}^{-1}$ ),  $V_d$  is the dry deposition (piston) velocity for  $\text{NH}_4^+$  ( $\text{m}\cdot\text{s}^{-1}$ ), and  $C_a$  is the  $\text{NH}_4^+$  aerosol concentration ( $\mu\text{M}\cdot\text{m}^{-3}$ ). Using a  $V_d$  value of 0.001, based on reported values of  $\text{NH}_4^+$  dry deposition to dry surfaces, and an  $\text{NH}_4^+$  aerosol concentration ( $C_a$ ) of 0.08 (reported in Robarge et.al. (2002) for coastal NC) one gets a daily dry deposition of about 7  $\mu\text{moles NH}_4^+ \cdot \text{m}^{-2} \cdot \text{d}^{-1}$ . This is similar to the results presented in table 10 suggesting our measurement is representative of  $\text{NH}_4^+$  dry deposition at UNCW.

The  $\text{NH}_x$  dry deposition measurement in table 10 is similar to other sites while  $\text{NO}_3^-$  deposition exceeds reported values by an order of magnitude; though it is similar to  $\text{NO}_3^-$  deposition measured at UNCW previously (1988-1990) (Table 11). The site's proximity to a major interstate and imbedded in a growing urban area where  $\text{NO}_3^-$  emissions are high would result in a comparatively higher deposition. Though  $\text{NO}_3^-$  aerosol concentrations are not known for Wilmington,  $\text{NO}_3^-$  concentrations are considerably higher in urban areas (Bari, 2003).

Table 12 compares current dry deposition at UNCW to amounts measured from 1988 through 1990 at the same site using the same method. Chloride ( $\text{Cl}^-$ ) is presented to provide a reference point for other analytes. Dominated by sea salt in coastal regions, the similarity between the two values validates the integrity of the dataset used in the current study. Small changes in  $\text{Cl}^-$  deposition most likely reflect natural variability in dry deposition. The results show that dry depositions of  $\text{SO}_4^{2-}$  as well as analytes of known anthropogenic origin -  $\text{NO}_3^-$  and NSS – remained relatively unchanged suggesting their aerosol concentrations have not increased. As well, the dry depositions of NSS and  $\text{NO}_3^-$  do not reflect local increases in known sources of these analytes - mainly automobiles, and industry. If dry deposition was governed by a local source we would expect to see an increase in  $\text{NO}_3^-$  and NSS dry deposition amounts. Consistent with the long-range transport potential of aerosols, these results probably reflect deposition from

Table 11. Particle dry deposition of  $\text{NH}_x$  and  $\text{NO}_3^-$  in  $\mu\text{moles} \cdot \text{m}^2 \cdot \text{d}^{-1}$  for UNCW and for various geographic locations.

<b>Location</b>	<b><math>\text{NH}_4^+</math> (<math>\mu\text{moles} \cdot \text{m}^2 \cdot \text{d}^{-1}</math>)</b>	<b><math>\text{NO}_3^-</math> (<math>\mu\text{moles} \cdot \text{m}^2 \cdot \text{d}^{-1}</math>)</b>	<b>Collection Method</b>	
<b>UNCW-Present</b>	5.55	13.8	Polyethylene Surface	
<b>UNCW-1988-1990</b>	4.4	13.2	Polyethylene surface	Willey and Kiefer, 1997
<b>Niwot Ridge, CO</b>	6.23	1.54	Gradient Method	Ratray and Sievering, 2001
<b>WY</b>	2.74	0.39	Inferential Model	Lawrence, 2000
<b>Oxford, OH</b>	14.7	2.94	Inferential Model	“
<b>Parsons, WV</b>	9.59	0.78	Inferential Model	“
<b>Tampa Bay, FL</b>	4.11	1.17	Inferential Model	Poor, 2001

Table 12. Particle dry deposition ( $\text{mmoles} \cdot \text{m}^{-2} \cdot \text{y}^{-1}$ ) and %Change of  $\text{NH}_x$ ,  $\text{NO}_3^-$ ,  $\text{SO}_4^{2-}$ , NSS, and  $\text{Cl}^-$  at UNCW for the periods from 1988 through 1990 and between August 2002 and August 2003.

	<b>1988 - 1990</b>	<b>Aug, 2002 – Aug, 2003</b>	<b>% Change</b>
<b><math>\text{NH}_4^+</math></b>	1.6	2.0	25%
<b><math>\text{NO}_3^-</math></b>	4.8	5.0	4%
<b><math>\text{SO}_4^{2-}</math></b>	4.2	4.2	0%
<b>NSS</b>	3.7	3.6	-3%
<b><math>\text{Cl}^-</math></b>	11.1	12.3	11%

regional sources. The 27% increase in ammonium deposition does, however, indicate an increase in ammonium aerosol concentration at this location. This may have resulted from a combination of increased livestock production in the region and increased local sources.

In lieu of the highlighted issues associated with the method of dry deposition collection used here, these results can still be considered representative of a long-term trend in analyte aerosol concentration since the sampling methods are the same. Research has demonstrated the conservative nature of aerosol particle size distributions (Zhuang, 1997; Ottley and Harrison, 1992; Yeatman, 2001). Therefore this change reflects an overall change in total aerosol concentration.

#### Gas-Phase Ammonia

Table 13 summarizes ammonia gas concentrations for various locations including the current study. Ammonia concentrations are high for the region, averaging 8.2 ppbv compared to 7.9 at Clinton located within a region of very high  $\text{NH}_3$  emissions. It has been suggested that a majority of ammonia gas is lost (by deposition and conversion to aerosols) within 2.5 kilometers of its source (Dragonsits et al., 2002); therefore our result most likely reflects the sampling site's proximity to  $\text{NH}_3$  sources. Studies have shown foliage and soils to be either  $\text{NH}_3$  sources or sinks based on the ambient concentration and temperature (Roelle, 2002; Schjoerring, 1997). As well, vehicles equipped with catalytic converters emit significant amounts of  $\text{NH}_3$  that can greatly alter local concentrations (Durbin, 2002). In Rome, Italy  $\text{NH}_3$  concentrations adjacent to major thoroughfares were consistently 5 times higher than the urban background due to traffic emissions ranging from 19.3 to 29.1 ppbv at traffic locations and 4.1 to 7.0 ppbv in the urban background (Perrino, 2002). A seasonal trend shows higher concentrations occurring during

Table 13. A comparison of NH<sub>3</sub> (g) measurements (ppbv) made at UNCW and different geographic locations in N. America.

<b>Location - Date</b>	<b>Annual</b>	<b>Winter</b>	<b>Spring</b>	<b>Summer</b>	<b>Fall</b>	
UNCW : Current Study	8.2	4.5	12.2	16.2	0.10	
Clinton, NC: Oct 1998 – Sept 1999	7.9	2.6	7.1	15.0	4.3	Robarge, 2002
Kinterbish, AL: 1992	-	-	-	0.69	-	Langford, 1992
Oak Ridge, TN	-	-	-	0.30	-	Langford, 1992
North Inlet, SC	-	-	-	0.30	-	Langford, 1992

warmer periods consistent with other studies revealing that atmospheric ammonia emissions vary in proportion to temperature (Perrino, 2002; Robarge, 2002; Schjoerring, 1997). No evidence was found that suggests rainwater ammonium is affected by surface ammonia gas concentrations; though a kinetic study of ammonia gas versus rainwater ammonium reveals similarities in long-term trends. Studies have consistently shown that ammonia gas at the surface is not a major contributor to rainwater concentrations (Chate, 2003; Asman, 1995; Shimshock, 1989). Gas measurements made throughout the span of one day show increased  $\text{NH}_3$  concentrations near noon (Figure 18). Similar studies have found diurnal patterns in ammonia concentrations based on numerous sources and sinks that depend on the time-of-day – mainly the effect of temperature on solubility and biological activity (Aneja, 2002; Ross and Jarvis, 2001; Schjoerring, 1997). Our results do not reflect diurnal variations in emissions from automobile traffic since the highest traffic emissions occur in the morning and afternoon, which could be a result of the high loss rate of ammonia due to dry deposition and conversion to aerosols within a short distance after emission.

#### Deposition to the Cape Fear River Estuary (CFRE)

The Cape Fear River Estuary is defined, for this study, as the body of water from Memorial Bridge in Wilmington, NC, south to Fort Fisher, NC. It has a water surface area of  $87.6 \text{ km}^2$  based on GIS calculations of on USGS digital hydrology maps. Raster-based model calculations determined the water volume for the estuary to be 253 million  $\text{m}^3$  (Ensign, In-Press). This yields an average depth of about 2.9 m for the entire estuary. Wet deposition per unit area for the sample year ( $D_{\text{total}}, \mu\text{moles} \cdot \text{m}^{-2}$ ) was calculated by multiplying the rainwater VWA

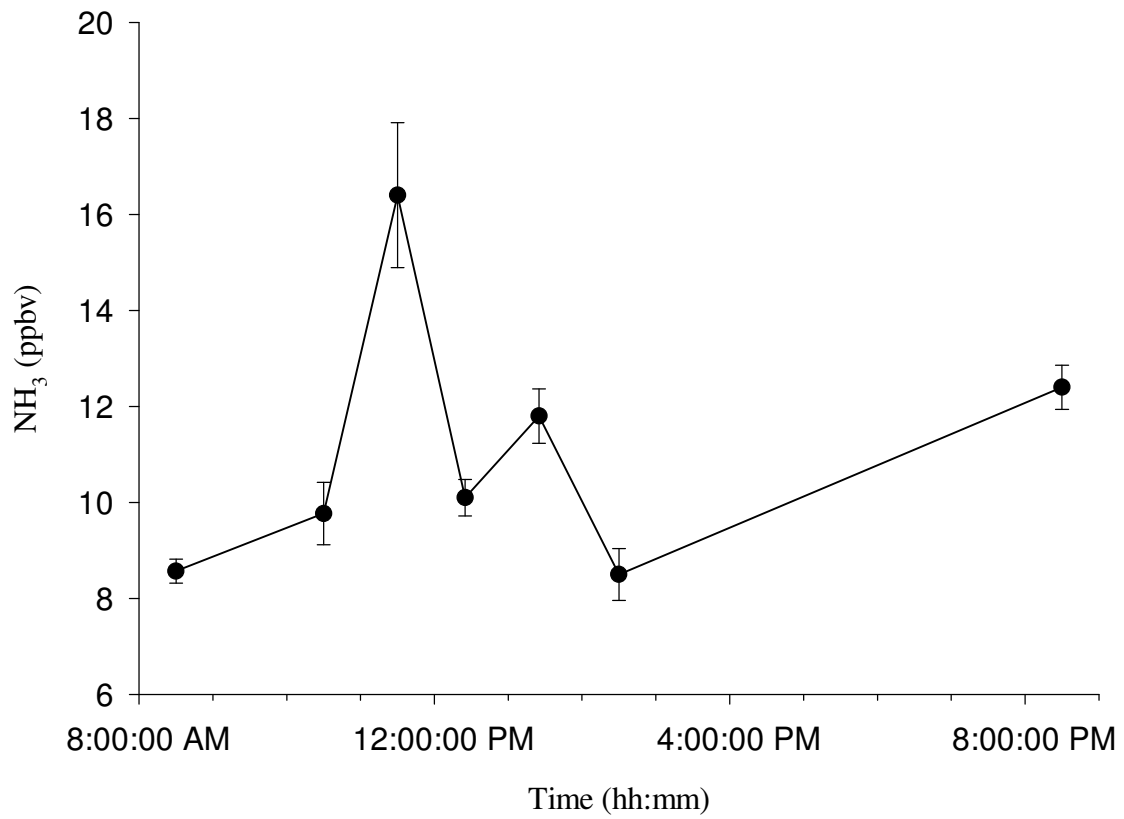


Figure 18. NH<sub>3</sub> (g) (ppbv) measured by condensate collection at UNCW throughout the day of July 29, 2003.

concentration of analyte X ( $C_x$ , in  $\mu\text{moles per liter}$ ) by the total rainfall ( $P_{total}$ , mm) measured at UNCW as

$$D_{total} = C_x \cdot P_{total} \cdot$$

Total wet deposition to the estuary ( $\mu\text{moles}$ ) is equal to  $D_{total} \cdot 8.762 \times 10^7 \text{ m}^2$ . Dry deposition to the CFRE is  $F_d \cdot 8.76 \times 10^7 \text{ m}^2$  where  $F_d$  is the dry deposition flux measured at UNCW. The results are given in table 14.

Overall, dry deposition rates of  $\text{NH}_4^+$ ,  $\text{NO}_3^-$  and AA represent 11%, 22% and 24% of their respective total depositions (wet + dry). Two assumptions are in this calculation. 1) There is no spatial variability in wet or dry deposition for the region including the CFRE and UNCW. Given the relatively small size of the CFRE, and the sampling site proximity to the estuary, this is likely a reasonable assumption. 2) Dry deposition to the polyethylene surface at UNCW is the same as to the CFRE water surface. Studies have shown, however, that, due to their hygroscopicity,  $\text{NH}_4^+$  and  $\text{NO}_3^-$  aerosols dry-deposit more efficiently to wet surfaces than dry ones (Pryor and Barthelmie, 2000; Wesely, 2000; Kou-Fang Lo, 1999; Dasch, 1985). This suggests that the measured dry deposition at UNCW for this study may underestimate actual dry deposition to the CFRE. Based on the fraction of coarse mode particles in total  $\text{NH}_4^+$  and  $\text{NO}_3^-$  aerosols (19% to 45% for  $\text{NH}_4^+$  and 51% to 81% for  $\text{NO}_3^-$ , Yeatman, 2001),  $\text{NH}_4^+$  and  $\text{NO}_3^-$  dry deposition measured at UNCW may also be underestimated because not all particle sizes are sampled with a polyethylene surface. Though  $\text{HNO}_3$  gas was not measured in this study, Poor et al. (2001) estimated a gas deposition of  $12 \mu\text{moles HNO}_3 \cdot \text{m}^2 \cdot \text{d}^{-1}$  to the Tampa Bay Estuary from a 3-year average  $\text{HNO}_3$  concentration of 0.50 ppbv. This value is similar to the 0.43 ppbv measured by Robarge et al. (2002) at Clinton, NC between October 1998 and September 1999. Given the uniformity of  $\text{NO}_3^-$  concentrations in rainwater, this value is likely a good regional estimate.

Table 14. Wet, Dry, and Total (Wet + Dry) Deposition of  $\text{NH}_x$ ,  $\text{NO}_3^-$ , AA, and TN to the CFRE. The %Dry Values are Calculated Relative to Total Depositions.

	<b>Deposition (<math>\mu\text{moles} \cdot \text{m}^2 \cdot \text{d}^{-1}</math>)</b>			
	<b>Wet</b>	<b>Dry</b>	<b>Total</b>	<b>%Dry</b>
$\text{NH}_4^+$	45.1	5.55	50.7	11%
$\text{NO}_3^-$	49.6	13.8	63.4	22%
AA	4.2	1.3	5.5	24%
TN	110.8	-	-	-

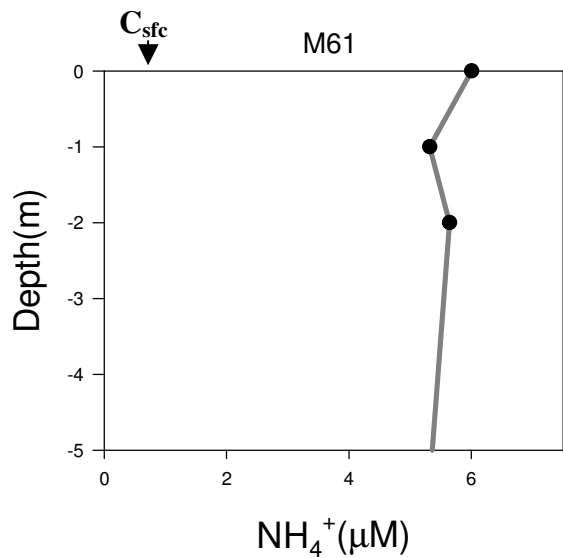
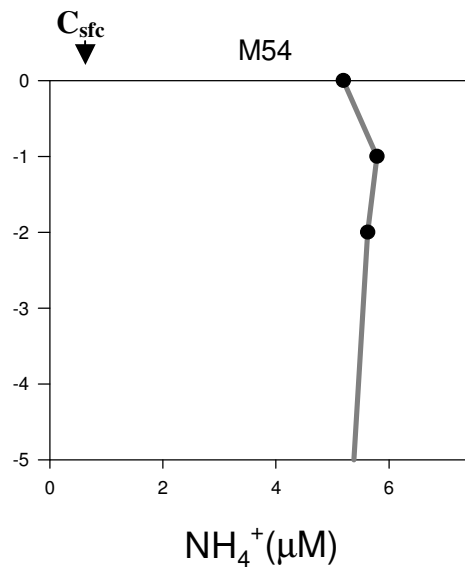
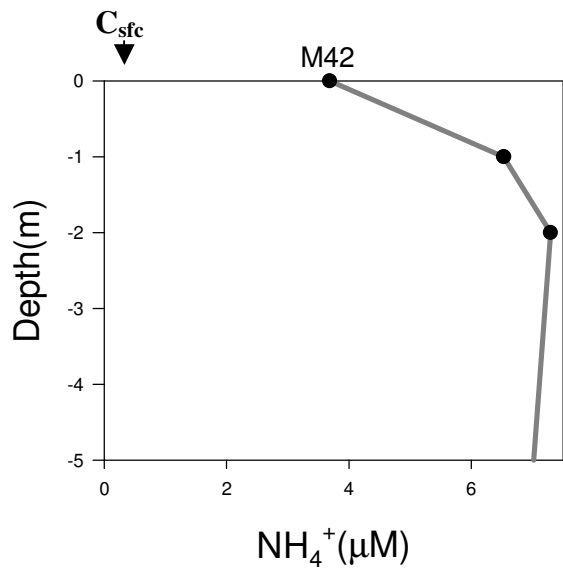
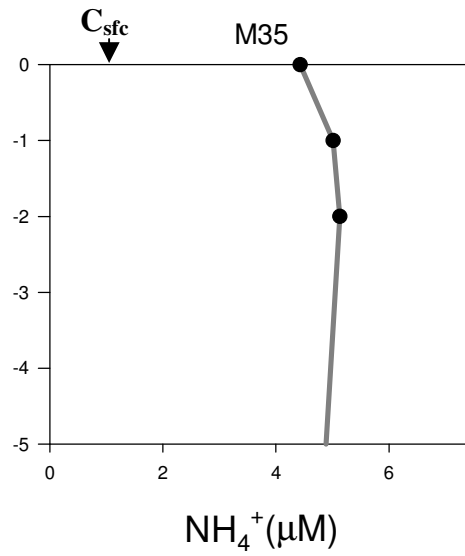
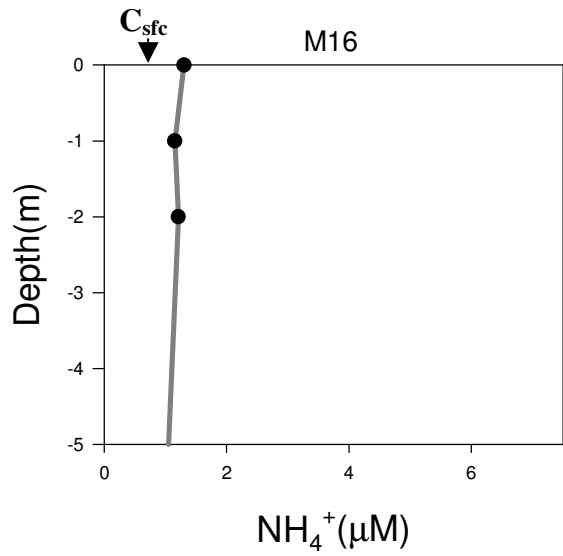
Since Dasch (1985) determined that a polyethylene surface does not collect gaseous HNO<sub>3</sub>, this suggests that there is a significant source of NO<sub>3</sub><sup>-</sup> to the CFRE in addition to the particle flux measurements taken for this study that could double our calculated daily flux to the CFRE.

Analysis of gas transfer at the air-water interface is important in determining the overall impact of total atmospheric deposition. Studies made in the North Sea have determined that estimates of total dry deposition may be considerably overestimated due to errors in flux calculations of ammonia gas (Sorensen, 2003). Predicted surface water NH<sub>4</sub><sup>+</sup> concentrations (C<sub>sfc</sub>) based on NH<sub>3</sub> (g) measurements taken at sites along the CFRE were calculated based on

$$C_{sfc} = P_{NH_3} \cdot [H^+] \frac{K_D \cdot K_H}{K_w}$$

where P<sub>NH<sub>3</sub></sub> is the NH<sub>3</sub>(g) concentration measured on the R.V. Cape Fear, and [H<sup>+</sup>] is the hydrogen ion concentration of the surface water. K<sub>D</sub> is the dissociation constant of aqueous ammonia and K<sub>H</sub> is the Henry's Law constant for NH<sub>3</sub>(g) adjusted for air-temperature. K<sub>w</sub> is the solubility product of water. These were compared to measured surface water NH<sub>4</sub><sup>+</sup> taken at the same time as the NH<sub>3</sub> (g) measurements. The results show that surface water concentrations exceed values predicted from gas-phase based calculations by 1 order of magnitude. Gas-phase measurements were made at approximately 2m above the water surface. From gas-exchange theory based on transfer through a stagnant surface layer, gas measurements made at a 2m sampling height would not represent concentrations at the air-water interface. In addition, an adequate determination of flux direction cannot be made from our gas-phase NH<sub>3</sub> measurements without more than one measurement in the vertical to determine a vertical gradient. Instead, vertical water column NH<sub>4</sub><sup>+</sup> profiles, given in Figure 19, taken at different sites along the CFRE can be used to determine a direction of flux. An analysis of gradients at the surface, calculated

Figure 19. CFRE water column measurements of  $\text{NH}_x$  from M18, M35, M42, M54, and M61 from 0 to 5 meters depth (based on measurements of the entire water column) taken on April 22, 2003.  $C_{\text{sfc}}$  is the surface water concentration of  $\text{NH}_x$  ( $\mu\text{M}$ ) calculated from  $\text{NH}_3$  (g) measurements taken over the CFRE on the same day.



from

$$\nabla_z \text{NH}_x = \frac{C_0 - C_{-1}}{\Delta z}$$

where  $C_0$  and  $C_{-1}$  are the concentrations of  $\text{NH}_x$  at 0 and 1 m depth respectively, indicates a general flux out of the water column. Exceptions are station M18 at the extreme southern end of the sampling transect. At M18 there is essentially no flux, which may be the result of higher seawater content, higher pH, and a significantly lower  $\text{NH}_4^+$  concentration than other sampling sites on the CFRE. At sites M54 and M61 in the north the water column gradient does not suggest an outward flux though the difference between  $C_0$  and  $C_{\text{sfc}}$  could, in fact, indicate this. The overall outward flux trend for these data indicates that total dry deposition to the CFRE could be less than particulate deposition as a result of  $\text{NH}_3$  outgassing.

The potential change in concentration of the CFRE was determined based on daily deposition results for measured N species. Daily deposition rather than annual deposition was used because the residence time of the CFRE is approximately 3 days. These values are compared to average annual analyte concentrations for the estuary based on measurements made for 2001 – 2002 by the Lower Cape Fear River Program (LCFRP):  $\text{NH}_4^+$  was 5.7  $\mu\text{M}$ ,  $\text{NO}_3^-$  was 9.3  $\mu\text{M}$ , and TN was 66.6  $\mu\text{M}$ . The results presented in Table 15 represent the potential impact of direct atmospheric nitrogen deposition to the CFRE nutrient nitrogen budget on a daily basis. Wet, dry and total depositions per day are a small fraction of the estuarine nitrogen budget adding about 0.32% and 0.29% of total  $\text{NH}_x$  and  $\text{NO}_3^-$  in the CFRE respectively. Wet deposition adds 0.07% of TN to the estuarine budget. It is more realistic, though, to consider wet deposition on an event basis. In this case the impact is more pronounced depositing about 1% of the total for both  $\text{NH}_x$  and  $\text{NO}_3^-$  per event in the CFRE. More significant deposition events occurred contributing 20% and 6% depositions for  $\text{NH}_x$  and  $\text{NO}_3^-$  respectively, in the spring. Total nitrogen deposition

Table 15. Potential change in concentration of  $\text{NH}_x$ ,  $\text{NO}_3^-$ , and TN for the entire CFRE due to wet, dry, and total direct atmospheric depositions ( $\mu\text{M} \cdot \text{d}^{-1}$ ). Percentages are calculated relative to 2002 average surface concentrations of each analyte based on data from the Lower Cape Fear River Program (LCFRP).

	<b>Wet</b>	<b>Dry</b>	<b>Total</b>	<b>Per Rain Event</b>
$\Delta[\text{NH}_4^+]_{\text{CFRE}} (\mu\text{M} \cdot \text{d}^{-1})$	0.016	0.002	0.018	0.073
$\%[\text{NH}_4^+]_{\text{CFRE}}$	0.28%	0.04%	0.32%	1.3%
$\Delta[\text{NO}_3^-]_{\text{CFRE}} (\mu\text{M} \cdot \text{d}^{-1})$	0.017	0.005	0.022	0.080
$\%[\text{NO}_3^-]_{\text{CFRE}}$	0.18%	0.05%	0.24%	0.86%
$\Delta[\text{TN}]_{\text{CFRE}} (\mu\text{M} \cdot \text{d}^{-1})$	0.039	-	-	0.18
$\%[\text{TN}]_{\text{CFRE}}$	0.06%	-	-	0.27%

represented about 0.26% per event of the total nitrogen budget (maximum deposition of about 2%). For the sample period,  $\text{NH}_x$  wet deposition exceeded 1% of the total CFRE  $\text{NH}_x$  43 times (2 times greater than 10%), and  $\text{NO}_3^-$  deposition exceeded 1% 48 times though never greater than 6%. TN exceeded 1% only 6 times. The frequency of rain was about once every five days – compared to a 3-day residence time of water in the CFRE. Dry deposition for any measured analyte never exceeded a 0.5% for the entire year.

Over extended periods, it can be concluded that direct atmospheric deposition is not a significant source of N to the total CFRE N budget; though episodic wet deposition events can make major contributions.

#### Hurricane Isabel

Hurricane Isabel made landfall just north of Cape Lookout, North Carolina on September 18 2003 as a category-2 hurricane. The National Weather Service at Wilmington International Airport (ILM) reported maximum sustained winds of 45 mph. Rainfall began on the UNCW campus at approximately 1:30AM on the 18<sup>th</sup> and lasted until approximately 9:00PM the same day netting 6.0 cm (compared to 5.0 at ILM). Sequential rainfall samples were taken on the UNCW campus: A) 8:30AM (17.5 mm), B) 11:20AM (11.4mm), C) 2:30PM (21.8mm), D) 5:40PM (7.1mm), and E) 8:30AM (2.3 mm) the following day. Results from sequential samples are shown in Figures 20 and 21. A bulk sample was taken as well. Five NOAA/ARL HYSPLIT back-trajectories were calculated (according to standards employed for all rain data in this study) with the end-point time set to that when each sequential sample was collected. Data on rainfall intensity was linked with the trajectory points during calculation. Relative wind intensities were calculated by hand for each trajectory point based on distance traveled per unit time. Figures 22 and 23 are trajectories plotted against rainfall intensity and wind fields.

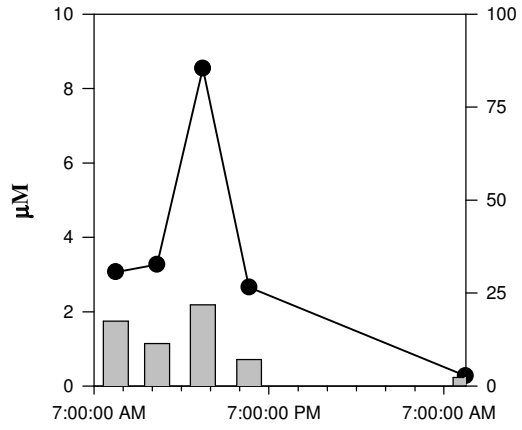
$\text{NH}_x$  and AA concentrations of the bulk sample were  $5.3 \mu\text{M}$  and  $1.8 \mu\text{M}$  respectively.  $\text{NH}_x$  and AA deposition values for the bulk samples were  $317 \mu\text{moles} \cdot \text{m}^{-2}$  and  $106 \mu\text{moles} \cdot \text{m}^{-2}$  respectively.  $\text{H}^+$  remains consistently low throughout the beginning and then jumps in acidity in sequential sample D after which it levels off again. The majority of a hurricane's moisture comes from seawater, which probably explains the low initial  $\text{H}^+$  concentrations. The increase may result from a transition from marine to continental air masses: trajectories D and E are completely terrestrial. This is supported by the  $\text{Cl}^-$  deposition sequence since the lowest values were from samples D and E. The highest  $\text{NH}_x$ , AA, NSS, and  $\text{Cl}^-$  depositions occurred in rain that fell between 11:20 AM and 2:30 PM (sequential sample C). The sequential profile suggests a complete washout of each of these analytes from the atmosphere by the end of the storm with the exception of AA.

The peak in  $\text{NH}_x$  concentration and deposition corresponds to trajectory C traversing major  $\text{NH}_x$  sources in conjunction with the high relative wind intensities that would aid  $\text{NH}_x$  transport. The concentration in trajectory C remains high in spite of heavy rain intensities that could scavenge  $\text{NH}_x$  from the air mass. Higher rain pH, though, would reduce scavenging efficiency. The washout of sequence sample E can be attributed to the air mass experiencing moderate rainfall intensity and a lower pH that would increase the aqueous retention of  $\text{NH}_x$  and promote scavenging.

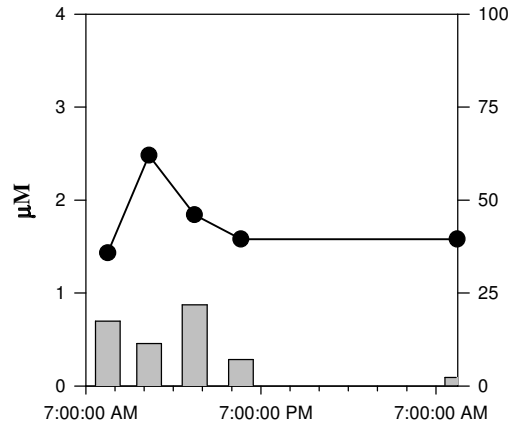
The variable initial concentrations and depositions of  $\text{Cl}^-$  highlight the abundance of seawater in tropical cyclones in conjunction with the extreme meteorological conditions associated with hurricanes. The reasons, though, for the dramatic drop in the  $\text{Cl}^-$  sequence at sample B are not clear. The sample C deposition maximum for NSS might indicate the influence of specific sources while the variability of  $\text{NO}_3^-$  depositions seems to reflect the widespread emissions

Figure 20. Results from sequential samples taken at UNCW during hurricane Isabel (September 18, 2003): a)  $\text{NH}_x$  concentration and Sequential rainfall amounts, b) AA concentration and sequential rainfall amounts, c)  $\text{H}^+$  concentrations, d)  $\text{NH}_x$  wet deposition amounts per sequential sample, and e) AA wet deposition amounts per sequential sample.

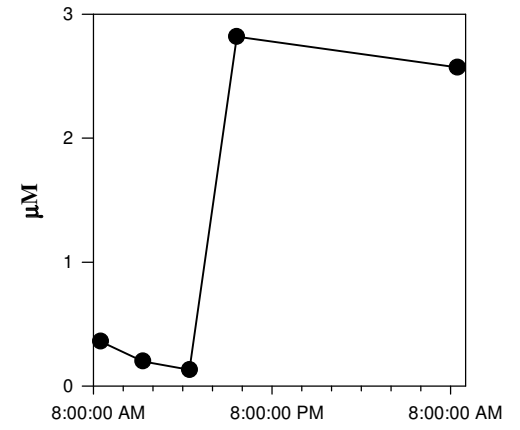
NH<sub>v</sub> Concentration



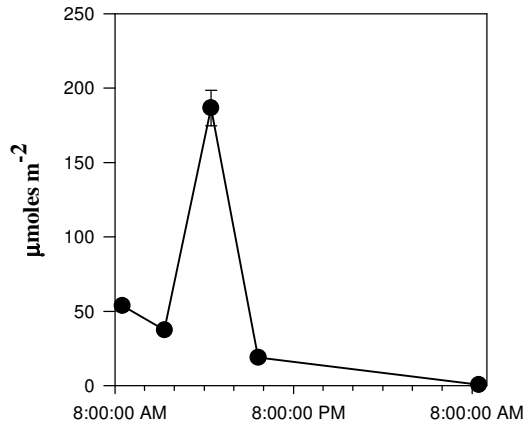
AA Concentration



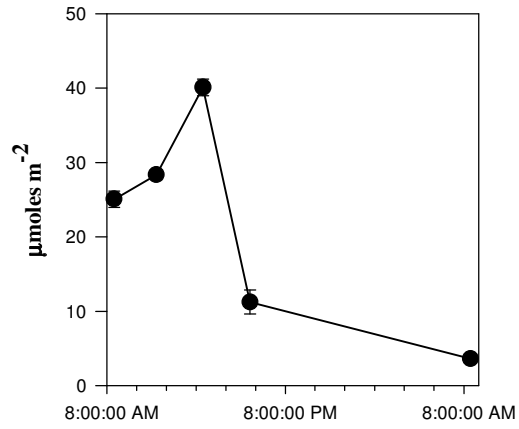
H<sup>+</sup> Concentration



NH<sub>v</sub> Deposition



AA Deposition



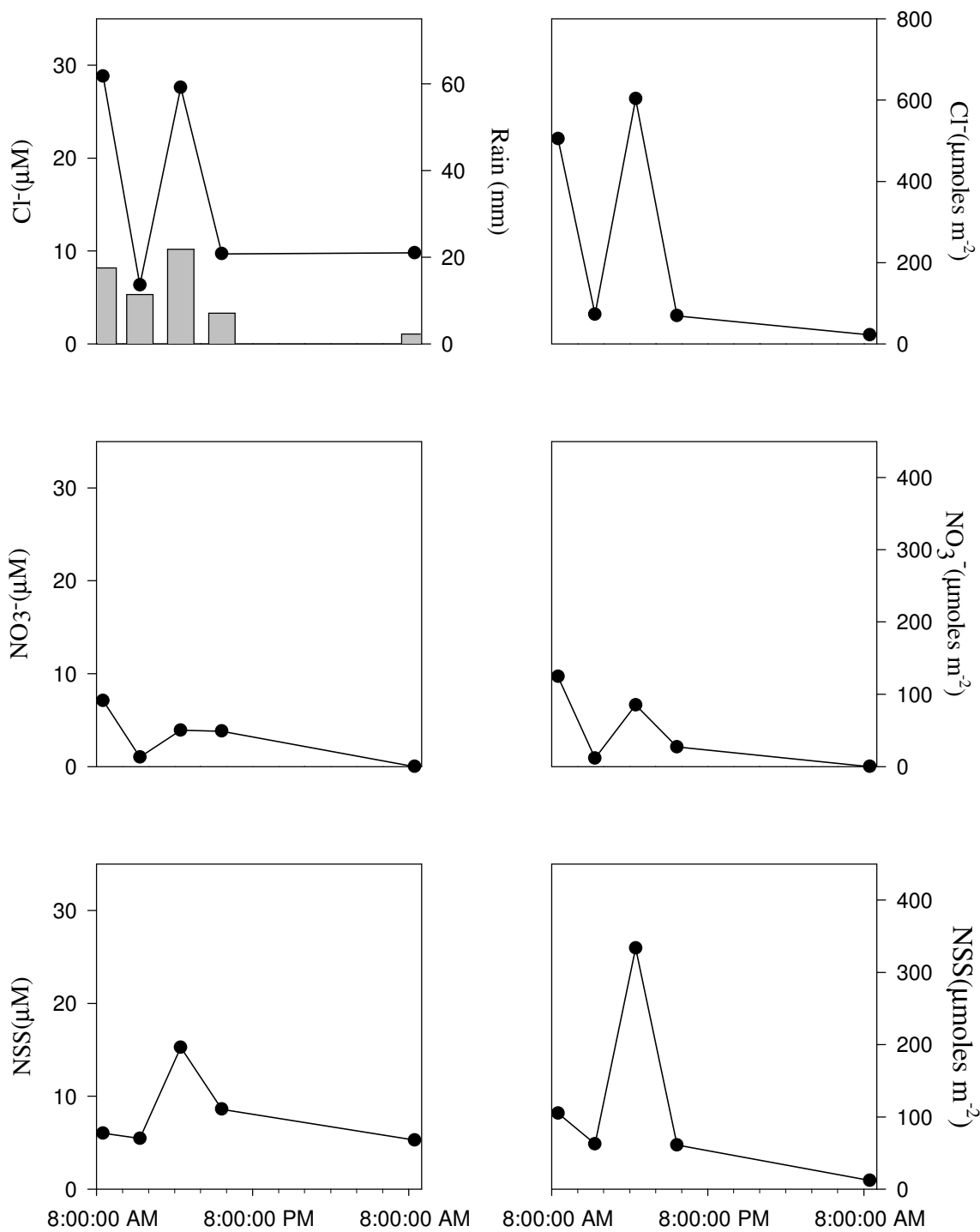


Figure 21. Concentrations and depositions of Cl<sup>-</sup>, NO<sub>3</sub><sup>-</sup>, and NSS in sequential samples taken at UNCW during hurricane Isabel (September 18, 2003). Bars in the Cl<sup>-</sup> concentration plot represent rainfall amounts for individual sequential samples.

Figure 22. Plots of back trajectories (calculated using the HYSPLIT model) and interpolated rainfall intensity field for hurricane Isabel sequential samples. Rainfall intensity (mm/h) is calculated from values given at each trajectory point.

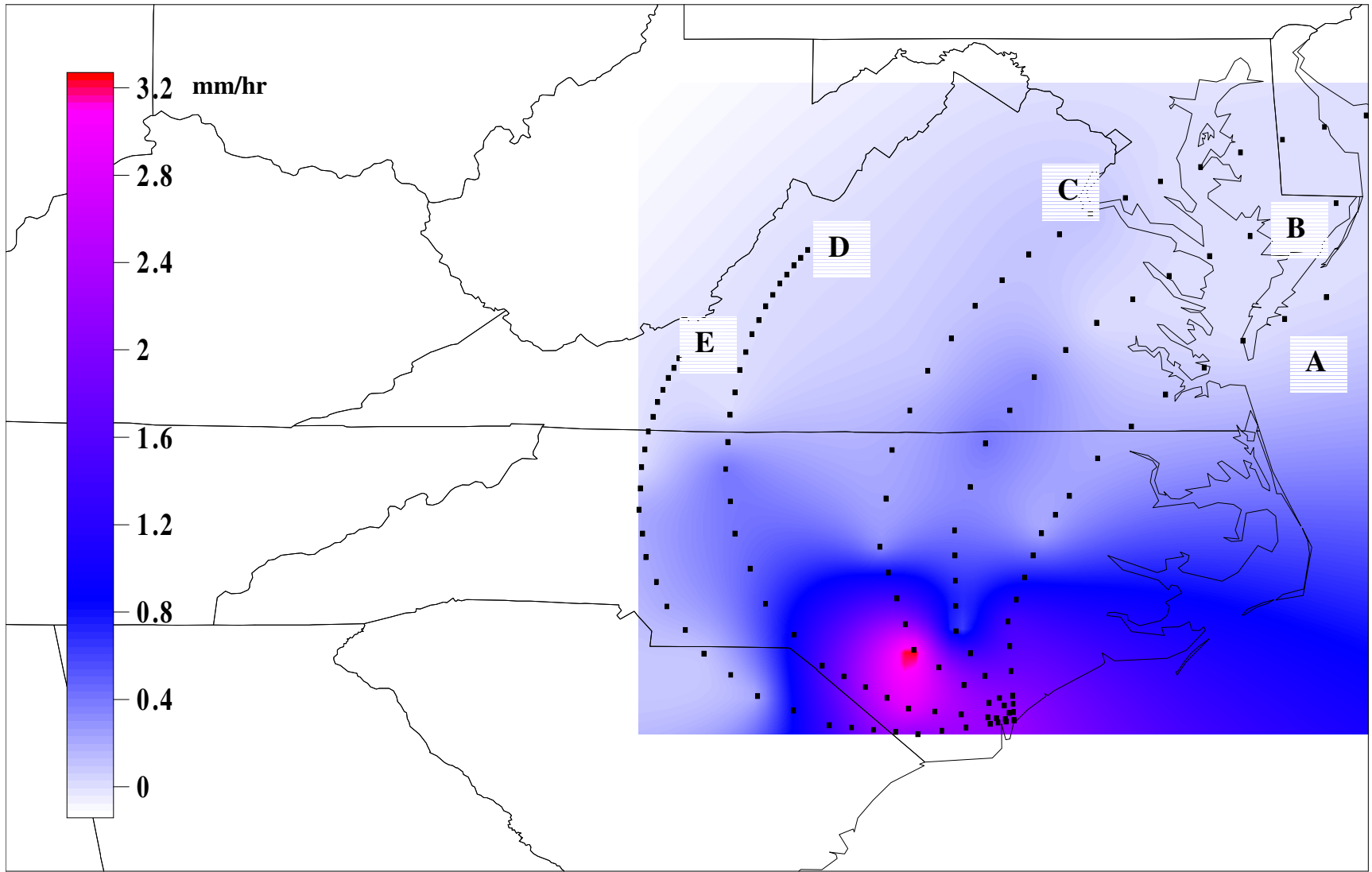
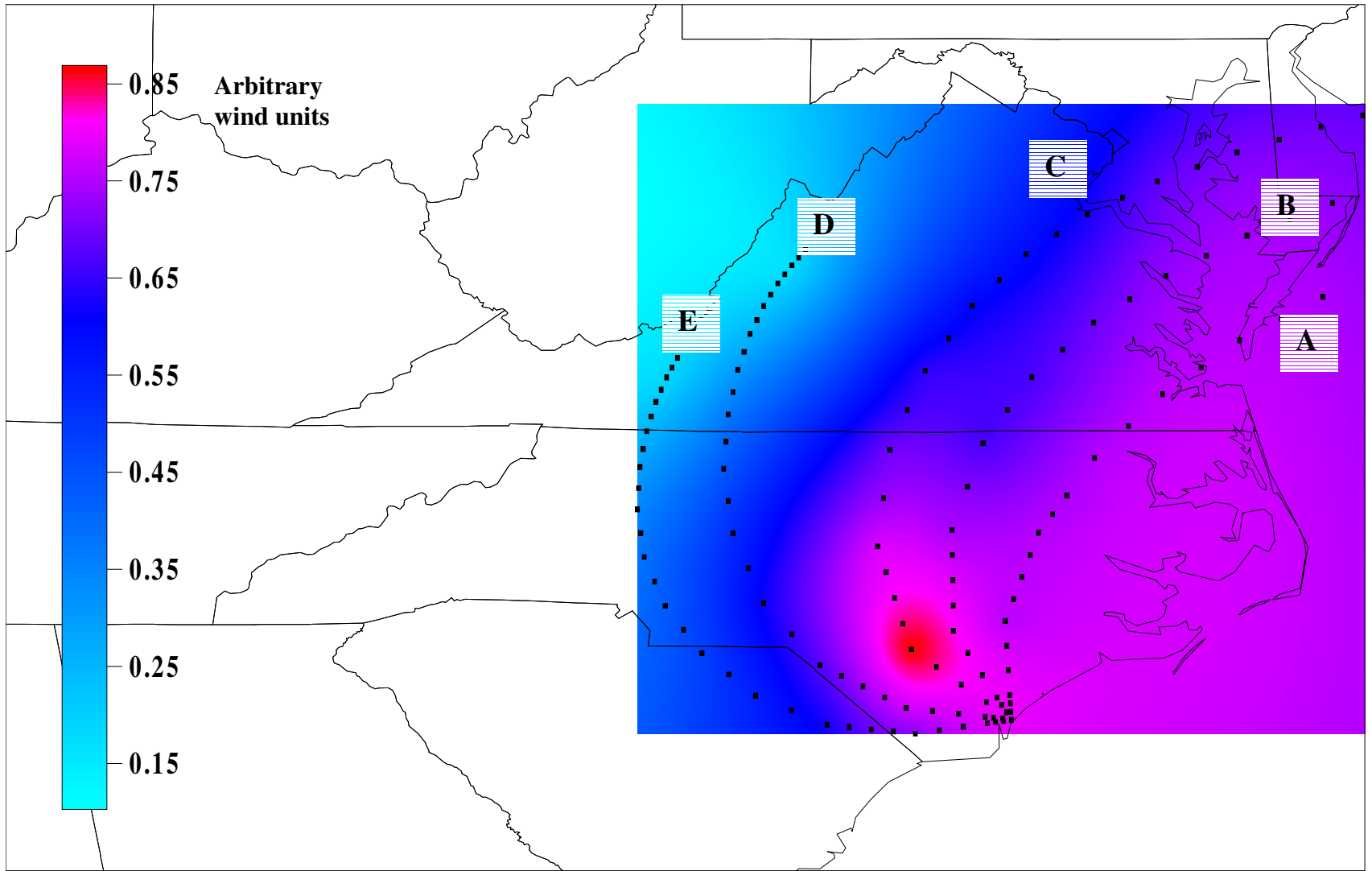


Figure 23. Plots of trajectories calculated using the NOAA/ARL HYSPLIT model and wind intensity field. The wind intensity Field is Calculated by Interpolation from Values Generated by Trajectory End Point Displacement. Values Represent Wind Intensities (arbitrary wind units) at the Specific Time and Position of the Modeled Air mass.



distribution. The reasons for the AA maximum in sequence sample C are not clear since sources of AA to the atmosphere are not well known though this suggests a similar source with  $\text{NH}_x$ . Changes in rain pH, though, might explain why AA does not wash out like  $\text{NH}_x$ . The nearly neutral rainfall throughout the event may prevent free amino acids from being effectively scavenged, thus retaining a significant portion of aerosolized AA in the atmosphere. When the  $\text{H}^+$  concentration increased toward the end of the event, scavenging efficiency increased.

On the whole, Hurricane Isabel's impact on the CFRE relative to  $\text{NH}_x$  and AA was significant in relation to the mean impact of summertime rain events. It contributed 2% to the total CFRE  $\text{NH}_x$  via direct wet deposition (versus 1% average for summer). Its total  $\text{NH}_x$  deposition ( $317 \mu\text{moles} \cdot \text{m}^{-2}$ ) was half the maximum ( $636 \mu\text{moles} \cdot \text{m}^{-2}$ ) of summer events used in this study and nearly three times the mean ( $119 \mu\text{moles} \cdot \text{m}^{-2}$ ). Considering  $\text{NO}_3^-$  deposition, Isabel was less important contributing less than 1% ( $243 \mu\text{moles} \cdot \text{m}^{-2}$ ) to the CFRE nitrate budget. Relative to the summertime, Isabel's nitrate deposition was only slightly higher than the  $190 \mu\text{moles} \cdot \text{m}^{-2}$  per event average.

## SUMMARY AND CONCLUSIONS

Concentrations of  $\text{NH}_x$ ,  $\text{NO}_3^-$ , AA, TN, ON,  $\text{SO}_4^{2-}$ ,  $\text{H}^+$ , and  $\text{Cl}^-$  were determined for 78 rain events between September 1, 2002 and August 31, 2003, at a coastal collection site on the campus of the University of North Carolina at Wilmington in southeastern North Carolina. Particle dry deposition of  $\text{NH}_x$ ,  $\text{NO}_3^-$ ,  $\text{SO}_4^{2-}$ ,  $\text{Cl}^-$ , and AA, and gas phase ammonia were also measured at this location during this time period. Rainwater composition data ( $\text{NH}_x$ ,  $\text{NO}_3^-$ ,  $\text{SO}_4^{2-}$ ,  $\text{H}^+$ , and  $\text{Cl}^-$ ) from the NADP monitored rain collection sites at Clinton, Lewiston, and Jordan Creek in Eastern North Carolina, along with data from Finley Farms near Raleigh, NC, and Cape

Canaveral, Florida, for the period from July 2002 through June 2003 was also studied. Vertical water column profiles of  $\text{NH}_x$  and measurements of above-water ammonia gas were taken on the Cape Fear River Estuary at five specified sites during the spring of 2003. As well, total and sequential samples of rainfall from Hurricane Isabel on September 18, 2003 were analyzed for  $\text{NH}_x$  and AA. Air mass back trajectories were calculated for all rain events during the sampling period and from Hurricane Isabel. These data support the following conclusions:

- 1) Of the total nitrogen (TN) in rain collected at UNCW in Wilmington, NC the majority (78%) is inorganic, occurring as  $\text{NO}_3^-$  and  $\text{NH}_x$  in approximately equal proportions. A decade ago, the comparable ratio of  $\text{NO}_3^-$  to  $\text{NH}_x$  was 1.4:1.0
- 2) Free amino acids make up a small portion of ON (17%).
- 3) Correlation analysis, back trajectory analysis, and emission vs. deposition comparisons indicate that regional sources, rather than local emissions, determine the concentrations of  $\text{NH}_x$  and  $\text{NO}_3^-$  in UNCW rainwater and particle dry deposition. In addition, similar temporal patterns in are seen at UNCW and the NADP monitored sites, with the exception of Clinton, NC, where  $\text{NH}_x$  concentrations and depositions have increased dramatically. Particle dry deposition of  $\text{NH}_x$  increased while NSS and  $\text{NO}_3^-$  dry depositions did not change over the last decade.
- 4) Concentrations of  $\text{H}^+$  and major N analytes considered in this study, with the exception of ON, vary significantly as a function of air mass origin. Analyses of back-trajectories indicate that rainwater constituents vary in accordance with the location of major regional emissions sources.
- 5) Seasonal and diurnal influences have a significant impact on the concentrations of  $\text{H}^+$  and N analytes in UNCW rainwater.

- 6) Overall,  $\text{NO}_3^-$  concentration in rainwater at UNCW has decreased from 1990 to the present while wet deposition increased due to increased rainfall and possibly increased emissions from growing population and expanding industry in North Carolina.
- 7) Wet and dry deposition, and rainfall concentrations of  $\text{NH}_x$  are higher compared with a decade ago. This probably reflects an increase in regional emissions due to growth in the livestock industry.
- 8) The rainwater concentration of NSS has decreased for the region as a whole.
- 9) The concentration of  $\text{H}^+$  decreased by a factor of approximately two in Wilmington, NC, rainwater over the last decade. This is more than can be explained by ion balance calculations using  $\text{NO}_3^-$ ,  $\text{SO}_4^{2-}$ , and  $\text{NH}_x$ .
- 10) Gas phase  $\text{NH}_3$  concentrations at UNCW are higher than for most other regions of North Carolina, possibly due to emissions from automobiles. The overall and seasonal values are similar to those measured at an agricultural site near Clinton, NC, which generally experiences high emissions of  $\text{NH}_3$  (Robarge et al., 2003).
- 11) Total long-term measurements of rainfall at UNCW are in good agreement with the total rainfall to the Cape Fear River Estuary. Comparisons of measured rainfall to that calculated from Doppler radar estimates showed good agreement. As well, estimates of total rainfall for the estuary from UNCW measurements were within 9% of those determined from the Doppler radar values.
- 12) Direct atmospheric deposition is not a major source of bioavailable nitrogen to the Cape Fear River Estuary. The average total daily  $\text{NH}_x$  and  $\text{NO}_3^-$  dry depositions were only 0.32% and 0.24%, respectively, in comparison to the total amount in the CFRE. Wet depositions of  $\text{NH}_x$  reached 20% for a single event with an average per event deposition

equivalent to 1.3% of  $\text{NH}_x$  in the CFRE. Wet deposition reached 4% and 1% for  $\text{NO}_3^-$  and TN respectively ( $\text{NO}_3^-$  average is 0.86%; TN average is 0.27%).

13) It is likely that dry deposition to the CFRE is underestimated in this study; perhaps by a factor of four, though there is evidence that the CFRE has a mean flux of  $\text{NH}_3$  out of the water.

14) In terms of direct deposition, hurricane Isabel did not contribute abnormal amounts of  $\text{NH}_x$  or AA to the CFRE.

15) The concentrations of  $\text{NH}_x$  in sequential samples collected from hurricane Isabel varied in conjunction with their back-trajectory's proximity to sources. Trends in  $\text{H}^+$  and AA concentrations in sequential samples seem to reflect a distinct transition from a marine to a terrestrial air mass.

## REFERENCES

- Atmospheric Loadings to Coastal Areas: Resolving Existing Uncertainties, in *Atmospheric Loadings Workshop*, Baltimore, MD. June 1994.
- Alvarez-Salgado, X.A., and A.E.J. Miller, Simultaneous determination of dissolved organic carbon and total dissolved nitrogen in seawater by high temperature catalytic oxidation: conditions for precise shipboard measurements, *Marine Chemistry*, 62, 325-333, 1998.
- Aneja, V.P., B. Bunton, J.T. Walker, and B.P. Malik, Measurement and analysis of atmospheric ammonia emissions from anaerobic lagoons, *Atmospheric Environment*, 35, 1949-1958, 2001a.
- Aneja, V.P., G. Murray, and J. Southerland, Proceedings of the Workshop on Atmospheric Nitrogen Compounds: emissions, transport, transformation, deposition, and assessment, pp. 299, North Carolina State University, Raleigh, NC, 1998.
- Aneja, V.P., A.B. Murthy, W. Battye, R. Battye, and W.G. Benjey, Analysis of ammonia and aerosol concentrations and deposition near the free troposphere at Mt. Mitchell, NC USA, *Atmospheric Environment*, 32 (3), 353-358, 1997.
- Aneja, V.P., D.R. Nelson, P.A. Roelle, J.T. Walker, and W. Battye, Agricultural ammonia emissions and ammonium concentrations associated with aerosols and precipitation in the southeast United States, *Journal of Geophysical Research D. Atmospheres*, 108 (D4), 2003.
- Aneja, V.P., P.A. Roelle, G. Murray, J. Southerland, J.W. Erisman, D. Fowler, W.A.H. Asman, and N. Patni, Atmospheric nitrogen compounds II: emissions, transport, transformation, deposition, and assessment, *Atmospheric Environment*, 35, 1903-1911, 2001b.
- Asman, W.A.H., Parameterization of below-cloud scavenging of highly soluble gases under convective conditions, *Atmospheric Environment*, 29 (17), 1359-1368, 1995.
- Asman, W.A.H., Modelling the atmospheric transport and deposition of ammonia and ammonium: an overview with special reference to Denmark, *Atmospheric Environment*, 35, 1969-1983, 2001.
- Asman, W.A.H., and J.A. van Jaarsveld, A variable-resolution transport model applied for NH<sub>x</sub> in Europe, *Atmospheric Environment*, 26A, 445-464, 1992.
- Avery Jr., G.B., Diurnal variations in major rainwater components at a coastal site in North Carolina, *Atmospheric Environment*, 35, 3927-3933, 2001.
- Bari, A., V. Ferraro, L.R. Wilson, D. Luttinger, and L. Husain, Measurements of gaseous HONO, HNO<sub>3</sub>, SO<sub>2</sub>, HCl, NH<sub>3</sub>, particulate sulfate and PM<sub>2.5</sub> in New York, NY, *Atmospheric Environment*, 37, 2825-2835, 2003.

- Barker, J. C., 1996a. Lagoon Design and Management for Livestock Waste Treatment and Storage. North Carolina Cooperative Extension Service EBAE 103-83. Retrieved January 29, 2004 from [http://www.bae.ncsu.edu/programs/extension/publicat/wqwm/ebae103\\_83.html](http://www.bae.ncsu.edu/programs/extension/publicat/wqwm/ebae103_83.html)
- Barker, J. C., 1996b. Utilization of Dairy Manure as Fertilizer. North Carolina Cooperative Extension Service EBAE 133-88. Retrieved January 29, 2004 from [http://www.bae.ncsu.edu/programs/extension/publicat/wqwm/ebae133\\_88.html](http://www.bae.ncsu.edu/programs/extension/publicat/wqwm/ebae133_88.html)
- Blando, J.D., and B.J. Turpin, Secondary organic aerosol formation in cloud and fog droplets: a literature evaluation of plausibility, *Atmospheric Environment*, 34, 1623-1632, 2000.
- Burkholder, J.M., H.B. Glasgow, and C.W. Hobbs, Fishkills linked to a toxic ambush-predator dinoflagellate: distribution and environmental conditions, *Marine Ecology Progress Series. Olendorf*, 124 (no 1-3), 43-61, 1995.
- Cahoon, L.B., J.A. Mikucki, and M.A. Mallin, Nitrogen and Phosphorous Imports to the Cape Fear and Neuse River Basins to Support Intensive Livestock Production, *Environmental Science and Technology*, 33, 410-415, 1999.
- Carta, R., Solubilities of L-cystine, L-tyrosine, L-leucine, and glycine in sodium chloride solutions at various pH values, *Journal of Chemical Thermodynamics*, 30, 379-387, 1998.
- Chate, D.M., P.S.P. Rao, M.S. Naik, G.A. Momin, P.D. Safai, and K. Ali, Scavenging of aerosols and their chemical species by rain, *Atmospheric Environment*, 37, 2477-2484, 2003.
- Clement, C.F., and I.J. Ford, Gas-to-particle conversion in the atmosphere: I. Evidence from empirical atmospheric aerosols, *Atmospheric Environment*, 33, 475-487, 1999.
- Cornell, S.E., T.D. Jickells, J.N. Cape, A.P. Rowland, and R.A. Duce, Organic Nitrogen Deposition on Land and Coastal Environments: A Review of Methods and Data, *Atmospheric Environment*, 37, 2173-2191, 2003.
- Cornell, S.E., T.D. Jickells, and C.A. Thornton, Urea in rainwater and atmospheric aerosol, *Atmospheric Environment*, 32, 1903-1910, 1998.
- Dasch, J.M., Direct measurement of dry deposition to a polyethylene bucket and various surrogate surfaces, *Environmental Science and Technology*, 19, 721-725, 1985.
- Dragosits, U., M.R. Theobald, C.J. Place, E. Lord, J. Webb, J. Hill, H.M. ApSimon, and M.A. Sutton, Ammonia emission, deposition and impact assessment at the field scale: a case study of sub-grid spatial variability, *Environmental Pollution*, 117, 147-158, 2002.
- Draxler, R.R. and Rolph, G.D., 2003. HYSPLIT (HYbrid Single-Particle Lagrangian Integrated Trajectory) Model access via NOAA ARL READY Website

- (<http://www.arl.noaa.gov/ready/hysplit4.html>). NOAA Air Resources Laboratory, Silver Spring, MD.
- Durbin, T.D., R.D. Wilson, J.M. Norbeck, J.W. Miller, T. Huai, and S.H. Rhee, Estimates of the emission rates of ammonia from light-duty vehicles using standard chassis dynamometer test cycles, *Atmospheric Environment*, 36, 1475-1482, 2002.
- Ensign, S.H., J.N. Halls, and M.A. Mallin, Application of digital bathymetry data in analysis of flushing times of two large estuaries, *Computers and Geoscience*, *In press*.
- EPA, National Air quality and Emissions Trends Report, 1999, United States Environmental Protection Agency, Office of Air Quality Planning and Standards, 2003.
- Gilbert, P.M., L. F., J.J. McCarthy, and M.A. Altabet, Isotope dilution models of uptake and remineralization of ammonium by marine plankton, *Limnology and Oceanography*, 27 (4), 1047-1056, 1982.
- Holmes, R.M., A. Aminot, R. Kerouel, B.A. Hooker, and B.J. Peterson, A simple and precise method for measuring ammonium in marine and freshwater ecosystems, *Canadian Journal of Fisheries and Aquatic Science*, 56, 1808-1808, 1999.
- Keene, W.C., J.A. Montag, J.R. Maben, M. Southwell, J. Leonard, T.M. Church, J.L. Moody, and J.N. Galloway, Organic Nitrogen in Precipitation Over Eastern North America, *Atmospheric Environment*, 36 (4529-4540), 2002.
- Kou-Fang Lo, A., L. Zhang, and H. Sievering, The effect of humidity and state of water surfaces on deposition of aerosol particles onto a water surface, *Atmospheric Environment*, 33, 4727-4737, 1999.
- Langford, A.O., F.C. Fehsenfeld, J. Zachariassen, and D.S. Schimel, Gaseous ammonia fluxes and background concentrations in terrestrial ecosystems of the United States, *Global Biogeochemical Cycles*, 6 (4), 459-483, 1992.
- Lawrence, G.B., D.B. Goolsby, W.A. Battaglin, and G.J. Stensland, Atmospheric Nitrogen in the Mississippi River Basin - Emissions, Deposition and Transport, *The Science of the Total Environment*, 248, 87-99, 2000.
- Lower Cape Fear River Program (LCFRP). (2004). University of North Carolina at Wilmington - Center for Marine Science, 5600 Marvin K. Moss Lane, Wilmington, NC 28409. <http://www.uncwil.edu/cmsr/aquaticceology/lcfrp>
- Maddox, R.A., J. Zhang, J.J. Gourley, and K.W. Howard, Weather radar coverage over the contiguous United States, *Weather and Forecasting*, 17, 927-934, 2002.
- Mallin, M.A., J.M. Burkholder, and L.B. Cahoon, North Carolina and South Carolina coasts, *Marine Pollution Bulletin*, 41 (no. 1-6), 56-75, 2000a.

- Mallin, M.A., L.B. Cahoon, M.R. McIver, D.C. Parsons, and G.C. Shank Alternation of factors limiting phytoplankton production in the Cape Fear River Estuary, *Estuaries*, 22 (4), 825-836, 1999.
- Mallin, M.A., K.A. Williams, E.C. Esham, and R.P. Lowe, Effect of human development on bacteriological water quality in coastal watersheds, *Ecological Applications*, 10 (4), 1047-1056, 2000b.
- Merriam, J., W.H. McDowell, and W.S. Currie, A high temperature catalytic oxidation technique for determining total dissolved nitrogen, *Journal of the Soil Science Society of America*, 60, 1050-1055, 1996.
- Metzger, S., F. Dentener, M. Krol, A. Jeuken, and J. Lelieveld, Gas/aerosol partitioning: 2. Global modeling results, *Journal of Geophysical Research D. Atmospheres*, 107 (D16), 2002.
- Minoura, H., and Y. Iwasaka, Rapid change in nitrate and sulfate concentrations observed in early stage of precipitation and their deposition processes, *Journal of Atmospheric Chemistry*, 24, 39-55, 1996.
- Mopper, K., and R.G. Zika, Free amino acids in marine rain: evidence for oxidation and potential role in nitrogen cycling, *Nature*, 325, 246-249, 1987.
- National Atmospheric Deposition Program (NRSP-3)/National Trends Network. (2004). NADP Program Office, Illinois State Water Survey, 2204 Griffith Drive, Champaign, IL 61820.
- Paasche, E., and S. Kristiansen, Ammonium regeneration by microzooplankton in the Oslofjord, *Marine Biology. Berlin, Heidelberg*, 69 (1), 55-63, 1982.
- Paerl, H.W., Nuisance phytoplankton blooms in coastal, estuarine, and inland waters, *Limnology and Oceanography*, 33 (4), 823-847, 1988.
- Parsons, T.R., Y. Maita, and C.M. Lalli, *A Manual of Chemical and Biological Methods for Seawater Analysis*, 173 pp., Pergamon Press, Oxford, 1984.
- Peierls, B., and H.W. Paerl, Bioavailability of atmospheric organic nitrogen deposition to coastal phytoplankton, *Limnology and Oceanography*, 42, 1819-1823, 1997.
- Pennock, J.R., Temporal and spatial variability in phytoplankton ammonium and nitrate uptake in the Delaware Estuary, *Coastal and Shelf Science*, 24 (6), 841-857, 1987.
- Perrino, C., M. Catrambone, D.M.D.B. A., and I. Allegrini, Gaseous ammonia in the urban area of Rome, Italy and its relationship with traffic emissions, *Atmospheric Environment, In Press*, 2002.

- Poor, N., R. Pribble, and H. Greening, Direct wet and dry deposition of ammonia, nitric acid, ammonium and nitrate to the Tampa Bay Estuary, FL, USA, *Atmospheric Environment*, 35, 3947-3995, 2001.
- Pradhan, A.A., and J.H. Vera, Effect of acids and bases on the solubility of amino acids, *Fluid Phase Equilibria*, 152, 121-132, 1998.
- Pryor, S.P., and R.J. Barthelmie, Particle dry deposition to water surfaces: processes and consequences, *Marine Pollution Bulletin*, 41, 220-231, 2000.
- Pryor, S.P., and L.L. Sorensen, Dry deposition of reactive nitrogen to marine environments: recent advances and remaining uncertainties, *Marine Pollution Bulletin*, 44, 1336-1340, 2002.
- Quantitative Precipitation Estimation and Segregation Using Multiple Sensors (QPESUMS). National Severe Storms Laboratory NSSL), 1313 Halley Circle, Norman, Oklahoma 73069. <http://www.nssl.noaa.gov/wrd/wish/qpe>
- Raes, F., R. van Dingenen, E. Vignati, J. Wilson, J.-P. Putaud, J.H. Seinfeld, and P. Adams, Formation and cycling of aerosols in the global troposphere, *Atmospheric Environment*, 34, 4215-4240, 2000.
- Robarge, W.P., J.T. Walker, R.B. McCulloch, and G. Murray, Atmospheric concentrations of ammonia and ammonium at an agricultural site in the southeast United States, *Atmospheric Environment*, 36, 1661-1674, 2002.
- Roelle, P.A., and V.P. Aneja, Characterization of ammonia emissions from soils in the upper coastal plain, North Carolina, *Atmospheric Environment*, 36, 1087-1097, 2002.
- Ross, C.A., and S.C. Jarvis, Measurement of emission and deposition patterns of ammonia from urine in grass swards, *Atmospheric Environment*, 35, 867-875, 2001.
- Russel, K.M., J.N. Galloway, S.A. Macko, J.L. Moody, and J.R. Scudlark, Sources of Nitrogen in Wet Deposition to the Chesapeake Bay Region, *Atmospheric Environment*, 32 (14), 2453-2465, 1998.
- Schjoerring, J.K., S. Husted, and M. Mattsson, Physiological parameters controlling plant-atmosphere ammonia exchange, *Atmospheric Environment*, 32 (3), 491-498, 1997.
- Scudlark, J.R., K.M. Russel, J.N. Galloway, T.M. Church, and W.C. Keene, Organic nitrogen in precipitation in the mid-Atlantic U.S. coast - methods evaluation and preliminary measurements, *Atmospheric Environment*, 32 (10), 1719-1728, 1997.
- Shahin, U.M., X. Zhu, and T.S. Holsen, Dry deposition of reduced and reactive nitrogen: A surrogate surfaces approach, *Environmental Science and Technology*, 33, 2113-2117, 1999.

- Shimshock, J.P., and R.G. De Pena, Below-cloud scavenging of tropospheric ammonia, *Tellus*, 41B (296-304), 1989.
- Sorensen, L.L., O. Hertel, C.A. Skjoth, M. Lund, and B. Pedersen, Fluxes of ammonia in the coastal marine boundary layer, *Atmospheric Environment*, 37, S167-S177, 2003.
- Stumm, W., and J.J. Morgan, *Aquatic Chemistry: Chemical Equilibria and Rates in Natural Waters*, John Wiley and Sons, Inc., New York, 1996.
- Walker, J.T., V.P. Aneja, and D.A. Dickey, Atmospheric transport and deposition of ammonium in North Carolina, *Atmospheric Environment*, 34, 3407-3418, 2000.
- Walsh, T.W., Total dissolved organic nitrogen in seawater: a new high temperature combustion method and a comparison with photo-oxidation, *Marine Chemistry*, 26 (295-311), 1989.
- Warneck, P., *Chemistry of the Natural Atmosphere*, pp. 426-441, Academic Press, New York, 1988.
- Wesely, M.L., and B.B. Hicks, A review of the current status of knowledge on dry deposition, *Atmospheric Environment*, 34, 2261-2282, 2000.
- Wheeler, P.A., P.M. Gilbert, and J.J. McCarthy, Ammonium uptake and incorporation by Chesapeake Bay phytoplankton: short term uptake kinetics, *Limnology and Oceanography*, 27 (6), 1113-1128, 1982.
- Whitall, D., B. Hendrickson, and H.W. Paerl, Importance of atmospherically deposited nitrogen to the annual nitrogen budget of the Neuse River Estuary, North Carolina, *Environment International*, 29, 393-399, 2003.
- Willey, J.D., and R.H. Kiefer, Atmospheric Deposition in Southeastern North Carolina: composition and quantity, *The Journal of the Elisha Mitchell Scientific Society*, 109 (1), 1 - 19, 1993.
- Wofsy, S.C., A simple model to predict extinction coefficients and phytoplankton biomass in eutrophic waters, *Limnology and Oceanography*, 28 (6), 1144-1155, 1983.
- Wofsy, S.C., M.B. McElroy, and J.W. Elkins, Transformations of nitrogen in a polluted estuary: nonlinearities in the demand for oxygen at low flow, *Science (Washington)*, 213 (4509), 754-757, 1981.
- Yeatman, S.G., L.J. Spokes, and T.D. Jickells, Comparisons of coarse-mode aerosol nitrate and ammonium at two polluted sites, *Atmospheric Environment*, 35, 1321-1335, 2001.

- Yevjevich, V., *Probability and Statistics in Hydrology*, Water Resources Publications, Colorado, 1971.
- Zhang, L., S. Gong, J. Padro, and L. Barrie, A size-segregated dry-deposition scheme for an atmospheric aerosol module, *Atmospheric Environment*, 35 (549-560), 2001.
- Zhang, Q., Free and combined amino compounds in atmospheric fine particles (PM<sub>2.5</sub>) and fog waters from Northern California, *Atmospheric Environment*, 37, 2247-2258, 2003.
- Zhuang, H., and C.K. Chan, Size distribution of inorganic aerosols as a coastal site, *Journal of Aerosol Science*, 28 (suppl. 1), 5213-5214, 1997.